Spatial, temporal and source contribution assessments of aerosol black carbon over the northern interior of South Africa

EK Chiloane

orcid.org 0000-0003-3504-3046

Thesis submitted in fulfilment of the requirements for the degree *Doctor of Philosophy in Environmental Sciences* at the North-West University

Promoter: Prof JP Beukes

Co-Promoter: Prof PG van Zyl

Graduation October 2019

20302177

PREFACE

The thesis model adopted by the Faculty of Natural Sciences in terms of the General Rules of the North West University (NWU) has been followed for this postgraduate study. This thesis presents the abstract, background and motivation (Chapter 1), literature review (Chapter 2), experimental (Chapter 3), results and discussion (Chapters 4, 5 and 6), as well as conclusion, project evaluation and future perspectives (Chapter 7).

It is currently a prerequisite for submitting a PhD thesis at the NWU that at least one research article was submitted to a reputable journal. This prerequisite was exceeded, since an extended paper was published in a very high impact factor journal (impact factor of 5.318 for 2016), i.e. **Kgaugelo Euphinia Chiloane**, Johan Paul Beukes, Pieter Gideon van Zyl, Petra Maritz, Ville Vakkari, Miroslav Josipovic, Andrew Derick Venter, Kerneels Jaars, Petri Tiitta, Markku Kulmala, Alfred Wiedensohler, Catherine Liousse, Gabisile Vuyisile Mkhatshwa, Avishkar Ramandh, Lauri Laakso, 2017. Spatial, temporal and source contribution assessments of BC over the northern interior of South Africa. Atmospheric Chemistry and Physics, 17, 6177–6196, 2017, www.atmos-chem-phys.net/17/6177/2017/, doi: 10.5194/acp-17-6177-2017.

Other articles, to which the author contributed as a co-author, which were published during the duration of this study include:

1. Sundström, A.-M., Nikandrova, A., Atlaskina, K., Nieminen, T., Vakkari, V., Laakso, L., Beukes, J. P., Arola, A., Van Zyl, P. G., Josipovic, M., Venter, A. D., Jaars, K., Pienaar, J. J., Piketh, S., Wiedensohler, A., **Chiloane, E. K**., De Leeuw, G., and Kulmala, M. Characterisation of satellite-based proxies for estimating nucleation mode particles over South Africa. Atmospheric Chemistry and Physics, 15, 4983–4996, **2015**. Doi: 10.5194/acp-15-4983-2015.
2. Backman, J., Virkkula, A., Vakkari, V., Beukes, J. P., Van Zyl, P. G., Josipovic, M., Piketh, S., Tiitta, P., **Chiloane, K**., Petäjä, T., Kulmala, M., and Laakso, L., **2014**. Differences in aerosol absorption Ångström exponents between correction algorithms for a particle soot absorption photometer measured on the South African Highveld. Atmospheric Measurement Techniques Discussion, 7, 4285-4298, doi: 10.5194/amt-7-4285, 2014.
3. K. Korhonen, E. Giannakaki, T. Mielonen, A. Pfüller, L. Laakso, V. Vakkari, H. Baars, R. Engelmann, J. P. Beukes, P. G. Van Zyl, A. Ramandh, L. Ntsangwane, M. Josipovic, P. Tiitta, G. Fourie, I. Ngwana, **K. Chiloane**, and M. Komppula, **2013**. Atmospheric boundary layer top height in South Africa: measurements with lidar and radiosonde compared to three atmospheric models. Atmospheric Chemistry and Physics, 13, 17407–17450.

4. L. Laakso, V. Vakkari, A. Virkkula, H. Laakso, J. Backman, M. Kulmala, J. P. Beukes, P. G. van Zyl, P. Tiitta, M. Josipovic, J. J. Pienaar, **K. Chiloane**, S. Gilardoni, E. Vignati, A. Wiedensohler, T. Tuch, W. Birmili, S. Piketh, K. Collett, G. D. Fourie, M. Komppula, H. Lihavainen, G. de Leeuw and V.M. Kerminen, **2012**. South African EUCAARI measurements: seasonal variation of trace gases and aerosol optical properties. Atmospheric Chemistry and Physics, 12, 1847–1864.

Book chapters that were published during the duration of this study, to which the author contributed, include:

1. Lauri Laakso, Johan Paul Beukes, Pieter Gideon Van Zyl, Jacobus Pienaar, Miroslav Josipovic, Andrew Venter, Kerneels Jaars, Ville Vakkari, Casper Labuschagne, **Kgaugelo Chiloane**, and Juha-Pekka Tuovinen, **2013**. Ozone concentrations and their potential impacts on vegetation in southern Africa. Developments in Environmental Science, Chapter 20, Volume. 13. Elsevier Ltd. 2013, http://dx.doi.org/10.1016/B978-0-08-098349- 3.00020-7.

ACKNOWLEDGEMENTS

I would like to express my gratitude to those who made the completion of this thesis possible:

- God the Almighty for being part of this journey and making it possible.
- Prof Paul Beukes and Prof Pieter van Zyl for supervising and co-supervising my studies, respectively.
- Specific thanks goes to Prof Beukes, for providing guidance and direction to all aspects of this work, including the long hours that he has put in working with me on the data analysis, interpretation and publications development. Much appreciated.
- Prof Lauri Laakso and Dr Ville Vikkari from the Finnish Meteorological Institute (FMI) for providing technical support and guidance on data collection and comments on the publication.
- My husband, Mr Dira Marule and our five children for their support and encouragement throughout this journey. Thank you so much Team. You are the Best!
- To my parents, Mr Platos Chiloane and Mrs Eunice Maabane, for always believing in me and inspiring me since the beginning of my career. I thank God for keeping you on this planet to witness this wonderful achievement with me. This is for you!
- All my family, friends and colleagues for their support and encouragement.
- A special thank you to all the funding institutions, the European Union Framework Programme 6 (EU FP6), the National Research Foundation (NRF), as well as national and international academic (North-West University, University of the Witwatersrand and University of Helsinki) institutions and companies (Eskom, Sasol and the Finnish Meteorological Institute) for their contribution to the success of aerosol black carbon (BC) measurements in South Africa.
- Eskom Holdings SOC Ltd is acknowledged for funding and making the Elandsfontein Air Quality Monitoring Station, as well as the technical team (Mr Abram Segopa, Mr Kgancho Komane and Ms Trinity Ngomane) available and accessible to support EUCAARI Project measurements in SA.
- Atmospheric Chemistry Research Group of the North-West University colleagues (Dr Andrew Venter, Dr Kerneels Jaars, Dr Mickey Josipovic and Dr Petri Tiitta) are thanked for their assistance on various aspects of this project. Ms Petri Maritz, thank you for providing the DEBITS data and information presented in this thesis.
- The North-West University administration is acknowledged for their assistance.

ABSTRACT

After carbon dioxide (CO_2), aerosol black carbon (BC) is considered to be the second most important contributor to global warming. Africa is one of the least studied continents, although it is regarded as the largest source region of atmospheric BC. Southern Africa is an important sub-source region, with savannah and grassland fires likely to contribute to elevated BC mass concentration levels. South Africa is the economic and industrial hub of southern Africa with large anthropogenic point sources. To date, little BC mass concentration data have been presented for South Africa in the peer-reviewed public domain. This thesis presents equivalent black carbon (eBC) (derived from an optical absorption method) data collected from three sites, where continuous measurements were conducted, i.e. Elandsfontein (EL), Welgegund (WG) and Marikana (MA), as well as elemental carbon (EC) (determined by evolved carbon method) at five sites where samples were collected once a month on a filter and analysed off-line, i.e. Louis Trichardt (LT), Skukuza (SK), Vaal Triangle (VT), Amersfoort (AM) and Botsalano (BS). All these sites are located in the interior of South Africa.

Analyses of eBC and EC spatial mass concentration patterns across the eight sites indicate that the mass concentrations in the South African interior are in general higher than what has been reported for the developed world, and that different sources are likely to influence different sites. The mean eBC or EC mass concentrations for the background sites (WG, LT, SK, BS) and sites influenced by industrial activities and/or nearby settlements (EL, MA, VT and AM) ranged between 0.7 and 1.1, and 1.3 and 1.4 μgm^{-3}, respectively. Similar seasonal patterns were observed at all three sites where continuous measurement data were collected (EL, MA and WG), with the highest eBC mass concentrations measured from June to October, indicating contributions from household combustion in the cold winter months (June-August), as well as savannah and grassland fires during the dry season (May to mid-October). Diurnal patterns of eBC at EL, MA and WG indicated maximum concentrations in the early mornings and late evenings, and minima during daytime. From these patterns, it could be deduced that for MA and WG, household combustion as well as savannah and grassland fires were the most significant sources, respectively. Possible contributing sources were explored in greater detail for EL, with five main sources being identified as coal-fired power stations, pyrometallurgical smelters, traffic, household combustion, as well as savannah and grassland fires. Industries in the Mpumalanga Highveld are often blamed for all forms of pollution in the area due to the NO_2 hotspot located in this area, which is attributed to NOx emissions from industries and vehicle emissions from the Johannesburg-Pretoria megacity. However, a comparison of source strengths indicated that household combustion, and savannah and grassland fires were the most significant sources of eBC, particularly during winter and spring months, while coal-fired power stations, pyro-metallurgical smelters and traffic contribute to eBC mass concentration levels all year round.

Keywords: aerosols, equivalent black carbon (eBC), temporal and diurnal, source strengths, combustion

TABLE OF CONTENTS

LIST OF TABLES

LIST OF FIGURES

Chapter 2

Chapter 3

CHAPTER 1: INTRODUCTION

This chapter provides a brief background to aerosol black carbon covering their potential impacts on human health, the environment and climate. This is followed by the problem statement demonstrating the motivation behind this study, concluding with the general aim as well as the specific objectives of this study.

1.1 Background

Aerosol black carbon (BC) is the carbonaceous fraction of ambient particulate matter that absorbs incoming short-wave solar radiation and terrestrial long-wave radiation, resulting in a warming effect on the atmosphere (IPCC, 2013; Seinfeld and Pandis, 2016). Although BC has a relatively short atmospheric lifetime (days to weeks), it has significant regional and local effects on atmospheric temperature, cloud amount and precipitation. Over snow-covered areas, the surface albedo can be significantly reduced due to the deposition of BC, and this may considerably influence the local and regional climate (Jacobson, 2004; Ramanathan and Carmichael, 2008). Direct observations of reduced albedo resulting from long-range-transported BC into Arctic areas have been reported by Stohl et al. (2006). Findings from this study estimated that BC may have contributed to more than half of the observed Arctic warming since 1890, most of this occurring during the last three decades (Stohl et al., 2006; Shindell et al., 2008). After carbon dioxide (CO_2), BC is considered to be the second most important contributor to global warming (Bond et al., 2004; Bond et al., 2016; IPCC, 2013). According to some authors, reducing BC emissions may be the fastest means of slowing global warming in the near future, because of its short atmospheric lifetime. In addition to the afore-mentioned effects, BC is a major contributor to fine particulate matter in the atmosphere that has negative health effects (Hansen et al., 1984, Cachier, 1995; IPCC, 2013).

Atmospheric BC is a primary species (Putaud et al., 2004; Pöschl, 2005; IPCC, 2013) that is emitted from combustion processes, particularly from fossil fuel combustion (industrial and residential), vehicle exhausts (mainly diesel engines), as well as open biomass fires (Cachier, 1995; Cooke and Wilson, 1996; Bond e al., 2004; IPCC, 2013). Globally, approximately 20% of BC is emitted from residential biofuel burning, 40% from fossil fuels and 40% from open biomass burning such as forest and savannah fires (Hansen et al., 1988; Cooke and Wilson, 1996; Wolf and Cachier, 1998; Pope, 2002). BC from fossil fuels is estimated to contribute a global mean radiative forcing of 0.04 watts per square metre (Wm^{-2}) (IPCC, 2013). There are many uncertainties associated with emissions of BC, its aging during atmospheric transportation and removal by precipitation (Bond et al., 2004), and these are reflected in uncertainties in its global effect (e.g. Bond et al., 2013). The majority of aerosol radiative impact assessments are currently based on models

that incorporate measured aerosol properties on local and global scales (Bond et al., 2013; IPCC, 2013). However, this approach involves several assumptions, such as assuming aerosol properties and the use of global instead of regional emission inventories for under-sampled or characterised regions.

Considering the relatively short atmospheric lifetime of BC, the above-mentioned assumptions could lead to significant uncertainties, especially on regional scales (Masiello, 2004; Andreae and Gelencser, 2006; Bond et al., 2013; Kuik et al., 2015). For a better understanding of the transport, removal and climatic impacts of atmospheric BC, accurate and up-to-date measurements covering large spatial areas and long temporal periods are required. Africa is one of the least studied continents, although it is regarded as the largest source region of atmospheric BC (Liousse et al., 1996; Kanakidou et al., 2005). Southern Africa is an important sub-source region, with savannah and grassland fires (anthropogenic and natural) being prevalent across this region, particularly during the dry season when almost no precipitation occurs (Formenti et al., 2003; Tummon et al., 2010; Laakso et al., 2012; Vakkari et al., 2014; Mafusire et al., 2016). Studies by Swap et al. (2004) found that savannah and grassland fire plumes from southern Africa affect Australia and South America. South Africa is the economic and industrial hub of southern Africa, with large anthropogenic point sources (Lourens et al., 2011). However, the relative importance of BC contributions from these anthropogenic sources in South Africa is still largely unknown and few BC-related papers have been published in the peer-reviewed public domain. Martins (2009) determined elemental carbon (EC) and organic carbon (OC) mass concentrations from three two-week winter campaigns and one two-week summer campaign at two sites, as part of the framework of the Deposition of Biogeochemical Important Trace Species (DEBITS)-International Global Atmospheric Chemistry (IGAC) in Africa project (Galy-Lacaux et al., 2003; Martins et al., 2007). However, the data from this study were not published in the peer-reviewed scientific domain.

Collett et al. (2010) only presented a single diurnal plot for BC mass concentrations measured at the Elandsfontein monitoring station in 2010. Venter et al. (2012) used BC mass concentration data collected at the Marikana monitoring station to verify the origin of CO and PM_{10}, but did not consider BC in detail. Hyvärinen et al. (2013) used BC mass concentration data collected at the Welgegund monitoring station to illustrate the use of a newly developed method to correct BC mass concentration values measured with a multi-angle absorption photometer (MAAP). Maritz et al. (2015) and Aurela et al. (2016) presented limited EC mass concentration data from some regional background sites in South Africa. Kuik et al. (2015) used BC data obtained from the South African Air Quality Information System (SAAQIS) to model the contribution of anthropogenic emissions to the total tropospheric BC load from September to December 2010 in South Africa. Significant underestimations and uncertainties with regard to BC mass concentrations were reported by the afore-mentioned authors.

In addition to the above-mentioned limited BC-related studies that were published, the availability of BC data in South Africa is improving due to several air quality stations being equipped to measure BC across the country. These stations are maintained by the South African Weather Service (SAWS) on behalf of the

National Department of Environmental Affairs (DEA). Data from these stations are archived in the SAAQIS online platform (http://www.saaqis.org.za/NAAQM.aspx, date accessed: 14 May 2018). Feig et al. (2015) published limited results from the DEA/SAWS stations.

1.2 Problem statement

Scientific evidence shows that aerosol BC contributes to adverse human health, as well as environmental and climatic impacts. Currently, there is a substantial level of understanding of climate forcing contributions by most greenhouse gases; whereas that by aerosols (particularly BC) remains one of the largest sources of uncertainties in estimating anthropogenic climate perturbations. This is mainly due to the large heterogeneities in the physical and chemical properties of aerosols in space and time (IPCC, 2013). BC is part of the aerosol load that affects the climate both directly and indirectly. The combined direct and indirect effects of aerosols constitute the largest uncertainty in the current radiative forcing estimates of the earth's climate system (Forster et al., 2007; Hansen et al., 2007 (a); Solomon et al., 2007; IPCC, 2013). BC is known to affect the climate by changing the way radiation is transmitted through the atmosphere. Direct observations of BC are limited in certain regions, resulting in the use of models to estimate the global climatic effect.

Detailed information on the temporal and spatial variability of aerosol BC can be obtained from a combination of model simulations, remote sensing and in-situ aerosol measurements. The limited studies on aerosol BC in South Africa, coupled with the potential significant impacts thereof on human health, the environment and climate are the main motivation behind this study.

1.3 Aims and objectives

The general aim of this study was to determine spatial and temporal concentration patterns of aerosol BC over the northern interior of South Africa, as well as assessing potential contributing sources. Specific objectives of this study were to:

- Assess spatial and temporal (seasonal and diurnal) trends of BC over the northern interior of South Africa. Data from several measurement sites will be considered and general deductions with regard to possible sources will be derived from the spatial and temporal trends.
- Determine potential contributing source strengths for at least one of the measurement sites for which high resolution continuous data were available.

- Use a multivariate statistical method to confirm that the above-mentioned deductions regarding source contributions were valid. Such a statistical evaluation will prevent biases that could have arisen due to preconceptions of the candidate.

1.4 Conclusion

Impacts of aerosol BC are significant on a regional and local scale due to its relatively short atmospheric lifetime. However, limited BC studies have been undertaken for South Africa with significant uncertainties with regard to BC mass concentrations and sources, and this is identified as the gap. The results presented in this study (Chapters 4-6) will make a contribution to address this research and knowledge gap.

CHAPTER 2: LITERATURE REVIEW

This chapter presents background information for this study, making particular reference to air pollution, climate change and aerosols, with a specific emphasis on black carbon (BC). A brief review on BC impacts on the climate, human health and the environment, measuring techniques, as well as the benefits of reducing BC are presented. An overview of BC measurement campaigns globally and in South Africa is also provided in this chapter.

2.1 Air pollution background

Air pollution is the introduction of chemicals, particulate matter or biological materials into the atmosphere that cause harm or discomfort to humans or other living organisms, or cause damage to the natural and built environment (Karnosky et al., 2003). The atmosphere is a complex dynamic natural system of mainly gases (and a bit of particulate matter) that is essential to support life on earth. Stratospheric ozone depletion due to air pollution has long been recognised as a threat to human health and the earth's ecosystems. Indoor air pollution and urban air quality are listed as two of the world's worst pollution problems. During the past decades, industrialisation, increased by population growth, and urbanisation have been the major determinants in shaping air quality (Karnosky et al., 2003; Seinfeld and Pandis, 2016).

Air pollution is widespread and a growing challenge with known global and regional impacts on health and the environment. The human need for transport, manufactured goods and services gives rise to air pollution and environmental impacts at local, regional and global scales. Governments are faced with a challenge to balance concerns over these impacts while maintaining and improving economic development. Science is the key to identify the nature and scale of air pollution impacts that are important in the formulation of effective policies and regulations. Knowledge of the fundamental science of air pollution and the application of this knowledge enables better prediction, assessment and mitigation of air pollution impacts on local, regional, national and international economic systems (Karnosky et al., 2003).

Scientists began to understand atmospheric pollution phenomena such as the Los Angeles photochemical smog during the 1950s. It is now known that surface-level ozone and photochemical smog are problems on regional, continental and global scales (Karnosky et al., 2003). As studies evolved, atmospheric processes (chemical, physical, meteorological, etc.), transport, transformations as well as removal mechanisms received more attention and understanding improved. In addition, knowledge of the effects of air pollutants on human health and welfare has improved substantially over the past decades. Furthermore, studies have also been directed to improve the levels of understanding of the accumulation

of persistent inorganic and organic chemicals and their impacts on sensitive receptors, including humans and the environment (Karnosky et al., 2003). Environmental literacy recently became an increasingly important factor, particularly in developing countries due to rapid population and industrial growth (Karnosky et al., 2003). Currently, scientific, public and political communities are concerned with increasing global air pollution and the consequent global climate change implications. Human health, environmental impacts, risk assessment and the associated cost-benefit analyses, coupled to the global economy, form essential components in dealing with air pollution issues (Seinfeld and Pandis, 2016).

Studies show that urban air pollution poses a significant threat to human health and the environment in both developed and developing parts of the world (Fenger, 1999; Gurja et al., 2008), and it also affects the regional and global climate. The world's population has more than doubled since the Second World War (Fenger, 1999). It is predicted that by the year 2030 approximately 80% of the population will be living in urban centres (Gurja et al., 2008; WHO, 2017). Even in less developed countries, the majority of people are, or will be, living in urban areas in the near future (WHO, 2017). Given these increasing trends, industries and local municipalities are constantly under pressure from governments to implement programmes to reduce concentrations of pollutants in the atmosphere and improve air quality, particularly in urban settlements. Therefore, air quality in urban and industrialised areas is a major concern for governments, industries and citizens worldwide.

The World Health Organization (WHO) estimated that air pollution caused nearly two million premature deaths per year. The latest WHO report indicates that, in 2012, approximately 7 million people died, where one in eight of total global deaths were premature as a result of air pollution exposure (WHO, 2017). This finding is more than double previous estimates and confirms that air pollution is now the world's largest single environmental health risk. Therefore, reducing air pollution could save millions of lives. In addition to air quality, climate change constitutes a serious threat to ecosystems and human welfare on local, regional and global scales. Changes in the atmospheric concentrations of greenhouse gases (GHGs) and aerosols, coupled with land cover changes and solar radiation, alter the energy balance of the climate system and are the drivers of climate variability and change (IPCC, 2013).

Air pollutants are emitted from both natural and anthropogenic (man-made) activities. Natural emission sources include biogenics, volcanic eruptions, fires (e.g. due to lightning, atmospheric conditions, etc.), dust and digestive gases emitted by animals (for non-anthropogenic species). Emissions from man-made activities primarily result from various industrial and residential combustion processes, solvent manufacturing and use, pyrometallurgical smelting, waste incineration or landfill, forestry/agriculture and vehicle emissions (Seinfeld and Pandis, 2016). Since the 19th century, the industrial revolution spread across the world resulting in an increase in anthropogenic emissions due to enhanced consumption of non-renewable resources for energy generation and transportation. Examples of air pollutants include organic and inorganic gaseous species such as SO_2, carbon monoxide (CO), NO_2, O_3, particulate matter with aerodynamic diameters smaller than 2.5 and 10 micrometres (μm) ($PM_{2.5}$ and PM_{10}, respectively), volatile

organic compounds (VOCs), toxic metals (e.g. mercury, lead, cadmium, copper) and their compounds chlorofluorocarbons (CFCs), ammonia (NH_3), and persistent organic pollutants (POPs) (organic pollutants resistant to environmental degradation, which are persistent in the environment and capable of bioaccumulation) (IPCC, 2001; Seinfeld and Pandis, 2016). Some of the aforementioned species are regarded as criteria air quality pollutants (within a legal framework) in many countries.

Apart from classifying pollutants as natural or anthropogenic, pollutants can also be classified as primary (directly emitted by source) or secondary (formed from chemical transformation of primary species in the atmosphere) (IPCC, 2001; EPA, 2006; Seinfeld and Pandis, 2016). Example of primary pollutants are sulphur dioxide (SO_2) emitted by a combustion process and windblown dust. An example of a secondary pollutant is ground-level ozone (O_3) that is formed from the photochemical reaction between oxides of nitrogen (NO_x), and VOC, and CO serving as precursors supplying the radical species for the enhanced oxidation of NO to NO_2 (Laban et al., 2018). However, other air pollutants such as GHGs and specific aerosols are not classified as criteria air quality pollutants but are of greater concern from a climate change perspective. Examples of GHGs include carbon dioxide (CO_2), methane (CH_4), nitrous oxide (N_2O), ozone (O_3), sulphur hexafluoride (SF_6) and halocarbons (a group of gases containing fluorine, chlorine or bromine). Examples of climatic relevant aerosol species include sulphates (SO_4^{2-}), nitrates (NO_3^-) elemental carbon (EC) or black carbon (BC) (definitions according to Petzold et al., 2013), organic carbon (OC), sea spray and dust (Seinfeld and Pandis, 2016).

Scientific and public awareness on air quality (related to health and environmental impacts) and climate change has increased dramatically in the past decade (IPCC, 2013). The Intergovernmental Panel for Climate Change (IPCC) conducts studies and compiles a report outlining scientific findings every six years. The latest IPCC Fifth Assessment Report (AR5): Climate Change 2013 concluded that the increase in global average atmospheric temperatures since the mid-twenties is likely to be due to the observed increase in anthropogenic greenhouse gases (GHGs) and aerosols (IPCC, 2013). GHGs and aerosols affect the absorption, scattering and emission of radiation within the atmosphere and at the earth's surface, resulting in positive or negative changes in the energy balance expressed as radiative forcing. Radiative forcing is used to quantify warming or cooling influences (IPCC, 2013). Atmospheric concentrations of GHGs increase when emissions are larger than natural removal processes. Studies show that global atmospheric concentrations of GHG gases such as CO_2, CH_4 and N_2O have increased considerably as a result of human activities since the 1750s, and now far exceed pre-industrial values determined from ice cores spanning thousands of years (IPCC, 2013).

Aerosols alter the earth's energy budget directly by scattering and absorbing radiation, and indirectly by modifying cloud microphysics and lifetime (Bohren and Huffman, 1983; Coakley et al., 1983; Ramanathan et al., 2001). Aerosol BC absorbs infrared radiation causing the earth's atmospheric temperature to increase, resulting in a large positive radiative forcing. In contrast, some aerosol species such as SO_4^{2-} and

NO_3^- act as light scatterers (Schmidt, 2000; IPCC, 2013; Seinfeld and Pandis, 2016) that can reflect radiation back to space, resulting in a cooling effect (Seinfeld and Pandis, 2016).

2.1.1 Air pollution in South Africa

South Africa is a developing country within the African continent, which is among the least studied continents in the world with respect to air quality and climate change (Laakso et al., 2008). In South Africa, air pollution issues were brought to public attention mainly as a result of large-scale annual savannah and grassland fires (Swap et al., 2003) that are endemic to southern Africa as well as concerns over the high emissions from industries, particularly those located on the Mpumalanga (province) Highveld area. A significant fraction of South Africa's coal is mined and consumed by industrial activities, such as coal-fired power generation, petrochemical processing, smelting and manufacturing taking place in this area (Van Tienhoven, 1999; Pretorius et al., 2015). Industrial-related air pollution is also of concern in other areas, such as the Vaal Triangle (Gauteng) and the western Bushveld Complex around Rustenburg/Brits (North West) (Venter et al., 2012). More recently, emissions from household combustion, particularly from in- and semi-formal settlements, have also been identified as problematic in these areas (Venter et al., 2012; Hersey et al., 2015).

With the rapid increase in industries and population growth in South Africa, effective emission control measures are essential to address escalating levels of air pollution in South Africa. However, methodological and data constraints affect air pollution studies on the African continent and in South Africa, despite the good understanding of the controlling mechanisms. The World Bank research study attests that air pollution results in 20 000 premature deaths in South Africa every year; and that this costs the economy nearly R300 million. This study further concluded that, globally, air pollution causes 5.5 million premature deaths each year, thereby making it co-responsible for one in every 10 deaths worldwide (World Bank, 2017). However, in South Africa, inadequate spatial and quantitative data are available for some of the criteria air pollutants covering sources and types, transport, transformations in the atmosphere, deposition and the associated health impacts. Furthermore, the influence of pollution on the regional climate also requires extensive attention, since South Africa is ranked the 13th largest GHG emitter globally and the biggest emitter on the African continent (Van Tienhoven, 1999; IEA, 2016).

2.1.2 Air pollution monitoring in South Africa

In comparison with first-world countries, research and monitoring of air pollution in South Africa have been largely fragmented and uncoordinated, although a substantial amount of information has been collected. Large internationally coordinated campaigns such as SAFARI 1992 and 2000 (Swap et al.,

2002) and smaller campaigns such as EUCAARI (Laakso et al., 2012) have stimulated research locally. Various South African research groups have been/are active in the field of atmospheric sciences at institutions such as the North-West University, Universities of the Witwatersrand, Johannesburg, Cape Town, KwaZulu-Natal, Pretoria and South Africa. South Africa's amended air pollution legislation in 2004 also stimulated activity in this field, resulting in legislation moving away from only regulating point sources to also include ambient air quality (SAAQIS, 2015). This resulted in local governmental bodies becoming active in air quality measurements and control. The Department of Environmental Affairs (DEA) in partnership with the South African Weather Service (SAWS) also became active in conducting measurements complementing industries and research groups' measurements. Bodies such as the National Association for Clean Air (NACA) (http://www.naca.org.za) and South African Society for Atmospheric Sciences (SASAS) (https://ifms.org/ifms/index.cfm/members/south-african-society-for-atmospheric-sciences) have also played an important role over the past couple of decades to promote air quality awareness in the country.

The South African National Environmental Management: Air Quality Act of 2004 (NEM AQA, 2004) is informed by the Bill of Rights contained in the Constitution. According to section 24 of the Constitution, every citizen has the right to an environment that is not harmful to their health or wellbeing. As part of the implementation mechanism of the afore-mentioned act, the South African National Department of Environment Affairs (DEA) declared the Vaal Triangle Airshed, Highveld, and the Waterberg Bojanala areas as three national air quality priority areas in 2006, 2007 and 2012, respectively. The declaration of the first two priority areas came about as a result of poor air quality due to industrial activities, domestic fuel burning, waste burning, mining and metallurgical activities in these areas; while the latter declaration was in line with the precautionary principle of the National Environmental Management Act (Act No. 107 of 1998) due to planned developments for the area. The declaration of the air quality priority areas resulted in a significant increase in measurements of criteria pollutants in these areas, which are reported on the SAAQIS online platform. The spatial extent of the three priority areas is indicated in Figure 2.1.

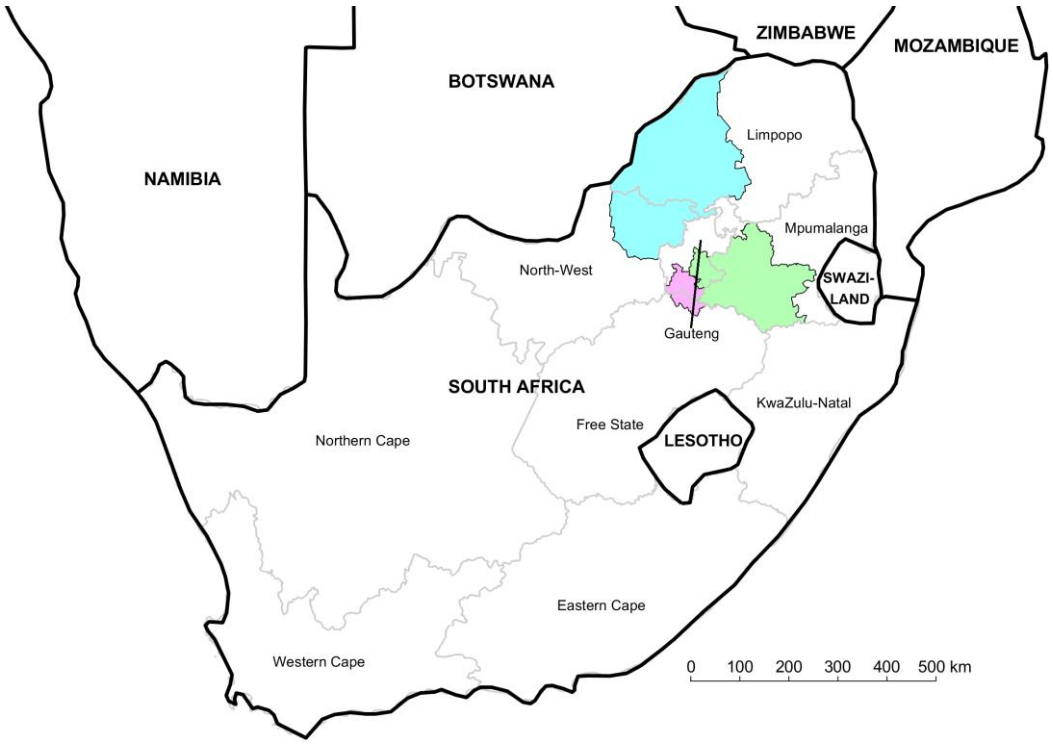

Figure 2.1: Spatial extent of the Vaal Triangle Airshed (blue), Highveld (pink), and Waterberg Bojanala (green) air quality priority areas *(Courtesy: JP Beukes)*

2.2 Climate change

Climate change refers to the variations in the earth's climate over time. It describes changes in the variability or state of the atmosphere or average weather over time scales ranging from decades to millions of years (IPCC, 2007; Seinfeld and Pandis, 2016). Within the context of environmental policy, the term climate change is often used to refer only to the ongoing changes in the modern climate, including the average rise in surface temperature known as global warming. As indicated, GHGs and aerosols significantly contribute to these climatic changes (IPCC, 2013).

The climate of the earth has always been changing, and the causes of this change prior to the industrial revolution were primarily of natural origin. Nowadays, although natural changes in the climate continue to occur, the term climate change is generally used when referring to changes in the earth's climate that have been identified since the early part of the 1900s. Many of the causes of these changes are mainly related to anthropogenic contributions to greenhouse gas and aerosol emissions in the atmosphere. Studies show that the increasing levels of GHGs such as CO_2 are currently changing the climate and are expected to continue to do so throughout the 21st century and beyond (IPCC, 2013). However, there are huge uncertainties about the scale and impacts of climate change, particularly at regional level. On the other hand, there is certainty that climate change is likely to have significant impacts on the global environment

through increases in temperature, increases in sea levels, changes in levels and patterns of precipitation, changes in the severity and frequency of extreme weather events, etc. Additional impacts include the shifting of climatic zones, disruption of ecosystems and of the services that they provide. This threatens habitats and the survival of some plant and animal species (IPCC, 2013; DEA, 2015). Furthermore, communities face various risks and pressures due to climate-related threats to food security, availability of water resources and human health. These communities need to adapt by strengthening their adaptive capacity and enhancing their resilience to these changing climatic conditions, while contributing to efforts towards stabilising atmospheric concentrations of greenhouse gases and aerosols (IPCC, 2013; Seinfeld and Pandis, 2016).

2.2.1 The greenhouse effect and GHGs

The earth's climate is driven by a continuous flow of energy from the sun that arrives predominantly in the form of visible light. Approximately 30% of this light is immediately scattered back into space, and most of the remaining 70% passes down through the atmosphere to warm the earth's surface. The earth then sends this energy back out into space in the form of infrared radiation. GHGs in the atmosphere block this infrared radiation from escaping directly from the surface to space. All GHGs, with the exception of industrial gases, occur naturally and make up less than 1% of the atmosphere. This small percentage of GHGs is enough to produce a natural greenhouse effect that keeps the planet some 30^{o}C warmer than it would otherwise be, which is essential for life (IPCC, 2001; Seinfeld and Pandis, 2016). Figure 2.2 shows a pictorial explanation of the greenhouse effect (IPCC, 2007).

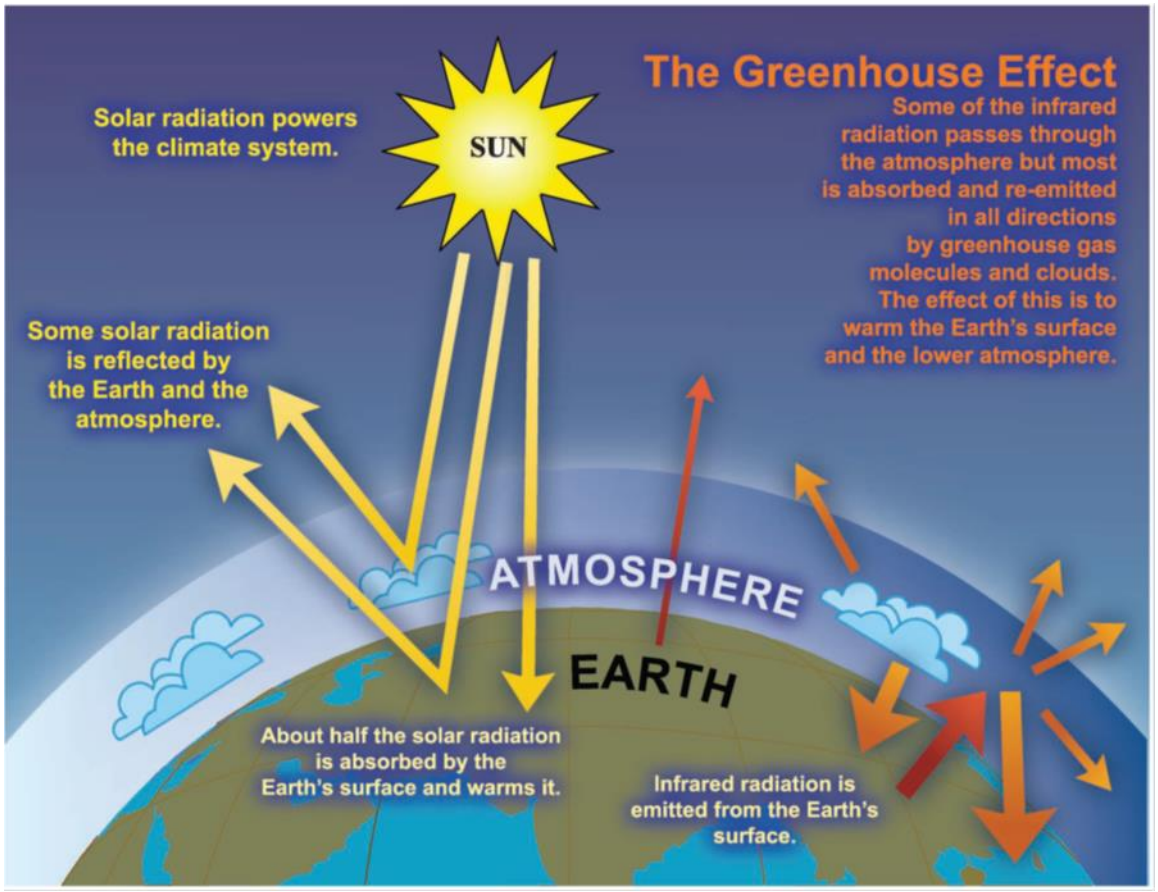

Figure 2.2: The greenhouse effect (IPCC, 2007 FAQ 1.3, Figure 1. Re-printed with permission of the IPCC)

Recent studies show that levels of all key greenhouse gases (with the possible exception of water vapour) and aerosols are rising at an unprecedented rateas a direct result of human activity (IPCC, 2013; IPCC, 2018). Emissions of CO_2 (mainly from combustion of fossil fuels such as coal, oil, and natural gas), CH_4 and N_2O (emitted from agriculture and changes in land use), O_3 and long-lived industrial gases such as CFCs, HFCs, and PFCs are increasing, resulting in influences on how the atmosphere absorbs energy (IPCC, 2013). The climate system must adjust to the rising GHG levels to keep the global energy budget in balance. In the long term, the earth must get rid of energy at the same rate at which it receives it from the sun. Since a thicker blanket of GHGs helps to reduce energy loss to space, the climate must change somehow to restore the balance between incoming and outgoing energy. This adjustment includes the global warming of the earth's surface and lower atmosphere. Warming up is the simplest way for the climate system to get rid of the extra energy. For instance, a small rise in temperature will be accompanied by changes in cloud cover and wind patterns, where some of these changes may act to enhance the warming (i.e. positive feedbacks) or counteract it (i.e. negative feedbacks) (IPCC, 2007; IPCC, 2013; Seinfeld and Pandis, 2016).

CO_2 emitted from both natural and anthropogenic sources is responsible for over 60% of the enhanced greenhouse effect (Seinfeld and Pandis, 2016). Figure 2.3 shows monthly mean CO_2 concentration levels

measured at Mauna Loa Observatory, Hawaii (IPCC, 2013), which clearly indicate a significant increase over time. CO_2 produced by human activity enters the natural carbon cycle. Billions of tonnes of carbon are exchanged naturally each year between the atmosphere, oceans and land vegetation; and these exchanges coupled with complex natural system are accurately balanced. In the 219 years since 1800, carbon dioxide levels have risen by over 40%. Even with half of man-made CO_2 emissions being absorbed by the oceans and land vegetation, atmospheric levels continue to rise by over 10% every 20 years (USEPA, 2012; IPCC, 2013; IPCC 2018).

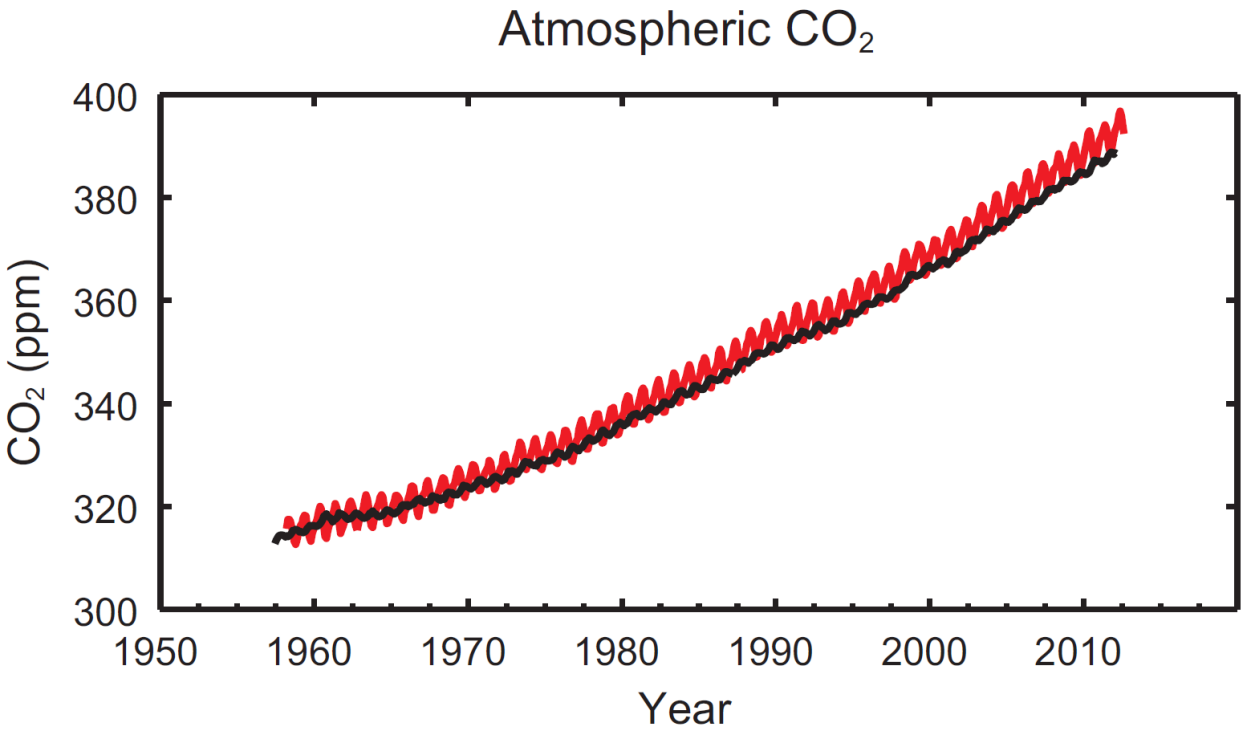

Figure 2.3: Monthly mean carbon dioxide measured at Mauna Loa Observatory, Hawaii (IPCC, 2013)

Levels of CH_4 have increased by a factor of two and a half during the industrial era, with agricultural activities (mainly flooded rice paddies and expanding herds of cattle) as a significant source of this important GHG. Emissions from landfills (waste dumps), and leaks from coal mining and natural gas production also contribute to CH_4 levels in the atmosphere (Seinfeld and Pandis, 2016). CH_4 is removed from the atmosphere by chemical reactions that are often difficult to model and predict. Methane from historical emissions currently contributes 20% of the enhanced greenhouse effect. The rapid rise in CH_4 levels started recently compared to CO_2, and its contribution to the greenhouse effect is likely going to increase at an unprecedented rate since it is a stronger greenhouse gas than CO_2 (UNEP and UNFCCC, 2002; IPCC, 2013).

Water vapour is the largest contributor to the natural greenhouse effect (IPCC, 2013; Seinfeld and Pandis, 2016), and its presence in the atmosphere is not directly affected by human activity. Nevertheless, water vapour matters for climate change due to its contribution to the positive feedback. Warmer air can hold more moisture, and models predict that a small global warming would lead to a rise in global water vapour levels, further adding to the enhanced greenhouse effect. Given the fact that modelling climate processes involving clouds and rainfall is challenging, the exact size of this feedback remains uncertain (Seinfeld and Pandis, 2016).

2.2.2 Climatic effect of atmospheric aerosols

Atmospheric aerosols are defined as a suspension of the fine solid or liquid particles in a gas, and are characterised by a particle size distribution (PSD) function. Aerosol science is the rapidly expanding field focusing on investigating the physical, chemical, and biological properties of aerosolised materials (airborne particles or liquids), which behave in ways that make them different from other forms of similar materials. Aerosols are generally classified according to their size, e.g. PM_{10} (aerodynamic diameter ≤ 10 μm), $PM_{2.5}$ (aerodynamic diameter ≤ 2.5 μm), PM_1 (aerodynamic diameter ≤ 1 μm) and $PM_{0.1}$ (aerodynamic diameter ≤ 0.1 μm) (Slanina and Zhang, 2004; Pöschl, 2005). The atmospheric science interest regarding aerosols revolves around their sources, concentrations, size, formation methods, transport, deposition and impacts. Aerosols are emitted from both natural (e.g. volcanic eruptions, natural forest, savannah and grassland fires, vegetation, and sea salt) and anthropogenic (e.g. household combustion, combustion of fossil fuels and various industrial processes,) sources. In addition, aerosols can be primary (directly emitted, e.g. dust), or secondary (e.g. oxidation of SO_2 to form SO_4^{2-}) (Seinfeld and Pandis, 2016).

Atmospheric aerosol composition includes wind-blown dust particles (e.g. pollen, bacteria, smoke, ash, and sea salt), black carbon (BC), organic carbon (OC), sulphates (SO_4^{2-}), nitrates (NO_3^-), ammonium (NH_4^+) and trace metal species, among others. The baseline of uncertainty in aerosol radiative forcing, i.e. climatic impact, is relatively large if compared to that of the greenhouse gases (Slanina and Zhang, 2004; IPCC, 2013). Apart from climate change, aerosols also pose adverse impacts on the environment, air quality and human health (IPCC, 2001; Seinfeld and Pandis, 2016). All these impacts are determined by the physical (e.g. size, shape, etc.) and chemical properties of aerosols. Aerosol species are removed from the troposphere on a time-scale of days to weeks (depending on their size and composition), primarily by wet scavenging and secondarily by dry deposition, resulting in spatially inhomogeneous distributions. Aerosols pose the second highest influence on climate after CO_2, by scattering sunlight back into space and by affecting clouds. They can block sunlight and provide seeding for the formation of clouds, resulting in a cooling effect. Over heavily industrialised regions, aerosol cooling may counteract nearly all the warming effects due to greenhouse gases (Seinfeld and Pandis, 2016). For instance, oxides of sulphur and nitrogen emissions from fossil fuels combustion and the burning of organic material produce microscopic

particles that can reflect sunlight back into space and also affect clouds. Since aerosols remain in the atmosphere for a relatively short time (days to weeks) compared to the long-lived greenhouse gases, their cooling or warming effect is mainly localised. They are also associated with acid rain and poor air quality (IPCC, 2001; Seinfeld and Pandis, 2016).

Specifically, aerosol particles affect the climate directly, by absorbing and scattering solar and infrared radiation in the atmosphere (Twomey, 1974; Seinfeld and Pandis, 2016). Aerosol particles that absorb radiation result in a warmer atmosphere. The result of the scattering of sunlight caused by aerosol particles is an increase in the amount of light reflected back into space, which results in a decrease in the amount of solar radiation that reaches the earth's surface (Nieuwenhuijsen, 2003). The indirect effect of aerosol particles is complex and difficult to assess. Changes in the numbers of concentration of atmospheric aerosols result in variations in the population and size of cloud droplets, for a set amount of water available for cloud formation. If enough aerosols, serving as cloud condensation nuclei CCN, are present, water can form large droplets within the clouds that could result in precipitation as a major removal mechanism for aerosols from the atmosphere. On the other hand, excess particulate matter in the atmosphere causes water to condense onto the particles resulting in smaller droplets in the clouds that increase the cloud albedo, leading to a decrease in precipitation. This suppression of precipitation results in excess water vapour remaining in the atmosphere (IPCC, 2001).

2.2.3 Impacts of atmospheric aerosols on the climate system

The direct and indirect radiative effects of aerosol particles constitute the largest uncertainty in current radiative forcing estimates of the earth's climate system. In order to reduce the uncertainties associated with atmospheric aerosols in climate systems, detailed information on the temporal and spatial variability of different aerosol properties is required. Such information can be obtained from a combination of continuous in-situ aerosol measurements, model simulations and remote sensing (Foster et al., 2007; Hansen et al., 2007 (b)).

Aerosols absorb and scatter solar and terrestrial radiation, which is quantified as the single scattering albedo (SSA). SSA tends to unity if scattering dominates with relatively little absorption and decreases as absorption increases – thereby becoming zero for infinite absorption. For example, sea-salt aerosol has an SSA of 1 and scatters radiation, whereas soot has an SSA of 0.23, showing that it is a major atmospheric radiationabsorber (IPCC, 2013). The chemical composition of aerosols directly affects the overall refractive index that determines how much light is scattered and absorbed (Coakley and Cess, 1985; Kim and Ramanathan, 2008; Gautam et al., 2009; Moorthy et al., 2009).

Natural and anthropogenic substances and processes that alter the earth's energy budget are drivers of climate change. Radiative forcing (RF) quantifies the change in energy fluxes caused by changes in these drivers that can be either positive or negative (IPCC, 2013). Positive RF leads to surface warming, while negative values lead to surface cooling. In climate science, RF is generally defined as the change in net irradiance between different layers of the atmosphere estimated based on in-situ and remote observations, properties of greenhouse gases and aerosols, and calculations using numerical models representing observed processes (IPCC, 2013). Therefore, RF of the surface-troposphere system due to the perturbation in or the introduction of an agent (such as change in greenhouse gas concentrations) is the change in net (down minus up) irradiance (solar plus long-wave in Wm^{-2}) at the tropopause after allowing for stratospheric temperatures to readjust to radiative equilibrium, but with surface and tropospheric temperatures and state held fixed at the unperturbed values (IPCC, 2001).

In simple terms, RF is the rate of energy change per unit area of the globe as measured at the top of the atmosphere (Rockstrom et al., 2009). Within the context of climate change, the term forcing is restricted to changes in the radiation balance of the surface-troposphere system imposed by external factors, with no changes in stratospheric dynamics, no surface and tropospheric feedbacks in operation (i.e. no secondary effects induced because of changes in tropospheric motions or its thermodynamic state), and no dynamically-induced changes in the amount and distribution of atmospheric water (vapour, liquid, and solid forms) (IPCC, 2001; IPCC, 2013; Rockstrom et al., 2009). According to the fifth Intergovernmental Panel on Climate Change Assessment Report (AR5) (2013), the RF value due to greenhouse gases may be determined to a reasonably high degree of accuracy. However, uncertainties relating to aerosol radiative forcings remain large and mostly rely on estimates from global modelling studies, which are currently difficult to verify (IPCC, 2013).

Figure 2.4 shows graphic contributions (at 2000, relative to pre-industrial) and uncertainties of various forcing species expressed in watts per square metre (Wm^{-2}). A positive forcing (more retained energy) tends to warm the climate system, while a negative forcing (more outgoing energy) tends to cool it. The term RF has been used in the IPCC assessments with a specific technical meaning to denote an externally imposed perturbation in the radiative energy budget of earth's climate system, which may lead to changes in climate parameters. The RF of the total aerosol effect in the atmosphere, which includes cloud adjustments due to aerosols, is –0.9 [–1.9 to −0.1] Wm^{-2} (medium confidence), and results from a negative forcing from most aerosols and a positive contribution from BC absorption of solar radiation. There is high confidence that aerosols and their interactions with clouds have offset a substantial portion of global mean forcing from well-mixed greenhouse gases. They continue to contribute the largest uncertainty to the total RF estimate (IPCC, 2013).

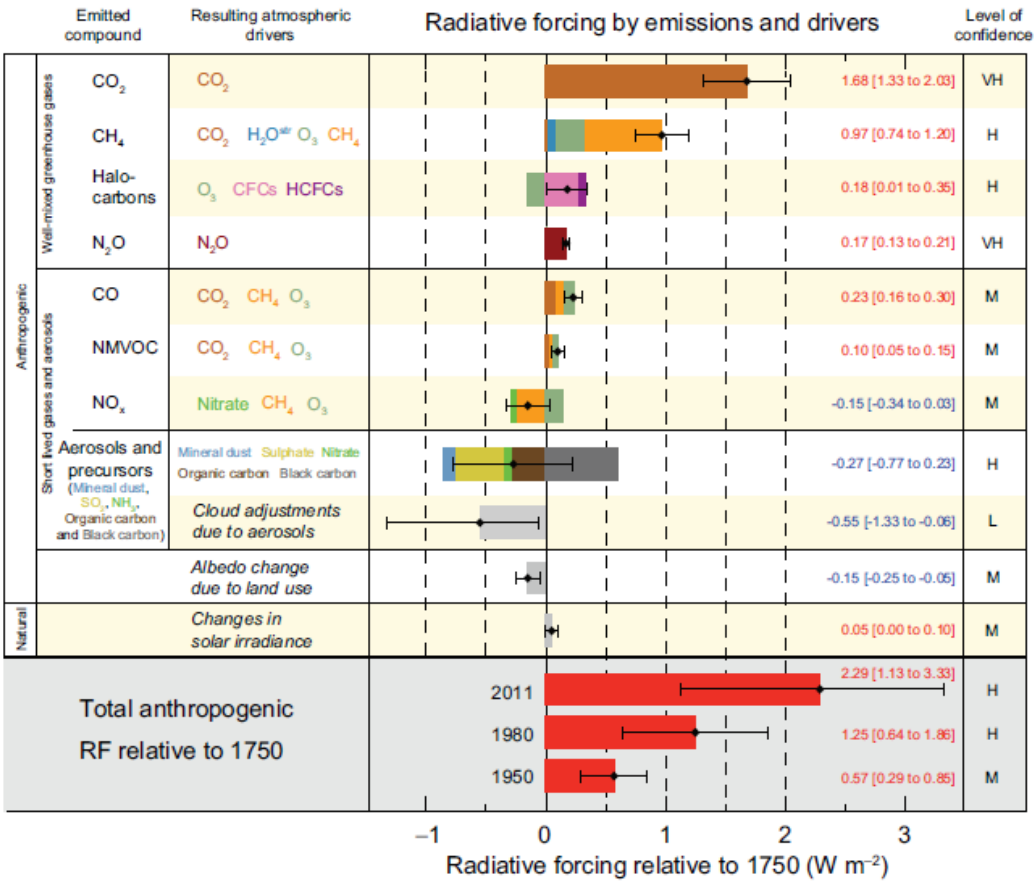

Figure 2.4: Radiative forcing estimates in 2011 relative to 1750 and aggregated uncertainties for the main drivers of climate change. Values are global average radiative forcing (RF14), partitioned according to the emitted compounds or processes that result in a combination of drivers. The best estimates of the net radiative forcing are shown as black diamonds with corresponding uncertainty intervals; the numerical values are provided on the right of the figure, together with the confidence level in the net forcing (VH – very high, H – high, M – medium, L – low, VL – very low). Albedo forcing due to black carbon on snow and ice is included in the black carbon aerosol bar. Small forcings due to contrails (0.05 Wm^{-2}), including contrail-induced cirrus, and HFCs, PFCs and SF_6 (total 0.03 Wm^{-2})) are not shown. Concentration-based RFs for gases can be obtained by summing the like-coloured bars. Volcanic forcing is not included as its episodic nature makes is difficult to compare to other forcing mechanisms. Total anthropogenic radiative forcing is provided for three different years (i.e. 2011, 1980 and 1950) relative to 1750 (IPCC, 2013)

2.3 Aerosol black carbon

Aerosol black carbon (BC) is the most strongly light-absorbing component of particulate matter (PM), emitted from both natural and anthropogenic sources directly into the atmosphere during incomplete combustion of fossil fuels, biofuel, and biomass (Bond, 2013; IPCC, 2013; Seinfeld and Pandis, 2016). It is emitted directly in the form of fine particles (mostly as $PM_{2.5}$), and is the carbonaceous fraction of ambient particulate matter that contains a significant fraction of elemental carbon (EC), with the remaining typically being highly polymerised organic material that has low hydrogen to carbon, and oxygen to carbon ratios (Seinfeld and Pandis, 2016; Cachier, 1995). However, the contribution of EC to BC can be higher closer to sources, such as traffic. BC is a major contributor to the fine particulate matter in the atmosphere and is almost solely responsible for the short-wave absorption of solar radiation caused by aerosol particles. BC can also be defined as the carbonaceous material having intense black or dark colour, which absorbs visible light efficiently (Hansen et al., 1984; Cachier, 1995; USEPA, 2012(a)). BC should be distinguished from organic carbon (OC), which is mostly reflective. However, as previously indicated, BC can contain certain OC species.

According to Pope (2001), approximately 20% of global BC is emitted from residential biofuel burning and 40% from fossil fuels (of which 14% are diesel engines for transportation; 10% from diesel engines for industrial use; 10% from industrial processes and power generation, usually from smaller boilers; and 6% residential coal burned with traditional technologies). The remaining 40% are emitted from open biomass burning (mostly forest and savanna fires). While biomass burning may be the dominant BC source over tropical regions and most of the southern hemisphere (Hansen et al., 1988; Cooke and Wilson, 1996; Wolf and Cachier, 1998), the contribution of fossil fuel combustion to BC is usually more important in cities, particularly over the northern hemisphere.

BC is a good indicator of primary anthropogenic air pollutants because of its shorter lifetime (days to weeks) in the atmosphere (Penner et al., 1993; Cachier, 1995; Cooke and Wilson, 1996). It is critical to highlight that BC sources vary by region. For instance, the majority of BC emissions in South Asia are due to biofuel used for cooking, whereas in East Asia, coal combustion for residential and industrial use is the main contributor. According to Ramanathan (2008), a reduction in BC emissions is a potential viable climate change mitigation strategy (Mokdad, 2004), since it is a primary species emitted by sources that can be controlled.

Additionally, the term black carbon is also used in soil sciences and geology referring either to deposited atmospheric BC or to directly incorporated BC from vegetation fires (Schmidt and Noack, 2000; Glaser, 2007). This type of BC significantly contributes to soil fertility, since it is able to adsorb important plant nutrients, particularly in the tropics. Large uncertainties prevail in terms of the global atmospheric radiative effect of BC due to insufficient data and its high spatial and temporal variability. Presently, the majority of BC radiative impact assessments are based on models (Zhou et al., 2006; USEPA, 2012; IPCC, 2013),

on both local and global scales, and incorporate measured aerosol properties (Harrison et al., 1997; Satheesh et al., 1999).

2.3.1 Climate forcing and climatic impacts of aerosol black carbon

The scientific understanding of the role of BC in climate change lags behind compared to carbon dioxide and other greenhouse gases. However, this gap appears to be closing as global research on BC has recently shown to be expanding rapidly (e.g. Shen, 2012; IPCC, 2013; Wang, 2014). BC is normally emitted with other particles and gases such as sulphur dioxide (SO_2), nitrogen oxides (NO_x), and organic carbon (OC) as co-emitted pollutants, with some of them exerting a cooling effect on the climate. Estimates of the net effect of BC emission sources on climate should take into account the offsetting effects of these co-emitted pollutants. Atmospheric processes such as mixing, aging, and coating that occur after BC is emitted can also contribute to the net influence of BC on climate. The short atmospheric lifetime of BC (days to weeks) coupled with the mechanisms by which it affects the climate differentiates it from long-lived carbon dioxide (CO_2). Reducing black carbon emissions may be the fastest means of slowing global warming and climate change in the near-term (Lippmann et al., 2003; USEPA, 2012; Bond, 2013; IPCC, 2013), whereas reductions in GHG emissions will take longer to influence atmospheric concentrations and will have less impact on climate on a short timescale. However, extensive reductions in GHG emissions are essential to limit climate change over the long term. Emission sources and ambient BC concentrations vary spatially and temporally, resulting in climate effects that are more regionally and seasonally dependent compared to the effects of other long-lived and well-mixed GHGs such as CO_2. It is therefore acknowledged that mitigation efforts for BC will produce different climate results depending on the region, season, and emissions sources. BC influences the climate through the following mechanisms, similar to the general mechanisms previously mentioned for aerosols in general (Seinfeld and Pandis, 2016):

- *Direct effect*: by absorbing both incoming and outgoing radiation of all wavelengths contributing to warming of the atmosphere and dimming at the surface; whereas, GHGs trap the outgoing infrared radiation from the earth's surface.
- *Snow/ice albedo effect*: whereby BC deposited on snow and ice darkens the surface and decreases reflectivity (albedo), thereby increasing absorption and accelerating melting of ice.
- *Other effects*: Similar to the indirect effects of general aerosols, BC also alters the properties and distribution of clouds, affecting cloud reflectivity and lifetime ('indirect effects'), stability ('semi-direct effect'), and precipitation.

The above-mentioned influencing mechanisms are graphically illustrated in Figure 2.5. The direct and snow/ice albedo effects of BC are widely understood to lead to climate warming. These combined effects likely also contribute more to current warming than any GHG other than CO_2 and CH_4. However, it is

critical to note that the climate effects of BC, via interaction with clouds, are more uncertain, and their net climate influence is not yet clear (IPCC, 2013; USEPA, 2012(b)).

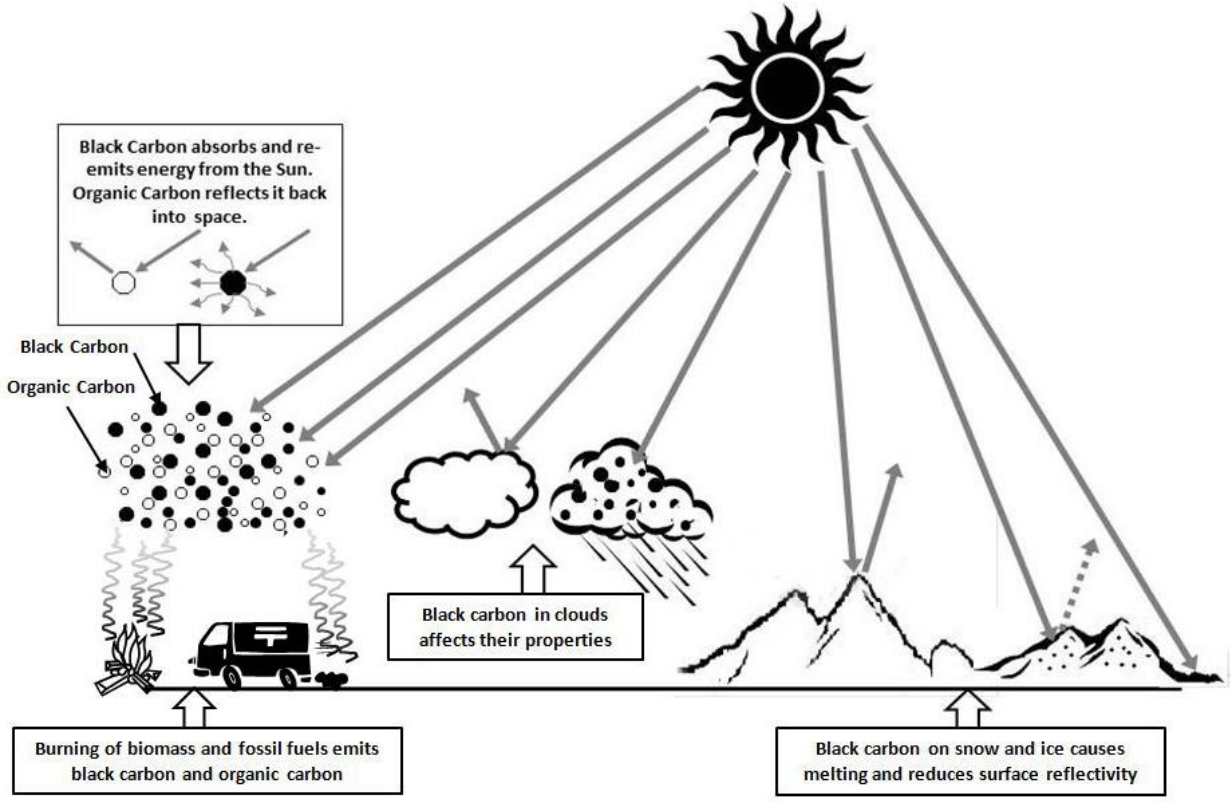

Figure 2.5: The impacts of aerosol black carbon on the global climate (Michael, 2011)

BC from fossil fuels was estimated by the IPCC in the Fifth Assessment Report (AR5) to contribute a global mean radiative forcing of +0.2 Wm^{-2}, compared to the +0.1 Wm^{-2} estimated in the Second Assessment Report (SAR) with a range +0.1 to +0.4 Wm^{-2} (IPCC, 1995; IPCC, 2013). Close to European and North American cities, industrial combustion plants usually have efficient cleaning facilities for particulate emissions. According to Hamilton and Mansfield (1991), more than 90% of BC originates from traffic emissions, particularly diesel vehicles that are known to emit EC (Watson et al., 1994) with a large mass fraction in the ultrafine (diameter of 0.1 μm) particle size range in most European cities (Kerminen et al., 1997). In addition to having a direct warming effect on the atmosphere, BC also affects cloud albedo and formation by changing the hygroscopicity of cloud condensation nuclei (Penner et al., 1991; Liousse et al., 1996). It has been suggested that the increasing level of BC in the atmosphere is an important driver in the observed trends of increased rainfall in the south and drought in the north of China over the past several decades (Menon et al., 2002). Evidence also suggests that large BC emissions in India and China contributed to shifts in the regional monsoon.

The direct radiative forcing effect of BC is augmented by deposition of BC on snow and ice. The snow albedo effect from BC has been estimated in recent studies to add approximately +0.05 Wm^{-2}, which is generally less than the +0.1 (±0.1) Wm^{-2} estimated by the IPCC (AR4). However, UNEP and WMO (2012) found that when the snow/ice albedo forcing estimates are adjusted to account for the greater warming efficacy of the snow deposition mechanism, the snow/ice albedo effect could add +0.05 to +0.25 Wm^{-2} of forcing. The sum of the direct and snow/ice albedo effects of BC on the global scale is likely comparable to, or larger than the forcing effect from methane, but less than the effect of carbon dioxide.

Findings from various studies (Hansen, 2005; Bond et al., 2013; IPCC, 2013) show that estimates of black carbon's climate forcing (combining both direct and indirect forcings) vary from the IPCC's conservative estimate of + 0.23 + 0.25 Wm^{-2} (Novakov et al., 1974; Chang and Novakov, 1975), to the most recent estimate of 1.0 -1.2 Wm^{-2}. This is larger than the forcing due to other GHGs such as CH_4, CFCs, N_2O, or tropospheric ozone (Nieuwenhuijsen, 2003). According to Ramanathan's (2008) global assessment, the forcing from black carbon equals 0.9 Wm^{-2}, which is more than the forcing from methane and it is 55% of that from CO_2 (Michael, 2010). Assessments by UNEP and WMO (2012) presented a narrower central range of +0.3 to +0.6 Wm^{-2} compared to the IPCC estimate of +0.34 (±0.25) Wm^{-2} (IPCC, 2007, USEPA, 2012). However, in some regions such as the Himalayas, the impact of black carbon on melting snowpacks and glaciers may be equal to that of CO_2. Findings from studies by Shindell (2008), who used a coupled ocean-atmosphere climate model to reconstruct twentieth-century influences on climate or forcings, with and without black carbon, found that increases in black carbon from Asia and reductions in sulphate pollution contributed to approximately 45% of the observed warming in the Arctic. This is critical because nothing in climate is more properly described as a tipping point than the 0°C boundary that separates frozen from liquid water. The bright, reflective snow and ice is in contrast to the dark heat-absorbing ocean (Adgate, 2011). Therefore, reducing black carbon emissions may be the most efficient way to mitigate the well-known Arctic warming (USEPA, 2012).

Recent studies by Myhre and Samset (2015) indicate underestimation of the positive radiative forcing (RF) of BC by 10% for global mean, all sky conditions, relative to the more sophisticated multi-stream models. RF of black carbon (BC) in the atmosphere is estimated using radiative transfer codes of various complexities. The two-stream radiative transfer codes used most in climate models give too strong forward scattering, leading to enhanced absorption at the surface and too weak absorption by BC in the atmosphere. This underestimation occurs primarily for low surface albedo, even though BC is more efficient for absorption of solar radiation over high surface albedo (Myhre and Samset, 2015).

2.3.2 Black carbon effects on human health and the environment

BC is a component of both fine and coarse PM. However, due to its small size, it is strongly associated with the fine particle ($PM_{2.5}$) fraction. Most of the literature evaluating the potential impacts of BC on human health as well as the health benefits of BC mitigation has focused on BC as part of $PM_{2.5}$. Short- and long-term exposures to $PM_{2.5}$ are associated with various adverse human health effects such as respiratory and cardiovascular effects, premature death, etc. Over the past decade, studies have focused increasingly on attempting to identify the health impacts of particular $PM_{2.5}$ constituents, such as BC (USEPA, 2012). However, EPA has determined that there is insufficient information at present to differentiate the health effects of the various constituents of $PM_{2.5,}$ thereby assuming that many constituents are associated with adverse health impacts (USEPA, 2012(a)). Studies show that black carbon, largely from combustion processes, contributes to poor air quality and induces respiratory and cardiovascular problems (Highwood and Kinnerslay, 2006).

The limited scientific evidence that is currently available about the health effects of BC is generally consistent with the general $PM_{2.5}$ health literature, with the most consistent evidence for cardiovascular effects. However, review studies undertaken by Janssen et al. (2011) found health effect estimates from mortality and morbidity time series studies and cohort studies to be higher for black carbon particles than for PM_{10} or $PM_{2.5}$ when expressed for a 1 μgm^{-3} increase in exposure. This shows that study results for BC are variable and that detailed research is required to address these uncertainties. Both ambient and indoor $PM_{2.5}$ is estimated to result in millions of premature deaths worldwide, the majority of which occur in developing countries. The World Health Organization (WHO) estimates that indoor smoke from the combustion of solid fuels is among the top ten major risk factors globally, contributing to approximately 2 million deaths annually, with women and children at a higher risk (WHO, 2017).

According to assessment approaches undertaken by the WHO and EPA, the health impacts of black carbon are considered equivalent to PM health impacts, and recent reports recognise associations between BC and a continuum of cardiovascular and respiratory effects. However, these studies conclude that it is not currently possible to distinguish the health impacts of BC from $PM_{2.5}$ (Janssen et al., 2012; U.S. EPA, 2012). Toxicological studies suggest that BC in its pure form may not be toxic, but it may function as a carrier of toxins to the lungs, the body's major defence cells, and possibly the blood circulation system (Janssen et al., 2012). Therefore, based on the evidence that black carbon is an efficient transporter of toxic compounds into the lungs, a strategy to reduce black carbon emissions from diesel vehicles (and by implication, particulate matter) would produce health benefits.

2.4 Black carbon emission reduction measures

Considering the link between $PM_{2.5}$ and BC, explained in the previous section, emission reduction of the former will automatically result in a reduction in the latter. For large industrial point sources, this implies process improvements (having lower emissions), installing of and improving abatement technologies (to capture PM), strict emission standards, compliance monitoring and enforcement of standards. Measures such as these can be regulated. However, it is less easy to regulate biomass burning fires and household combustion, both of which are also significant sources of BC. Reduction of BC emissions from vehicles can be achieved using various measures, including improved technology, introduction of standards, replacing older engines, using cleaner fuels, reducing idling time, and ensuring proper maintenance (EPA, 2006; EPA 2012 a and b; EC, 2015).

According to Ramanathan (1998), technology exists for a drastic reduction of fossil fuel-related black carbon. Studies assert that given proper conditions and incentives, soot emitting technologies can be rapidly phased out. For instance, several effective technologies are available to reduce BC emissions from diesel vehicles. In addition, diesel oxidation catalysts that can be used on almost any diesel vehicle have been in use for over 30 years and can eliminate 25 to 50% of black carbon emissions (Hansen and Makiki, 2001). Furthermore, newer and efficient diesel particulate filters (DPFs) or traps can eliminate over 90% of black carbon emissions from motor vehicles that use ultra-low sulphur diesel fuel (ULSD). The United States Environmental Protection Agency (US EPA) requires a nationwide shift to ULSD to ensure compliance with new particulate rules for new on-road and non-road vehicles, and introduced legislation on the use of DPFs in diesel vehicles in order to meet the standards. Due to recent EPA regulations, BC emissions from diesel vehicles are expected to decline by approximately 70 percent from 2001 to 2020 (Hansen and Nazarenko, 2007(a)). Overall, BC emissions in the United States are projected to decline by 42 % from 2001 to 2020 (Hansen and Makiki, 2001), as a result of the implementation of these regulations.

2.5 Benefits of reducing black carbon emissions

Mitigation of BC offers a clear opportunity where continued reductions in BC emissions can provide significant near-term benefits for climate, human health, and the environment (Bond and Sun, 2005). It is generally impossible to reduce BC in isolation from other co-pollutants, and most BC mitigation strategies involve reductions in total emissions of fine particles, including other $PM_{2.5}$ constituents. All control measures that reduce $PM_{2.5}$ pollution, BC and other constituents will achieve substantial health, environmental and climate change mitigation benefits. Therefore, mitigation strategies targeting BC that also reduce total direct $PM_{2.5}$ emissions could potentially result in hundreds of thousands of avoided economic losses and premature deaths among communities, resulting in large health benefits (Seinfeld and Pandis, 2016).

According to U.S. EPA (2012), the benefits from controlling direct $PM_{2.5}$ emissions are 7 to 300 times greater than the benefits per ton estimated for reductions of PM precursors such as NOx and SOx. The magnitude of human health benefits of emission reductions depends both on how much exposure is reduced, as well as the size of the affected population. The largest health benefits from $PM_{2.5}$ including BC control strategies will be achieved in areas near the emissions sources and where exposure affects a large population (USEPA, 2012).

Studies by Bond and Sun (2005) demonstrated benefits of BC reduction on the mitigation of climate change; and found that many BC emission reductions measures are less expensive and/or easier to endorse/implement if compared with greenhouse gases. These studies further proposed the role of black carbon in climate mitigation strategies and show that reducing BC emissions is a promising way to reduce climatic interference, as well as adverse impacts on health and regional air quality.

2.6 Global and regional black carbon studies

Interest in black carbon emerged in the 1980s following studies on light reflective properties of snow by Warren and Wiscombe (1980), after experiencing difficulties in developing a mathematical model of snow reflectance or albedo. This study found that calculations could not align with the latest albedo measurements in the Arctic due to snow reflecting less light than expected. In this study, snow samples collected downwind from a diesel generator that might be contributing to black carbon were analysed. Other studies concluded that black carbon soot could have a measurable effect on the Arctic climate (Rosen and Hansen., 1985). Further studies by Hansen et al. (1984) concluded that the fastest way to combat global warming was to reduce black carbon, methane and other powerful warming pollutants that could be controlled and reduced easier than CO_2 (Rosen and Hansen, 1985). Regional sources indicate that developed countries were once the primary source of black carbon emissions, but this trend started changing during the 1950s as a result of the adoption of pollution control technologies by these countries. The U.S. was found to be contributing approximately 21% of the world's CO_2, while accounting for 6.1% of the world's soot (US Department of Energy, 1985).

Various recent studies found that the majority of black carbon emissions are from developing countries and this trend is expected to increase (Jacobson, 2004; Ramanathan and Carmichael, 2008). The largest sources of black carbon are Asia, Latin America, Africa, China and India (IPCC, 2013; Wang, 2014). Emissions from China have doubled from 2000 to 2006 (Jacobson, 2004b) and were estimated to account for approximately 30% of global anthropogenic BC emissions (Bond et al., 2004). These high emission levels were mainly attributed to high rates of consumption of coal and biofuels in this country (Bond et al., 2013). Furthermore, annual emissions of BC in China were estimated to be 1.3 Tg in 1995 (Bond et al., 2004), 1.1 Tg in 2000 (Streets et al., 2003a, b) and 1.8 Tg in 2006

(http://www.cgrer.uiowa.edu/EMISSION_DATA_ new/index_16.html, accessed: June 2018). These estimates are subject to large uncertainties because of the difficulty in obtaining accurate data on activity and emission factors for some emission sources. For instance, the level of uncertainty was approximately 800% for 1995 and 484% for 2000, for anthropogenic sources (at a 95% confidence interval). Although recent inventories have reduced this level of uncertainty, improvement is necessary (Streets et al., 2003).

Existing and well-tested technologies used by developed countries, such as clean diesel and coal could be implemented in developing countries to reduce black carbon emissions (Jacobson, 2004). According to Jacobson (2002), black carbon emissions peak close to major source regions and give rise to regional hotspots of these emissions. Such hotspots include the Indo-Gangetic plains in South Asia, eastern China, most of Southeast Asia, including Indonesia, regions of Africa between sub-Sahara and South Africa, Mexico and Central America, and most of Brazil and Peru in South America (Hansen and Sato, 2001). China is a major emitter of carbonaceous aerosols (Saikawa et al., 1999; Cao et al., 2006) and sulphur dioxide (SO_2) (Streets et al., 2003). Despite its rapid industrial growth, China has passed and continues to develop many environmental regulations (Liu and Diamond, 2005). However, future emissions remain highly uncertain and are of interest for regional and global air quality and climate change. Most emissions of SO_2, OC and BC in China result from fossil fuel and biofuel combustion (Ohara et al., 2007). In addition, the two most important sources of atmospheric black carbon are fossil fuel combustion (such as automobile exhaust, industrial and power plant emissions, aircraft emissions, etc.) and biomass burning (burning of agricultural wastes and forest fires) (Saha and Despiau, 2001). While biomass burning may be the dominant BC source over tropical regions and most of the southern hemisphere, the role of fossil fuel combustion is usually more important in cities, especially over the northern hemisphere. Knowledge of long-term changes in BC is vital for the assessment of its regional and global climate effect, and measurements have been carried out in the remote and marine environments (Cooke et al., 1997). However, limited long-term measurements exist from certain source regions.

2.7 Global BC measurements

To date, several field experiments and campaigns have been carried out in recent years such as Smoke, Clouds, Aerosols, Radiation-Brazil (SCAR-B), Tropospheric Aerosol Radiative Forcing Observational Experiment (TARFOX), Aerosol Characterisation Experiment – Asia (ACE-Asia), Indian Ocean Experiment (INDOEX), Experience sur Site pour Contraindre les Modeles de Pollution atmospherique et de Transport d'Emissions (ESCOMPTE), Mediterranean Intensive Oxidant Study (MINOS), etc. However, most of these experiments provide only snapshot information and data for limited periods. Additional studies are necessary to obtain a more complete picture of the global distribution of aerosol BC in the atmospheric boundary layer (Cooke et al., 1997).

Globally, very few countries have robust networks for ambient measurements of $PM_{2.5,}$ (and probably even fewer for BC measurement) with the most available global ambient BC data being produced in the United States, Canada, Europe and China. However, the majority of the data is based on the more widely used thermal measurement techniques, with limited light absorption measurements available to supplement them, particularly in the United States and Europe. In addition, there are networks of BC monitoring sites across the globe in remote areas that provide information about background levels. Figure 2.6 provides a map showing the extent of known BC monitoring networks around the globe, highlighting locations of the sites that use light absorption, thermal, or both measurement techniques (USEPA, 2012). According to this published map, BC was monitored in South Africa at the Global Atmospheric Watch site at Cape Point in 2012, as well as EC that was monitored during a campaign on the Mpumalanga Highveld. However, the monitoring network for BC and EC in South Africa has expanded significantly since, as articulated in the next section.

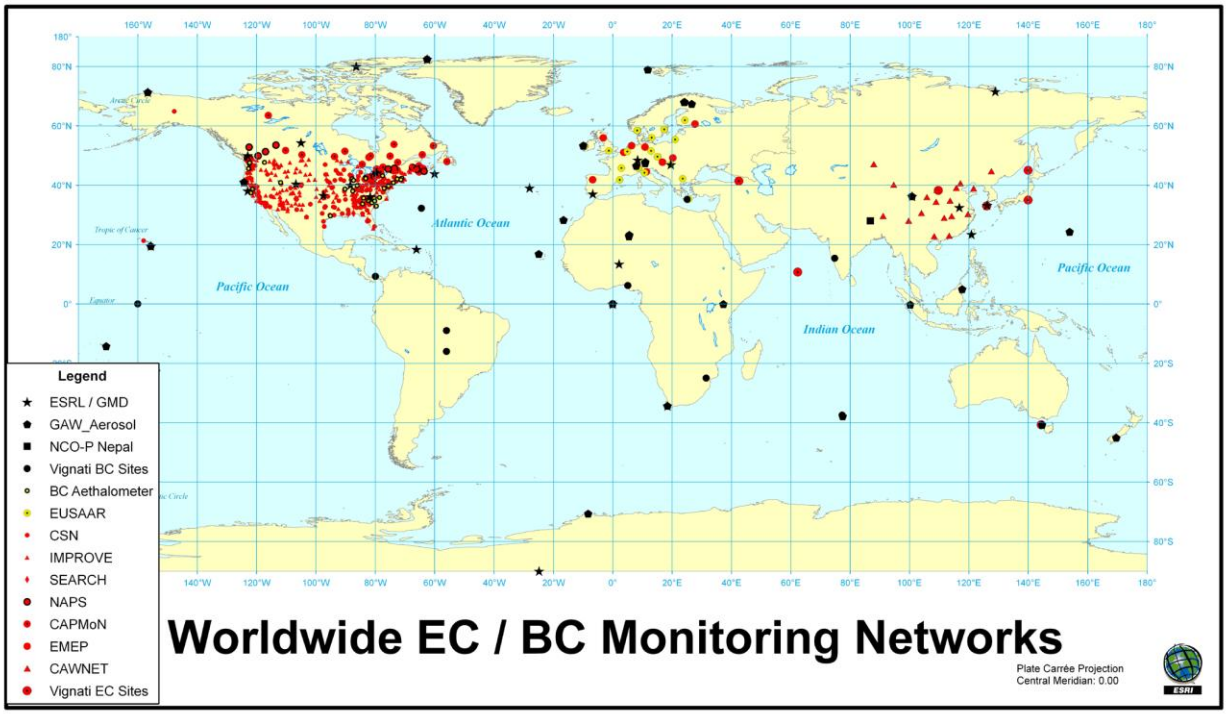

Figure 2.6: Ambient EC and BC measurement locations worldwide, with light absorption measurement locations and thermal measurement locations coloured black and red, respectively. A small subset of locations with both measurements is coloured yellow (USEPA, 2012)

2.8 BC measurements in South Africa

Limited equivalent black carbon (eBC)monitoring is currently undertaken by various institutions in South Africa, including the national Department of Environmental Affairs (DEA) and the South African Weather Service (SAWS), the North-West University and Eskom (electricity generating state-owned company).

The locations of these sites, within the context of sites where data were gathered during this study, will be indicated in Chapter 3 (Measurements, Locations, Techniques and Analyses). In South Africa, the relative significance of BC contributions from anthropogenic sources is still largely unknown, and few BC-related papers have been published in the peer-reviewed public domain to date. Venter et al. (2012) used BC mass concentration data collected at the Marikana monitoring station to verify the origin of CO and PM_{10} but did not consider BC further. Ramsuchi and Kornelius (2013) presented aethalometer BC data, measured for a period of almost a year in the Carletonville gold mining area. Collett et al. (2010) only presented a single diurnal plot for BC mass concentration measured at the Elandsfontein monitoring station in 2010. Hyvärinen et al. (2013) used BC mass concentration data collected at the Welgegund monitoring station to illustrate the use of a newly developed method to correct BC mass concentration values measured with a multi-angle absorption photometer (MAAP).

In addition, Martins (2009) determined elemental carbon (EC) and organic carbon (OC) mass concentrations from three two-week winter campaigns and one two-week summer campaign at two sites, as part of the framework of the Deposition of Biogeochemical Important Trace Species (DEBITS)-International Global Atmospheric Chemistry (IGAC) in Africa project (Galy-Lacaux et al., 2003; Martins et al., 2007). However, this data have not yet been published in the peer-reviewed scientific domain. Maritz et al. (2015) and Aurela et al. (2016) presented limited EC mass concentration data from some regional background sites in South Africa. Kuik et al. (2015) used the Weather Research and Forecasting model, including chemistry and aerosols (WRF-Chem) to analyse the contribution of anthropogenic emissions to the total tropospheric BC mass concentrations from September to December 2010 in South Africa. However, significant underestimations and uncertainties with regard to BC mass concentrations were reported by the afore-mentioned authors. Feig et al. (2015) published limited results from the DEA/SAWS stations. From the afore mentioned, the need for improved BC mass concentration data for South Africa is evident.

2.9 BC measurement techniques

BC mass concentration can be measured using both online and offline techniques. The two most common online and offline approaches to quantify and characterise BC are light-absorption and thermo-optical methods, respectively. The former exploits light-absorbing properties of BC by relating the amount of light absorbed or attenuated in a sample to the mass of the absorbing material, assumed to be equivalent to the mass of equivalent BC (eBC). The latter measures elemental carbon (EC) by heating a sample and measuring the carbon that evolves from a filter at different temperatures and controlled atmospheric conditions (Petzold and Schönlinner, 2004). These methods will be explained in greater detail in Chapter 3.

In addition to the above-mentioned, online measurements of eBC can also be undertaken with the Aethalometer, the Particle Soot Absorption Photometer (PSAP) and the Photoacoustic Extinction Meter (PAX). The first two instruments use a light attenuation method that measures the attenuation of a light signal through a filter medium loaded with the aerosol sample; whereas the PAX instrument directly measures absorption on the sample while it is still suspended in air. A sample volume is illuminated by modulated laser light, which heats absorbing particles, which, in turn, heat the surrounding air and cause a pressure/sound wave. The absorption coefficient can be calculated directly from the amplitude of the sound wave. BC mass can then be calculated using an assumed mass absorption cross-section (Petzold and Schönlinner, 2004).

2.10 BC emissions and sources in South Africa

Aerosol BC emissions depend on the location of point sources, population density, economic state and growth, technological state (e.g. Euro specifications of vehicles), and social trends. Little has been published to link sources in South Africa to BC emissions; therefore, it is one of the main objectives of this study.

2.11 Climatology of South Africa

Although this study does not focus specifically on meteorology, meteorological conditions are critical for understanding and interpretation of the results. Therefore, a brief overview of meteorology over South Africa is considered in this section. Meteorological conditions in South Africa are influenced by strong seasonal variability. The atmospheric circulation pattern around the central Highveld is dominated by anticyclonic circulation during winter and frequent easterly disturbances during summer. Westerly disturbances occur approximately 20% of the time throughout the year (Garstang et al., 1996). Precipitation is characterised by strong seasonal variation with rainfall experienced during the wet season, typically between October and March. The precipitation cycle strongly affects local pollutant concentrations via primary emissions from wildfires during the dry season, as well as wet scavenging by precipitation and clouds during the wet season (Garstang et al., 1996).

Cloud cover over this region is often limited due to a dominant high pressure system created by the high altitude and the subtropical subsidence (Tyson et al., 1996; Tyson and Preston-Whyte, 2004). This, combined with low heat capacity of the soil, creates frequent inversion layers that significantly reduce the vertical mixing of pollutants in the atmosphere (Garstang et al., 1996). These inversion layers are most prominent just before sunrise and break due to convective heating in the presence of sunlight, resulting in the increase in the height of the mixing layer (Tyson et al., 1996; Tyson and Preston-Whyte, 2004). These

meteorological conditions modify pollutant levels on the South African interior and other parts of the country. In addition, given the high occurrence of anticyclonic circulations, pollutants can be trapped over this region for several days before exiting the sub-continent towards the east coast via a well-defined plume (Garstang et al., 1996; Freiman and Piketh, 2002).

2.12 Conclusion

There is considerable understanding of climate forcing contributions by most greenhouse gases, whereas those by aerosol BC remain one of the largest sources of uncertainties in estimating anthropogenic climate perturbations. As indicated in Chapter 1, limited BC studies have been undertaken for South Africa, with significant uncertainties regarding BC mass concentrations being reported by the above-mentioned authors. This thesis presents spatial and temporal assessments of equivalent black carbon (eBC) derived from an optical absorption method and elemental carbon (EC) determined by an evolved carbon method (definitions according to Petzold et al., 2013), mass concentrations over the northern interior of South Africa, as well as potential contributing sources of eBC at the Elandsfontein monitoring site. The results presented in this study (Chapters 4-6) contribute towards addressing these gaps.

CHAPTER 3: MEASUREMENT LOCATIONS, TECHNIQUES AND DATA ANALYSES

This chapter provides a description of the locations where equivalent black carbon (eBC) and elemental carbon (EC) measurements were undertaken, including overlay back trajectory plots showing the percentage of plume passing over online monitoring sites during sampling periods. Measurement techniques as well as an overview of ancillary measurements that were used are also presented. Furthermore, the data quality assurance and analysis processes that were followed are also explained and outlined in this chapter.

3.1 Measurement locations

This thesis presents eBC or EC mass concentration data from eight measurement stations located over the northern interior of South Africa. At three of these stations, continuous high resolution measurements were conducted, i.e. Elandsfontein (EF), Marikana (MA), and Welgegund (WG), while at the remaining five stations, i.e. Louis Trichardt (LT), Skukuza (SK), Vaal Triangle (VT), Amersfoort (AF) and Botsalano (BS), samples were collected once a month on a filter for a period of 24 hours and analysed offline in the laboratory. Figure 3.1 shows the locations of these sites together with the relatively newly commissioned eBC sites by the Department of Environmental Affairs (DEA) and the South African Weather Service (SAWS), which are presented within a regional context (SAAQIS, 2015). However, data from the DEA and SAWS measurement sites were not considered in the study, since this were not yet available at the inception of the study and certain data quality issues were not resolved. In order to contextualise the locations of the sites that were considered, a brief description of each site is presented below.

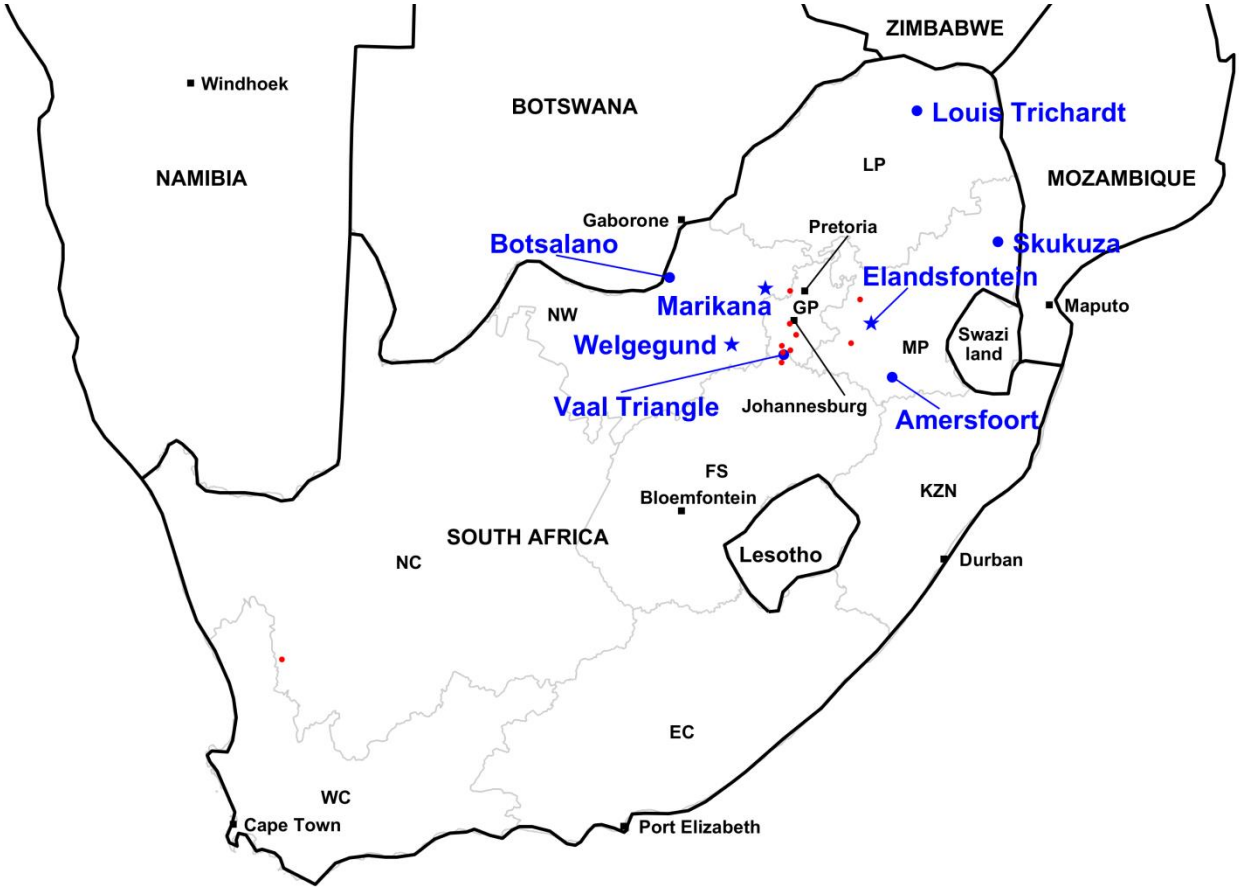

Figure 3.1: Locations of the Elandsfontein (EF), Marikana (MA), Welgegund (WG), Louis Trichardt (LT), Skukuza (SK), Vaal Triangle (VT), Amersfoort (AF) and Botsalano (BS) measurement stations within a regional context. The sites where continuous high resolution data were gathered are indicated with blue stars, while the sites where filters were gathered and analysed offline are indicated with blue dots. Additionally, DEA and SAWS sites, where eBC is also measured, but not considered in this study, are indicated with red dots. Neighbouring countries, some major cities and South African provincial borders are also indicated for additional regional contextualisation (Provinces: WC = Western Cape; EC = Eastern Cape; NC = Northern Cape; FS = Free State; KZN = KwaZulu-Natal; NW = North West; GP = Gauteng; MP = Mpumalanga and LP = Limpopo)

3.1.1 Elandsfontein

The Elandsfontein monitoring station (26.25°S 29.42°E; 1750 metres above mean sea level - m.a.m.s.l) is located on the top of a hill approximately 200 km east of Johannesburg in the highly industrialised South African Highveld (Collett et al., 2010). The site is relatively frequently affected by plumes from coal-fired power stations, metallurgical smelters and a large petrochemical operation located within an approximately 60 km radius around the site (Laakso et al., 2012). This site was used for the European Integrated Project

on Cloud Climate, Aerosols and Air Quality Interactions (EUCAARI) for measurements outside Europe; and was equipped with state-of-the-art instruments for comprehensive aerosol measurements (Laakso et al., 2012; Kulmala et al., 2009). Measurements were conducted from February 2009 to January 2011 with a PM_{10} inlet. The vegetation around the site is typically dry grassland pasture and farmland with annual precipitation of approximately 700 mm (Carruthers, 1997). The rain season is during the October-March period with little rain during winter months (SAWS, 2017). The average maximum daytime temperatures in summer and winter are 26°C and 17°C, respectively, with corresponding average night temperatures of 14°C and 1°C. Figure 3.2 (a) shows an image of the Elandsfontein air quality monitoring station that was equipped with state-of-the-state of the art aerosol and trace gas monitoring equipment, and (b) shows the Google Earth image showing the surroundings of Elandsfontein.

(a)

(b)Figure 3.2: (a) Google Earth image of the immediate surroundings of the site (indicated using a red icon) (*Google Earth, 2018*). (b) Elandsfontein monitoring site shelter and setup (*Courtesy: JP Beukes*)

As stated in section 2.10, the atmospheric circulation pattern over the South African interior is dominated by anticyclonic circulation. Figure 3.3 illustrates this circulation, representing the statistical distribution of HYSPLIT 96-hours back trajectories (Draxler and Hess, 2004) for the duration of the EUCAARI project measurements period at Elandsfontein.

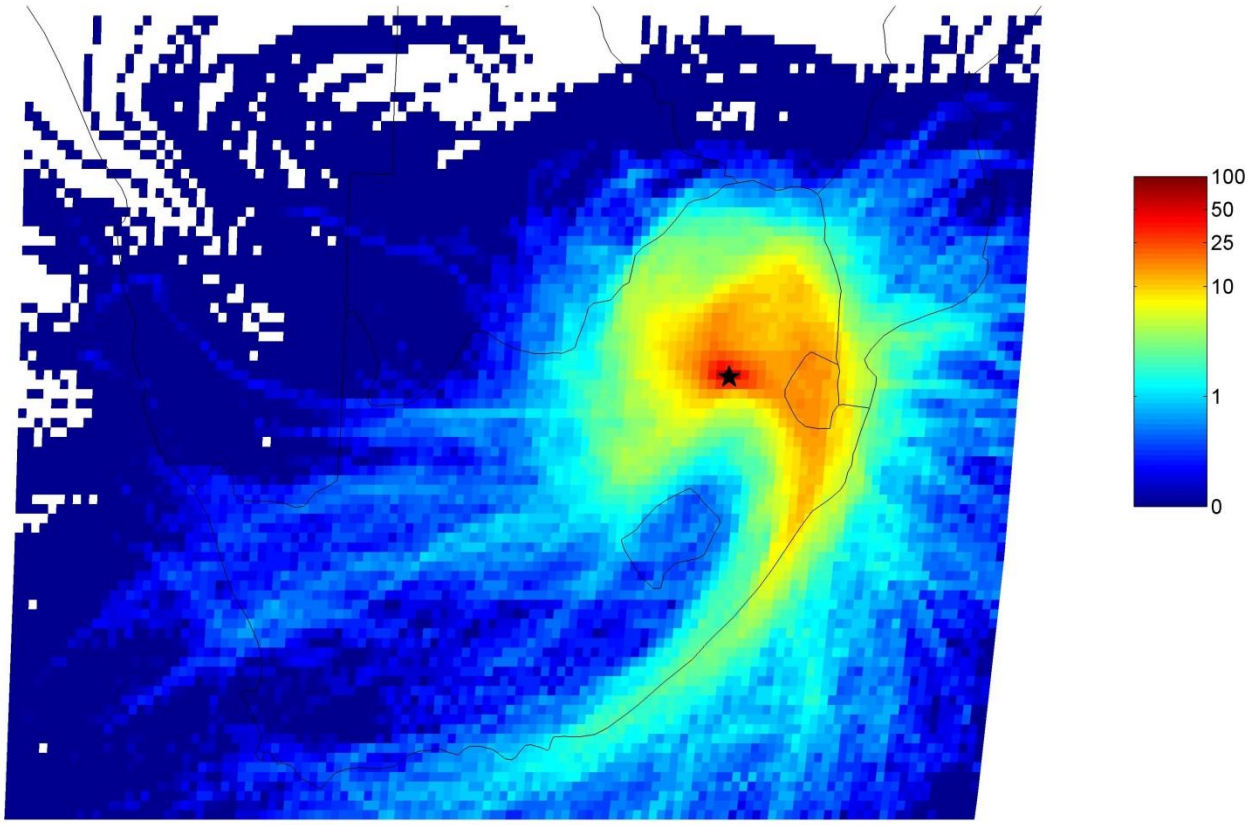

Figure 3.3: Overlay back trajectory plot showing the percentage of trajectories passing over 0.2 X 0.2° grid cells, before arriving at Elandsfontein for the period 11 February 2009 to 31 January 2011

3.1.2 Marikana

The Marikana monitoring station (25.70°S 27.48°E; 1170 m.a.m.s.l.) is located in a small village situated approximately 35 km east of the city of Rustenburg, in the North West Province of South Africa. Within an approximately 55 km radius from this site there are 11 pyrometallurgical smelters and at least twice as many mines (feeding the afore-mentioned smelters) (Venter et al., 2012). However, there are no mining and/or industrial activities within a 1 km radius of the site. The closest surroundings include semi-formal (government-built housing developments, mostly with some form of informal housing additions by the occupants) and informal (self-erected, sometimes unauthorised, mostly without municipal services) settlements, a formal residential area with a gas station and shops, as well as tarred and untarred roads serving the communities in this area (Venter et al., 2012; Hirsikko et al., 2012). Figure 3.4 presents a Google Earth image, which gives some sense of the area and surrounding sources, while Figure 3.5 represents the statistical distribution of HYSPLIT 96-hours back trajectories for the September 2008 to May 2010 measurement period with a PM_{10} inlet.

(a)

(b)

Figure 3.4: (a) Google Earth image of the immediate surroundings of Marikana monitoring site (indicated using blue star) (*Google Earth, 2018*), while (b) shows the measurement site shelter and setup (*Courtesy: V. Vikkari*)

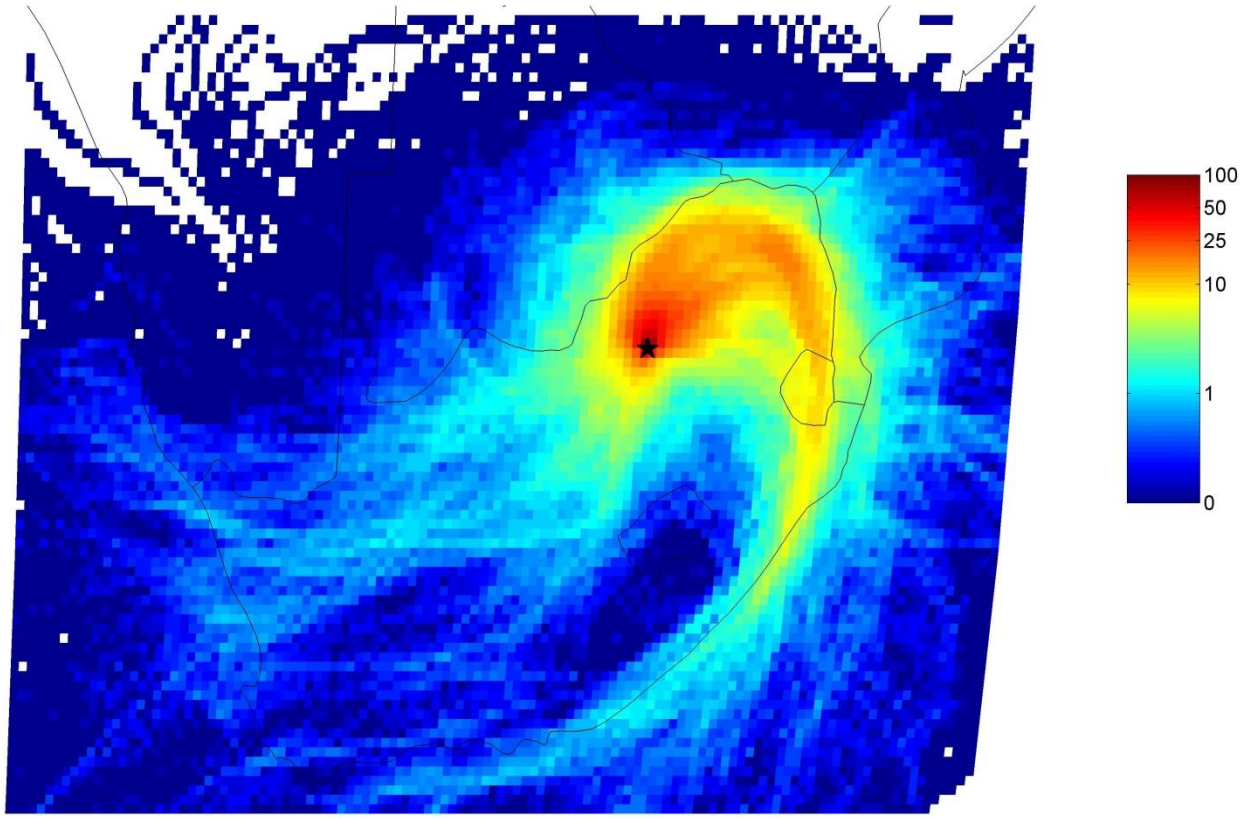

Figure 3.5: Overlay back trajectory plot showing the percentage of trajectories passing over 0.2 X 0.2° grid cells, before arriving at Marikana for the September 2008 to May 2010 measurement period

3.1.3 Welgegund

The Welgegund measurement station (www.welgegund.org, 26.57°S 26.94°E, 1480 m.a.m.s.l.) is situated approximately 115 km west of Johannesburg and 23 km from the Potchefstroom central business district (CBD) on the property of a commercial farmer. It is representative of a regional background site with no impacts from local pollution sources in its close proximity, resulting in clean air masses frequently arriving at this site. The entire western sector contains no major sources and is considered a relatively clean regional background area. However, this site is affected by aged plumes from major source regions in the South African interior, which include the western Bushveld Igneous Complex (WBIC), the eastern Bushveld Igneous Complex (EBIC), the Johannesburg-Pretoria metropolitan conurbation (> 10 million people), the Vaal Triangle priority area, the Mpumalanga Highveld priority area and also a region of anticyclonic recirculation of air mass over the interior of South Africa (Beukes et al., 2013; Jaars et al., 2014; Tiitta et al., 2014; Venter et al., 2016). In addition, impacts of regional biomass combustion occurring mainly in the dry winter and spring are also observed at this site. A detailed description of the Welgegund measurement station and related source regions is presented by Beukes et al. (2014). Measurements reported in this thesis covered the period June 2010 to May 2012, with either PM_{10} (1 June 2010 to 25

August 2010, as well as 1 September 2011 to 31 May 2012) or PM_1 (26 August 2010 to 31 August 2011) inlets being employed. Figure 3.6 (a) shows a Google Earth image of the immediate surroundings of the Welgegund monitoring site, while (b) shows the actual measurement site shelter and other measurements.

(a)

(b)

Figure 3.6: (a) Google Earth image of the immediate surroundings of Welgegund monitoring site (indicated using a red icon) (*Google Earth, 2018*), while (b) shows the measurement site shelter and setup (*Courtesy: JP Beukes*)

The main research aim at this site is to observe different atmospheric parameters relevant for climate

change, regional pollution, atmosphere-ecosystem interactions, aerosol chemistry and physics based on long-term measurements. The specific research topics include formation and growth of aerosol particles, concentrations of aerosol particles of natural and anthropogenic origin, aerosol optics, atmospheric trace gases, grassland-savannah carbon balance, ecosystem interactions and water balance in a water-limited ecosystem. The back-trajectory overlay map for Welgegund, indicated in Figure 3.7, clearly indicates that it often samples air masses that have recirculated around the main anthropogenic source regions in the South African interior. The back trajectories have been calculated for Welgegund from 20 May 2010 to 15 April 2012.

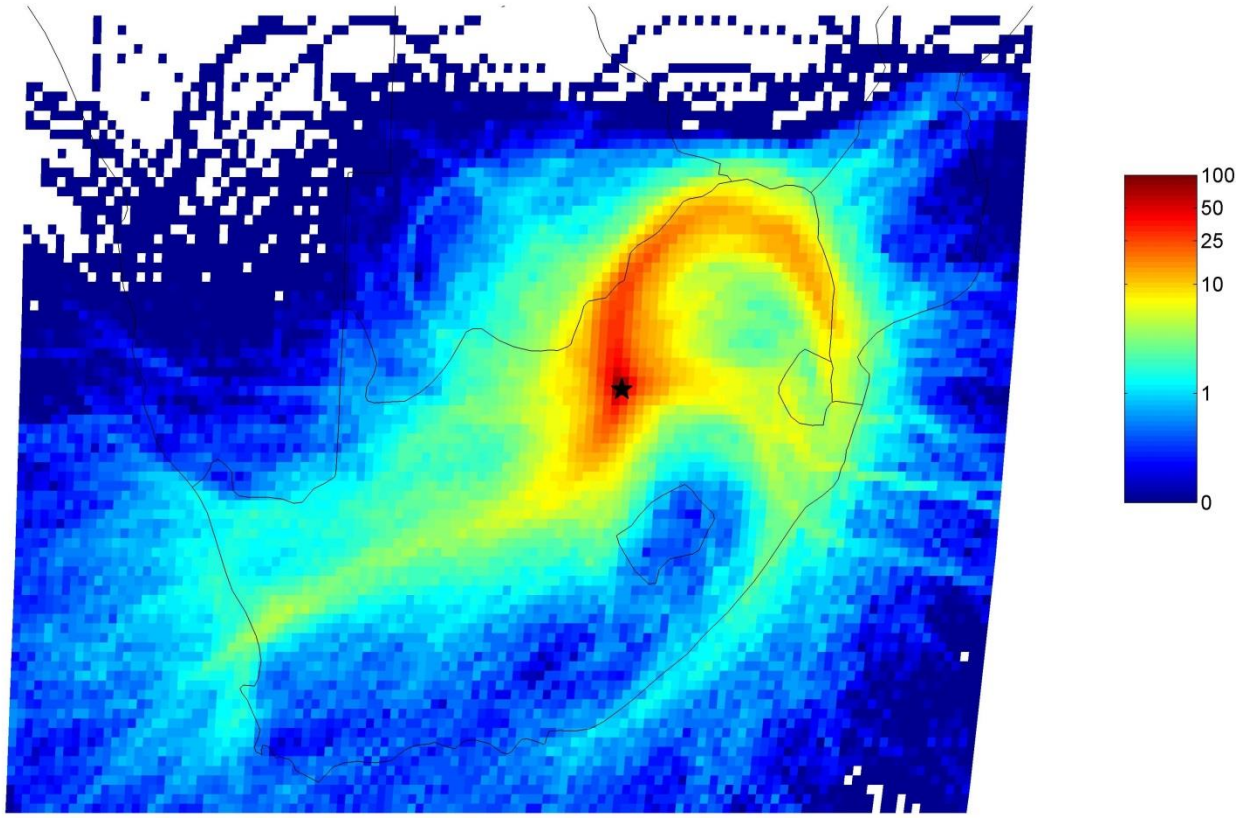

Figure 3.7: Overlay back trajectory plot showing the percentage of trajectories passing over 0.2 X 0.2° grid cells, before arriving at Welgegund for the period June 2010 to May 2012

3.1.4 Sites where filters were collected and analysed offline

Maritz et al. (2015) introduced all the Deposition of Biogeochemical Import Trace Species (DEBITS) sites for which data are presented. The DEBITS project is an international project that was established in the 1990s as a long-term initiative to measure the deposition of atmospheric pollutants. It is a joint initiative of the International Global Atmospheric Chemistry (IGAC) programme and the World Meteorological Organisation (WMO). The main objectives of the DEBITS initiative are to monitor the removal rates (e.g.

dry and wet deposition processes) of bio-geochemically important trace species and to determine which factors (e.g. physical or chemical) control deposition fluxes (Galy-Lacaux et al., 2003; Mphepya et al., 2004; Conradie et al., 2016). Average monthly atmospheric gaseous and 24-hour aerosol samples per month have been collected since 2009 at these sites.

The Louis Trichardt (LT) (22.99 S 30.02 E; 1300 m.a.m.s.l.), Skukuza (SK) (24.99 S 31.58 E; 267 m.a.m.s.l.), Vaal Triangle (VT) (26.72 S 27.88 E; 1320 m.a.m.s.l.), Amersfoort (AF) (27.07 S 29.87 E; 1628 m.a.m.s.l.) and Botsalano (BT) (25.54 S 25.75 E; 1424 m.a.m.s.l.) sites were operated within the afore-mentioned programme. Louis Trichardt is a rural site that is predominantly used for agricultural purposes located within the savannah biome. Skukuza is a regional background site located within the savannah biome, within the Kruger National Park. The Kruger National Park is located in the north-eastern side of South Africa and is one of Africa's largest game reserves, featuring a high density of wild animals, which include the Big 5 (lions, leopards, rhinos, elephants and buffalos, as well as hundreds of other mammals and diverse bird species such as vultures, eagles and storks). Mountains, bush plains and tropical forests are all part of the landscape. The Vaal Triangle site is within the grassland biome and is situated in a highly industrialised area, affected by emissions from various industries, traffic and household combustion. Some of South Africa's largest petrochemical refineries and steel smelters are located in this area. This site lies within the Vaal Triangle Airshed Priority area that has been declared a national air pollution hotspot in terms of the South African National Environmental Management: Air Quality Act (Government Gazette Republic of South Africa, 2005). Amersfoort lies southeast of the internationally well-known NO_2 hotspot that is clearly visible from satellite observations over the Mpumalanga Highveld of South Africa (Lourens et al., 2012) and is located in a grassland biome. It is likely to be affected by anthropogenic activities within the Highveld Priority Area (Lourens et al., 2012) wherein it lies. Botsalano is a regional background site that is situated within the 5 800 hectare Botsalano Game Reserve, which is situated in the savannah biome. It is also located in the relatively recently declared Waterberg-Bojanala priority area (SAAQIS, 2015). LT, SK and BT are considered to be background sites. Mphepya et al. (2006) and Martins et al. (2007) provide detailed descriptions for the LT and SK sites. All these DEBITS sites are likely to be impacted by local, as well as regional biomass burning fire emissions. In this thesis, EC sampled at these sites with a PM_{10} inlet was reported for the period March 2009 to April 2011.

3.2 eBC, EC and ancillary measurement techniques

In this study, online analysis, as well as offline sampling and analysis, of either eBC or EC, were undertaken. These methods are described below.

3.2.1 eBC online sampling

This thesis presents equivalent black carbon (eBC) results measured at EL, MA and WE with the multi-angle absorption photometer (MAAP) that were measured at 1-minute resolutions and converted to 15 minute averages for further use. All the instruments at all the three sites were positioned behind a PM10 inlet. The MAAP measures light absorption by particles at a single wavelength (λ) of 637 nm and eBC mass loadings based on aerosol optical absorption. Figures 3.2 shows an image of the MAAP instrument used in this study. It collects aerosol particles on a quartz tape at a flow rate of 16.7 litres per min ($Lmin^{-1}$) and measures the light attenuation caused by the sampled particles. It reports black carbon concentrations by measuring light absorption and uses the mass absorption efficiency of 6.6 m^2 g^{-1} to calculate the concentrations of black carbon. Black carbon concentrations are then multiplied by this efficiency to calculate light absorption coefficient σAP at 637 nm wavelength. It is mathematically calibrated from the correlation between the optical absorption and mass of BC multiplied by its absorption cross-section. The response between absorption and BC concentration has some variation depending on the chemical composition of the black carbon sampled (Petzold and Schönlinner, 2004). The optical absorption coefficient of aerosol collected on the filter is determined by radiative transfer considerations, which include multiple scattering effects and absorption enhancement due to reflections from the filter. This calculation is based on the transmitted and reflected phase functions defined by directly measured values of transmission, direct and diffuse back scattering. Full details of the algorithms used are presented by Petzold et al. (2002 and 2004).

Figure 3.8: An image of the MAAP instrument used to measure eBC at 637nm wavelength in this study

According to Hyvärinen et al. (2013), an artefact may occur if the automated filter change in MAAP occurs at a high eBC concentration. This artefact was corrected, as recommended by the afore-mentioned authors. Furthermore, the MAAP instruments at EL and WE were operated at reduced flow rates, which decreased the number of such filter change artefacts.

3.2.2 Offline sampling and analysis of EC

Twenty four (24)-hour PM_{10} aerosol samples were collected on quartz filters (with a deposit area of 12.56 cm^2) once a month at the LT, SK, VT, AM and BT sites for the entire measurement period reported. Sample preparation and analysis were according to the methods described by Maritz et al. (2015), where quartz filters were prebaked at 900°C for four hours and cooled down in a desiccator, prior to sample collection. MiniVol samplers developed by the United States Environmental Protection Agency (US-EPA) and the Lane Regional Air Pollution Authority were used during sampling (Baldauf et al., 2001). Samples were collected at a flow rate of 5 $Lmin^{-1}$, which was verified using a handheld flow meter. All filters were handled with tweezers, while wearing surgical gloves as a precautionary measure to prevent possible contamination. Thermally pre-treated filters were visually inspected to ensure that there were no weak spots or flaws. After inspection, acceptable filters were weighed and packed in airtight Petri dish holders

to be used for sampling. After sampling, the filters were placed in Petri dish holders, sealed off, bagged and stored in a portable refrigerator and transported to the laboratory for analysis. At the laboratory, the sealed filters were stored in a conventional refrigerator. Twenty four (24) hours prior to analysis, samples were removed from the refrigerator and weighed before analysis. Several methods can be used to analyse EC collected on filters (Chow et al., 2001).

In this study, the IMPROVE thermal/optical (TOR) protocol (Chow et al., 1993; Chow et al., 2004; Environmental Analysis Facility, 2008; Guillaume et al., 2008) was applied using the Desert Research Institute (DRI) analyser. Figures 2.5a and b show photos of the DRI thermal optical carbon analyser used, while examples of sampled filterers are presented in Figures 2.5c and d. With this method, the filters are subjected to volatilisation at temperatures of 120, 250, 450 and 550°C in a pure helium (He) atmosphere and at temperatures of 550, 700 and 800°C in a mixture of He (98%) and oxygen (O_2) (2%) atmosphere. Carbon compounds released are converted to CO_2 in an oxidation furnace with a manganese dioxide (MnO_2) catalyst at 932°C. Then, the flow passes through a digester where the CO_2 is reduced to methane (CH_4) on a nickel-catalysed reaction surface. The amount of CH_4 formed is detected by a flame ionisation detector (FID), which is converted to carbon mass using a calibration coefficient. The carbon mass peaks detected correspond to the different temperatures at which the seven separate carbon fractions, which include three elemental carbon (EC) fractions, are released. These fractions are depicted as different peaks on the thermogram, of which the surface areas are proportional to the amount of CH_4 detected. The DRI thermal optical carbon analyser can detect EC as low as 0.1 $\mu g\ cm^{-2}$.

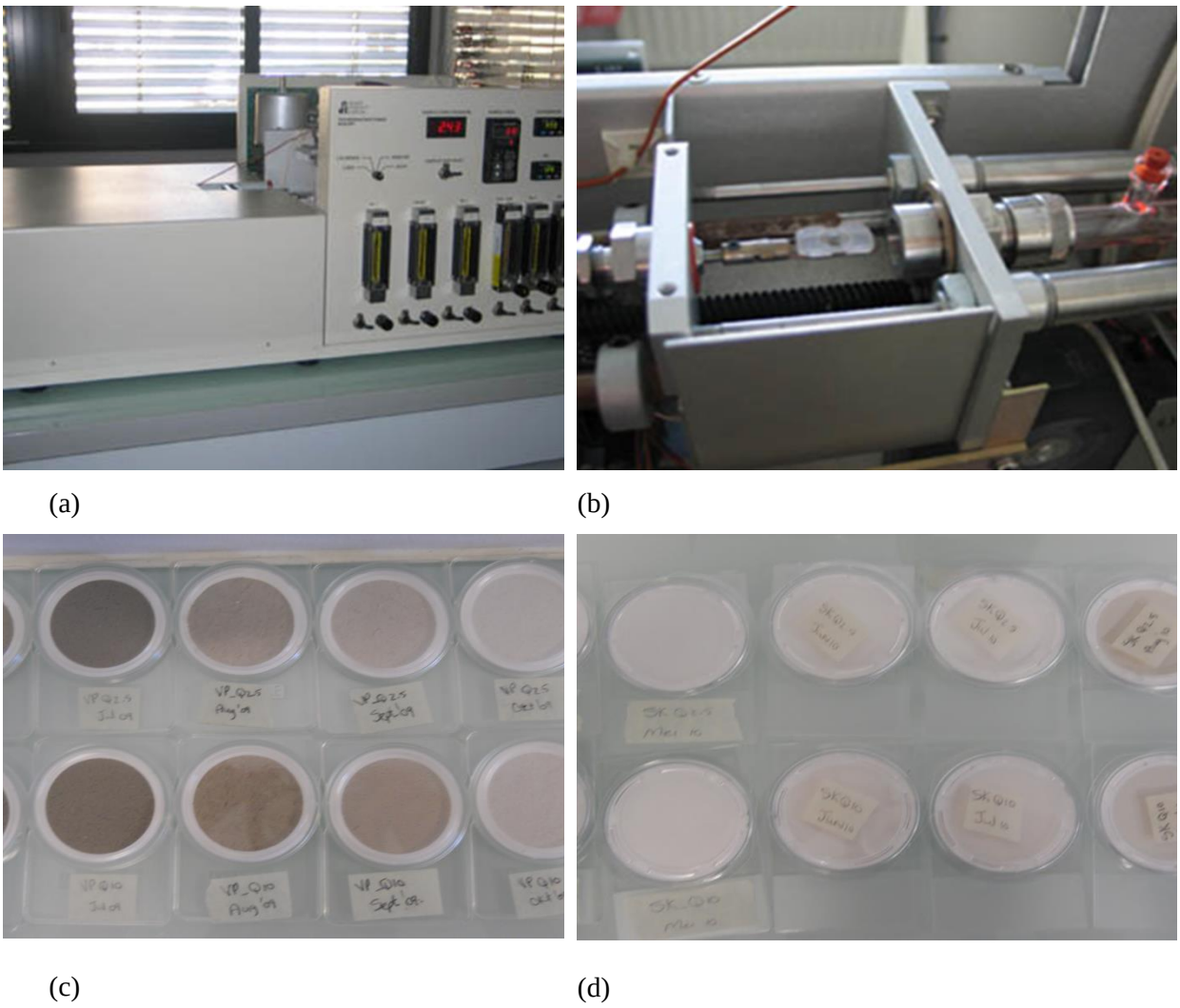

(a) (b)

(c) (d)

Figure 3.9: (a) Desert Research Institute (DRI) thermal optical carbon analyser, (b) components and filter mounting instrument setup used to analyse the filters collected from offline DEBITS sites; (c) and (d) are some sampled filters for the LT and SK sites, respectively (*Courtesy: Maritz, 2017*)

3.3 Ancillary measurements at EL, MA and WE

Various ancillary measurements covering trace gases and meteorological parameters were undertaken at the three sites where on-line eBC sampling was undertaken. Meteorological parameters, vertical structure, black carbon and ancillary measurements undertaken at Elandsfontein, Marikana and Welgegund are presented in Tables 3.1, 3.2 and 3.3, respectively.

Table 3.1: Measured meteorological parameters and instrumentation at Elandsfontein monitoring site during the sampling period

Measurement property and instrumentation	**Parameter**
Meteorology	Temperature, relative humidity, wind speed and direction, ambient pressure and precipitation
Vertical structure measurements	PollyXT Raman Lidar planetary boundary layer measurements
Trace gas measurements	Mercury (Hg), SO_2, NO_x, H_2S, NH_3, O_3, VOCs
Aerosol measurements	
Aerosol light absorption measurements	
Multi-Angle Absorption Photometer (MAAP) at λ = 637 nm	eBC (Light absorption by PM_{10}-aerosol)
3-3 wavelength Particle Soot Absorption Photometer (PSAP) at λ = 467, 530, and 660 nm (Virkkula, 2010; Backman et al., 2014).	eBC
Aerosol light scattering measurements	
Ecotech Aurora 3000 3-13 wavelength Nephelometer	Measured light scattering by PM_{10}-aerosol at λ = 450 nm, 525 nm, and 635 nm wavelength
Number size distributions	
Particles between 10 and 870 nm diameter at a 5-minute time resolution.	Scanning Mobility Particle Sizer (SMPS) particles between 10 and 870 nm diameter at a 5-minute time resolution.
Particle number size distribution in the diameter range 0.3–20 μm	Optical particle counter (OPC, Grimm Model 1.108)
Solar irradiance and aerosol optical depth measurements	
Cimel multichannel 26 Sun photometer	Solar irradiance

Table 3.1 (continued): Measured meteorological parameters and instrumentation at Elandsfontein monitoring site during the sampling period

Aerosol sampling and analysis of chemical composition - Aerosol chemistry (filter sampling and offline analysis) (Gilardoni et al., 2010)	
Dichotomous 3 aerosol sampler – 2025 Partisol equipped with a PM10 inlet.	Aerosol particles were collected for chemical analysis at a flow rate of 1 m^3 h^{-1} (at ambient conditions) on 47 mm quartz filters. Fine particles (aerodynamic diameter below 2.5 μm) and coarse particles (aerodynamic diameter between 2.5 and 10 μm) were collected simultaneously every 6 days for a collection period of 24 hours starting from 8:00 am Organic carbon (OC) and elemental carbon (EC) were measured by thermo-optical analysis with a Sunset Laboratory Dual-Optical analyser
Vertical aerosol back scattering profiles	
Portable aerosol Raman LIDAR system extended PollyXT (Korhonen et al., 2014)	*Vertical aerosol back scattering profiles*

Table 3.2: Measured meteorological parameters and vertical structure, and various black carbon instrumentation that were installed at Marikana monitoring site during the sampling period

Measured property	**Parameter**
Meteorological parameters	Temperature, relative humidity, wind speed and direction, ambient pressure and precipitation
Solar radiation	Direct and reflected PPFD (PAR)
Aerosol number size distribution	Particle size in the range 10-840 nm
Air ion size distribution	Particle size in the range 0.4-40 nm
Aerosol mass	PM_{10}
Trace gas concentrations	SO_2, NO, NO_2, O_3, CO
Light absorption by aerosol particles (Equivalent black carbon)	eBC
Aerosol chemistry	Campaign-based filter sampling and offline analysis

Table 3.3: Measured meteorological parameters and vertical structure, and various black carbon instrumentation that were installed at Welgegund monitoring site during the sampling period

Measured property	**Parameter**
Meteorology	Temperature, relative humidity, wind speed and direction, ambient pressure, vertical temperature gradient and precipitation
Solar radiation	Direct and reflected PPFD (PAR), direct and reflected global radiation, net radiation
Aerosol number size distribution	DMPS 10-840 nm
Air ion size distribution	AIS 0.4-40 nm
Aerosol mass	PM_{10}
Trace gas concentrations	SO_2, NO, NO_2, O_3, CO, VOCs
Light absorption by aerosol particles	Multi-angle aerosol absorption photometer (MAAP)
Light scattering by aerosol particles	3-wavelength nephelometer
Vertical aerosol profile	Vaisala CT25K ceilometer
Flux measurements	H_2O, CO_2 and sensible heat fluxes (eddy covariance) SO_2 and NO_2 fluxes (eddy covariance)
Soil measurements	Soil temperature and moisture at different depths, soil heat flux

3.4 Data quality assurance

Data cleaning and quality verification of the large datasets acquired during the operation of the comprehensively equipped long-term atmospheric stations (EL, WE, MA) are summarised in this section. Keeping an electronic diary wherein notes and observations are made is important. Information captured in the electronic diaries for all the sites was transferred together with all the other data daily to a server to prevent the loss thereof. Information captured in this diary serves as an institutional memory documenting how to solve problems that had occurred in the past. In addition, it contains arrival and departure times of personnel visiting the sites, as well as their names and dates. Figure 3.10 shows an example of an electronic diary file that was recorded at the WE site. The personnel names are just as important as the times, especially if the site is maintained by different personnel. If data or instrument abnormalities are encountered later, the appropriate person (that the diary indicates as the person who successfully resolved a similar problem in the past) was normally consulted to resolve the matter (in a case where the person visiting the site at that time is unable to resolve the problem). Secondly, all activities with associated time stamps are recorded, including routine checks. Furthermore, *ad hoc* procedures such as the installation of a new systems or casting of a cement floor as well as abnormal observations or events of interest, e.g. nearby savannah or grassland fires were also described in detail and logged, since these are vital in

understanding abnormally high or low concentrations of species monitored. In addition, simple diagnostics such as indoor air temperature and operation of the air conditioning units were also logged, since they have the potential of influencing the functioning of the equipment.

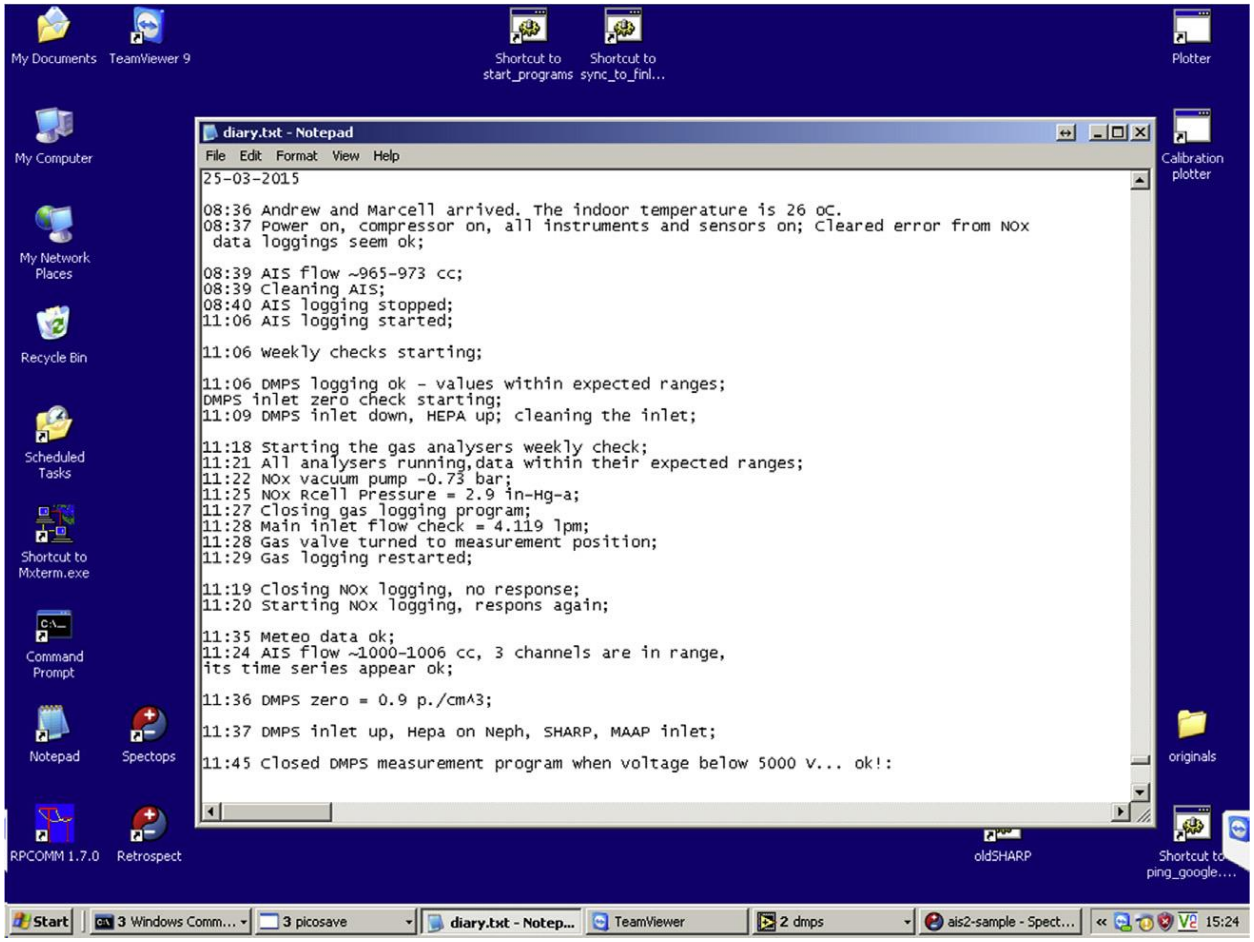

Figure 3.10: Example of an electronic diary file recorded at Welgegund measurement site (Beukes et al., 2015)

The data were cleaned once a year for all the measurement sites, where the arrival and departure times of site visits during which work was performed that could have affected the measurements are transferred from the electronic diary into a simple data file. This data file was then read into an appropriate data processing program and all the data collected during these site visits are taken out of the dataset to remove interferences caused by the site visits. In addition, artefacts caused by power failures were also removed from the dataset. All instruments were protected by operating through uninterrupted power supplies (UPSs) to ensure safe shutdowns (mainly due to power failures). However, UPS cannot be used to operate the instruments for significant periods of time, thereby resulting in the gap in the data, due to a significant spike in the data that was normally observed after the power is restored. The instrument needed to stabilise after a power failure before accurate readings are measured. Furthermore, these power-related data artefacts were also removed in a semi-automated manner from the dataset to ensure that the data are not biased by

such events, during annual data clean-up.

3.4.1 Regular checks and data transfer

Various aspects were considered as critical to ensure the production of quality data during automated continuous atmospheric species monitoring. For instance, regular inspections of the instrument and data coupled with the ability to immediately act on errors/concerns have proven critical in the operation of the online stations. As a result, routine maintenance was performed weekly as set out in the standard operating procedures (SOPs) for all the instrumentation at all the online sites. In addition, *ad hoc* issues identified were also addressed as and when required. Furthermore, scheduled weekly visits were also undertaken irrespective whether there were any problems or not. Every night, the entire dataset was automatically transferred with third generation mobile telecommunications technology (3G) to a server. This daily data are then visualised with an appropriate processing program and reviewed the next morning to identify any problems or concerns. In addition, diagnostic data such as instrument temperatures, pressures, flows, relative humidity and error messages were also checked, since these are very important in ensuring proper instrument function and data quality. Such data were also logged to ensure that data quality issues related to error messages and/or diagnostic data could be resolved.

Another tool used to ensure data quality is an appropriate live-feed viewer that allows viewing diagnostic and signal data as they are being generated by instruments. Figure 3.11 shows an example of a screenshot demonstrating how actual live flux data, radiation, as well as soil temperature and moisture can be viewed remotely for the WE site. If any data and/or instrumental operational errors/concerns were identified with either the daily data overview or live-feed viewing, the monitoring station was visited as soon as possible. The contributions of effective data transfer, daily data evaluation, live-feed viewing, the ability to immediately visit the site if issues are identified and the existence of an instrument workshop to assist with

more technical issues cannot be underestimated.

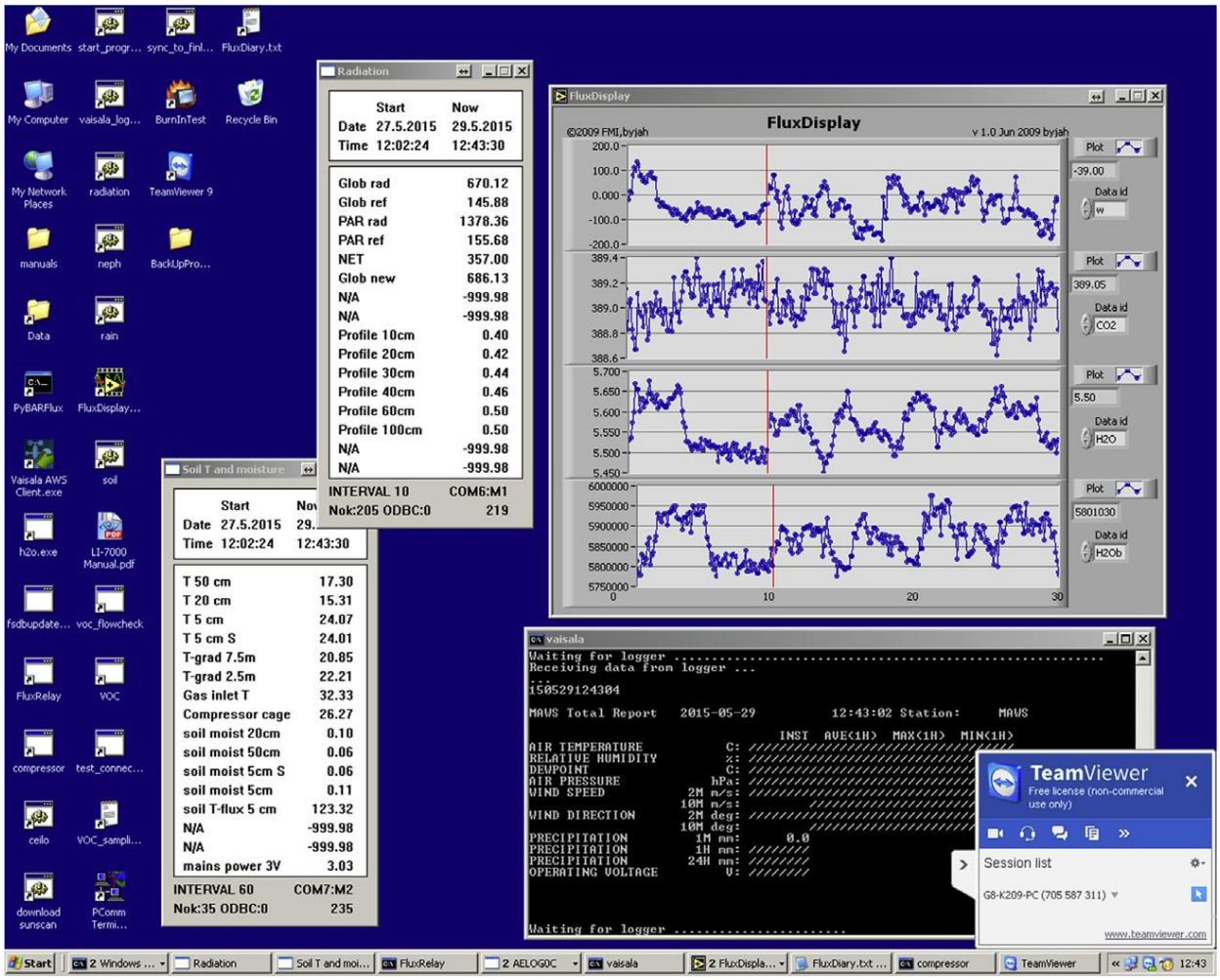

Figure 3.11: An example of real-time view of data being recorded by automated continuous monitoring devices at WE measurement site (Beukes et al., 2015)

3.5 Data analysis

Various statistical tools, which included the Matlab software package, were used to analyse the data, and are discussed in the subsequent sections. In addition, uncommon techniques that were also used in data analysis are discussed in detail in these sections.

3.5.1 Savannah and grassland fire locations

A number of products can be used to obtain savannah and grassland fire locations. In this thesis, remote sensing observations of fires from the MODIS collection 5 burned area product were used to obtain fire locations (Roy et al., 2008; MODIS, 2014).

3.5.2 Air mass back trajectory analysis

The Hybrid Single-Particle Lagrangian Integrated Trajectory (HYSPLIT 2014) model (version 4.8), developed by the National Oceanic and Atmospheric Administration (NOAA) Air Resources Laboratory (ARL), was used to calculate air mass histories (Draxler and Hess, 2004). Meteorological data from the GDAS archive of the National Centre for Environmental Prediction (NCEP) of the United States National Weather Service (USNWS), archived by the ARL (Air Resources Laboratory, 2014a), were used as input in this analysis. This dataset have a 40 or 80 km grid resolution, depending on the year considered (NASA, 2015), with all the data used in this study having 40 km grid resolution. All trajectories were calculated for 24 hours backwards, to arrive on the hour at an arrival height of 100 m above ground level. An arrival height of 100 m was chosen, since the orography in HYSPLIT is not well defined, which could result in increased error margins on individual trajectory calculations if lower arrival heights are used (Air Resources Laboratory, 2014c). For such calculated back trajectories, maximum error margins of 15 to 30% of the trajectory distance travelled have been estimated (Stohl, 1998; Vakkari et al., 2011).

3.5.3 Linking ground-based measurements with point sources using HYSPLIT back trajectories

This method was introduced and used by Maritz et al. (2015) to link ambient organic carbon (OC) and EC concentrations to potential sources. The same method was also applied in this study to assess whether large point sources and in- or semi-formal settlements contributed to ambient eBC concentrations. This method relates eBC concentrations measured at a particular sampling site with the closest distance between the hourly arriving trajectory and the afore-mentioned sources (large point sources, as well as in- and semi-formal settlements). Figure 3.12 presents an illustration of the method applied for a specific sampling site to determine the shortest distance between a 24-hour back trajectory and large point sources. The distances between the large point sources (indicated by the black markers) and a specific back trajectory were calculated for each of the hourly locations of the 24-hour back trajectory (indicated by the red dots on Figure 3.12). The red line indicates the shortest distance between hourly locations of this specific trajectory and large point sources (i.e. petrochemical operations, coal-fired power stations and pyro-metallurgical smelters). The weaknesses of the afore-mentioned method were that downwind point sources and/or in- or semi-formal settlements, very close to the monitoring site, could in some instances be the closest point source/in- or semi-formal settlements. Additionally, dilution due to distance travelled by the trajectories was not considered.

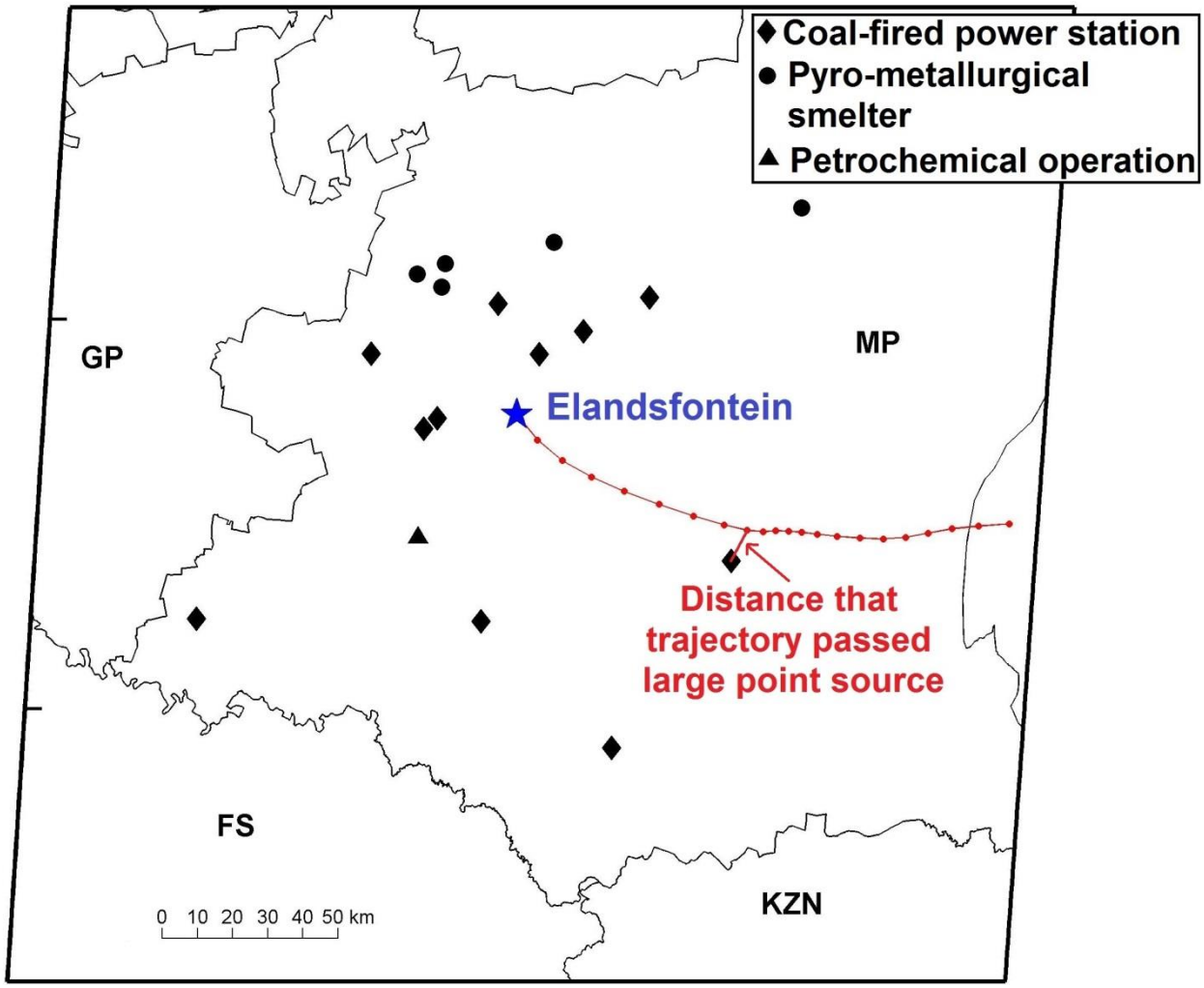

Figure 3.12: Example to illustrate the method applied to determine the shortest distance that each 24-hour back trajectory passed through large point sources and/or in- or semi-formal settlements

3.5.4 Determining the relative contribution of eBC from sources

In order to determine the relative strength of eBC mass concentration sources, detailed correlation analyses were performed for eBC peaks. For instance, it is well known that plumes from coal-fired power stations on the Mpumalanga Highveld are characterised by a simultaneous increase in NO, NO_2 and SO_2 concentrations (Collet et al., 2010; Lourens et al., 2011). Figure 3.13 shows the eBC, SO_2, NO_2, NO and H_2S data that were measured on 14 February 2009. In this figure, it is evident that two well-defined coal-fired power plant plumes were observed between 09:15 and 11:30 based on SO_2, NO_2 and NO time series, as well as between 18:00 and 21:00. However, both of these coal-fired power plant-associated plumes did not raise the eBC baseline meaningfully. There was, however, a significant eBC plume between 02:00 and 08:30, which coincided perfectly with a simultaneous increase in H_2S. This eBC plume was therefore associated with the source that emitted the H_2S. For each such plume, excess eBC (Δ eBC) was determined, with Δ eBC defined as the eBC concentration above the baseline, as indicated in the top panel of Figure

3.13.

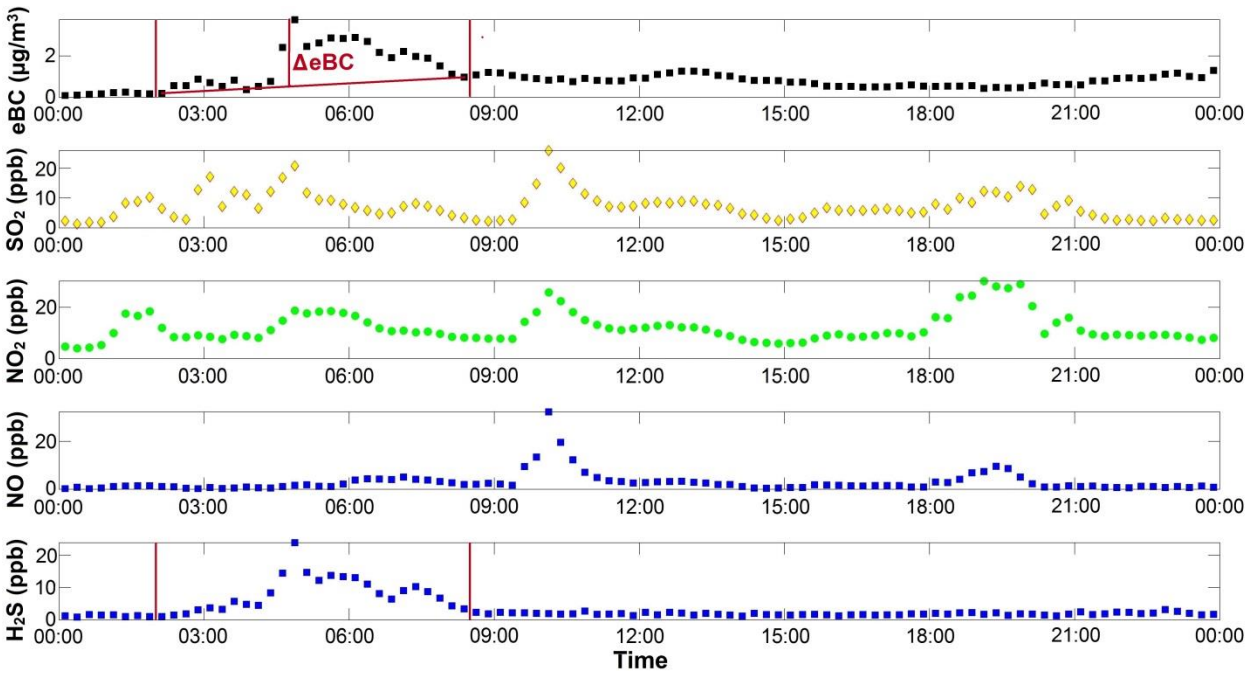

Figure 3.13: Example to illustrate how species were correlated with eBC in order to separate sources from one another. Excess eBC (Δ eBC), defined as the eBC concentration above the baseline for this example is also indicated in the top panel

3.5.5 Multiple linear regression analysis

Several techniques were applied in this thesis to characterise possible sources of BC mass concentrations measured at the various stations, e.g. seasonal patterns, diurnal patterns, back trajectory analyses, and identifying sources based on coincidental increases in species time series. In an attempt to further critically evaluate deductions made from these methods, multiple linear regression (MLR) analyses were conducted. Linear regression is denoted by constants or known parameters (c), an independent variable (x) and a dependent variable (y) by fitting a linear equation to the observed data. MLR is characterised by more than one independent variable (x). In MLR, the relationship between the dependent variable (y) and independent variables (x) is denoted by Equation 2 below.

$$y = c_0 + c_1x_1 + c_2x_2 + c_3x_3 + \ldots\ldots\ldots\ldots c_zx_z \qquad \text{Eq. 2}$$

In this study, MLR was used to determine an equation for the dependent variable concentration of eBC. MLR was used to determine the optimum combination of independent variables to derive an equation that could be used to predict eBC mass concentrations. MLR analysis models the relationship between two or more explanatory independent variables and a dependent variable by fitting a linear equation to the observed

data. The equation obtained can be utilised to calculate values for the dependent variable. Root mean square error (RMSE) was used to compare the calculated values with the measured values. Several authors have previously applied similar methods for various atmospheric species (e.g. Awang et al., 2015; Du Preez et al., 2015; Venter et al., 2015).

CHAPTER 4 SPATIAL AND TEMPORAL ASSESSMENT OF BC OVER THE NORTHERN SOUTH AFRICAN INTERIOR

This chapter presents spatial and temporal variations of aerosol black carbon measured at sites located in the in northern parts of South Africa. In order to extend the spatial coverage, sites where active sampling, i.e. Elandsfontein (EL), Marikana (MA) and Welgegund (WE), as well as sites where filter based sample collection and off-line analysis , i.e. Louis Trichardt (LT), Skukuza (SK), Vaal Triangle (VT), Amersfoort (AF) and Botsalano (BT) were conducted are considered. To elucidate temporal patterns, only sites where active sampling (EL, MA and WE) was conducted, are considered and presented in this chapter.

4.1 Spatial variations of eBC

In Figure 4.1, a box and whisker plot indicating statistical equivalent black carbon (eBC) and elemental carbon (EC) mass concentrations for each of the sites is presented. The significant difference in number of samples (N) is due to the fact that at the DEBITS sites EC mass concentrations were only measured once per month over a 24 hour sampling period, whereas at the other sites collected one-minute eBC data that were converted to 15 min averages. Precaution should be taken when directly comparing eBC and EC, since it has been proven that eBC and EC concentrations can differ by up to a factor of 7 among different methods, with a factor of 2 differences being common (Watson et al., 2005). However, an unpublished 12 month intern-comparison of eBC and EC at the Welgegund measurement site, with the actual sampling and analysis equipment used to acquire data for this study, proved that eBC and EC were within the same order of magnitude (Sehloho, 2017). Therefore, notwithstanding the limitations in directly comparing EC and eBC data, Figure 4.1 provides the most realistic spatial perspective for the northern interior of South Africa, especially within the context of very little eBC data being available in the peer reviewed public domain.

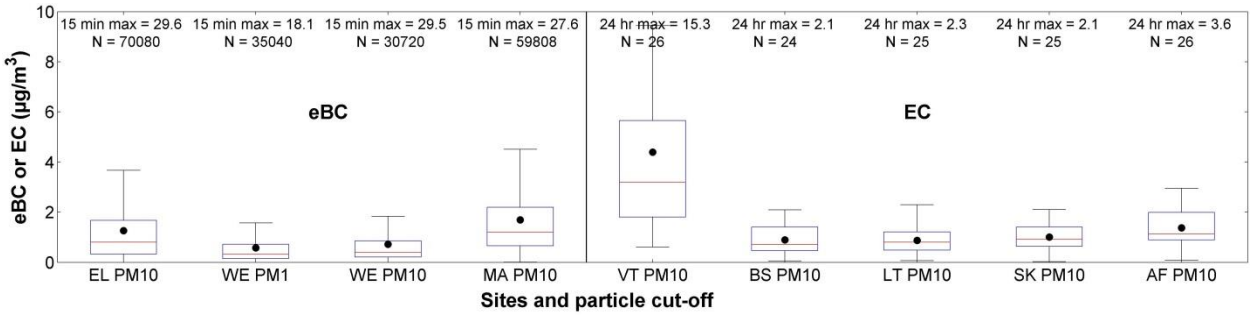

Figure 4.1: Box and whisker plot indicating statistical eBC mass concentrations at the EL, WE and MA

sites, as well as EC mass concentrations at the LT, SK, VT, AF and BT sites. The red line of each box indicates the median, the black dot the mean, the top and bottom edges of the box the 25th and 75th percentiles and the whiskers ±2.7σ (99.3% coverage if the data has a normal distribution). The 15-minute and 24-hour maximum mass concentration values measured at the sites with continuous and off-line analyses, respectively, as well as the number of measurements (N) are indicated

Of all the sites considered, the highest mass concentrations were measured at VT that had a median EC of 3.2 $\mu gm^{-3}$and a mean of 4.4 μgm^{-3} for the entire measurement period. Although sources will be considered in greater detail later, the higher EC mass concentration levels at VT can be attributed to various possible sources. Firstly, this area is densely populated with large semi-formal and informal settlements (See Figure 4.2). This indicates that household combustion for space heating and cooking could be a significant source of EC. Secondly, the area experiences relatively high traffic volumes and several large point sources (including petrochemical and related chemical industries, two coal-fired power stations and numerous metallurgical smelters) occur in the area. Thirdly, the site experiences less dilution of pollutants due to the close proximity of the sources to the measurement site that contribute to the observed elevated levels of EC mass concentration.

Figure 4.2: Google image showing the position of the Vaal Triangle monitoring site (showed by yellow place mark). Although this is an image of a large area, indications of the relatively high population density (formal and informal housing) and potential large industrial sources are evident *(Google Maps, 2017)*

The eBC at EL and MA as well as EC at AF sites indicated to be somewhat high levels with median and mean values of 0.8 and 1.3, 1.2 and 1.7, and 1.1 and 1.4 μgm^{-3} respectively. EL and AF lie within the well-known NO_2 hotspot over the Mpumalanga Highveld identified from satellite observations (Lourens et al., 2012) and are therefore likely to be influenced by industrial activities in this area. Figures 4.3a and b present Google Earth images of areas surrounding the EL and AF sites. Since the large industrial points sources and towns are relatively far from one another on the Mpumalanga Highveld, the potential BC sources are not that evident from these Google Earth images. However, surface scarring due to coal mining in the sector between north-east and north-west from EL (Figure 4.3a) and the coal-fired power station south-west from the AF measurement site (Figure 4.3b) are clearly visible in these two images. Marikana can be affected by household combustion from in - and semi-formal settlements that are located close to the measurement site, as well as the large pyrometallurgical processing plants located in the area (Venter et al., 2012; Hirsikko et al., 2012). Figure 4.3b shows a Google Earth image of the area surrounding MA, which clearly indicates surface scarring due to mining and pyrometallurgical activities.

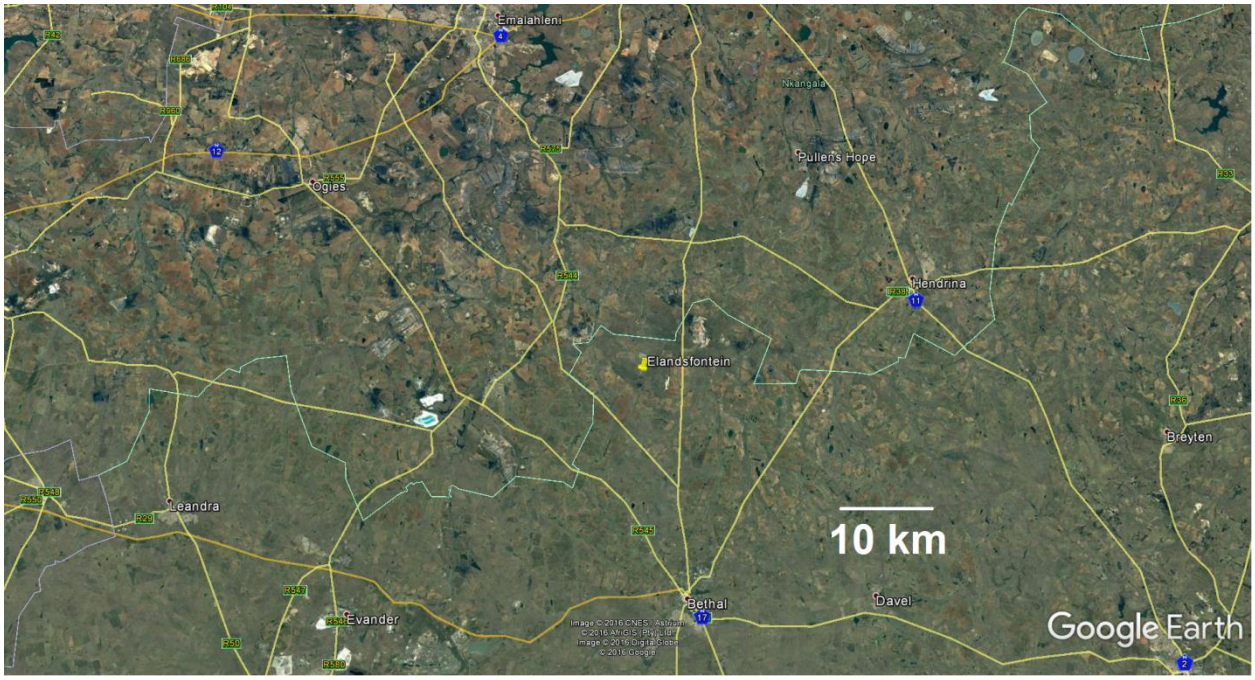

(a) Elandsfontein

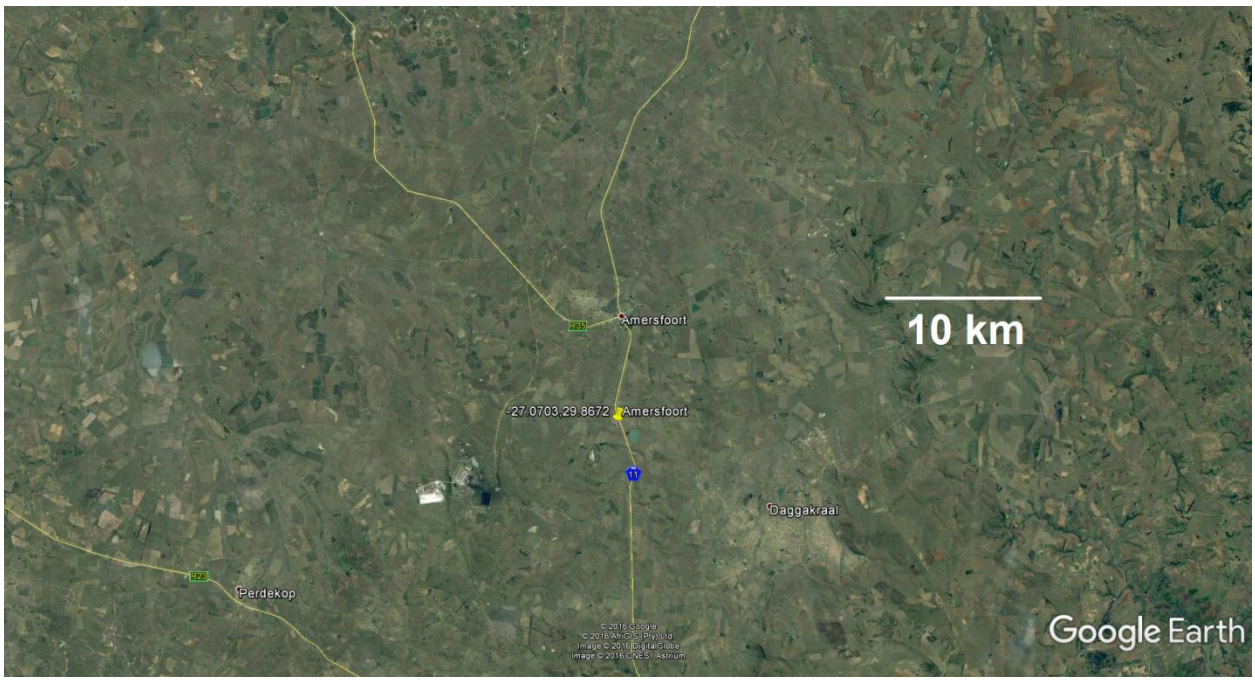

(b) Amersfoort

Figure 4.3: Google Map showing the locations and surrounding areas of (a) Elandsfontein, (b) Amersfoort and (c) Marikana monitoring stations (showed by yellow place marks) *(Google Maps, 2017)*

(c) Marikana

Figure 4.3 (*continued)*: Google Map showing the locations and surrounding areas of (a) Elandsfontein, (b) Amersfoort and (c) Marikana monitoring stations (showed by yellow place marks) *(Google Maps, 2017)*

The background sites, i.e. WE, BT, LT and SK (Google Earth images of the surrounding areas are presented in Figure 4.4) had lower eBC or EC levels compared to other locations, with median and mean

concentrations of 0.4 and 0.7, 0.7 and 0.9, 0.8 and 0.9, and 0.9 and 1.1 µgm^{-3}, respectively. All these background sites are likely to be affected most by regional savannah and grassland fires that are common in southern Africa or by pollutants transported from other parts of the country. However, WE, which is the furthest west of these sites, is likely to be affected less by savannah and grassland fires due to the dryer biomes, i.e. the Kalahari and Karoo that are located to the west of this site. These drier biome regions produce less biomass that can burn (Mafusire et al., 2016). In Figure 4.7, which will be presented later (Section 4.2.3) spatial distribution patterns of fires across southern Africa are indicated, to support the previous statements. It is therefore understandable that WE had lower eBC levels than the other background sites. Obviously, EL, MA, VT and AF will also be affected by regional savannah and grassland fires, in addition to the possible sources already mentioned.

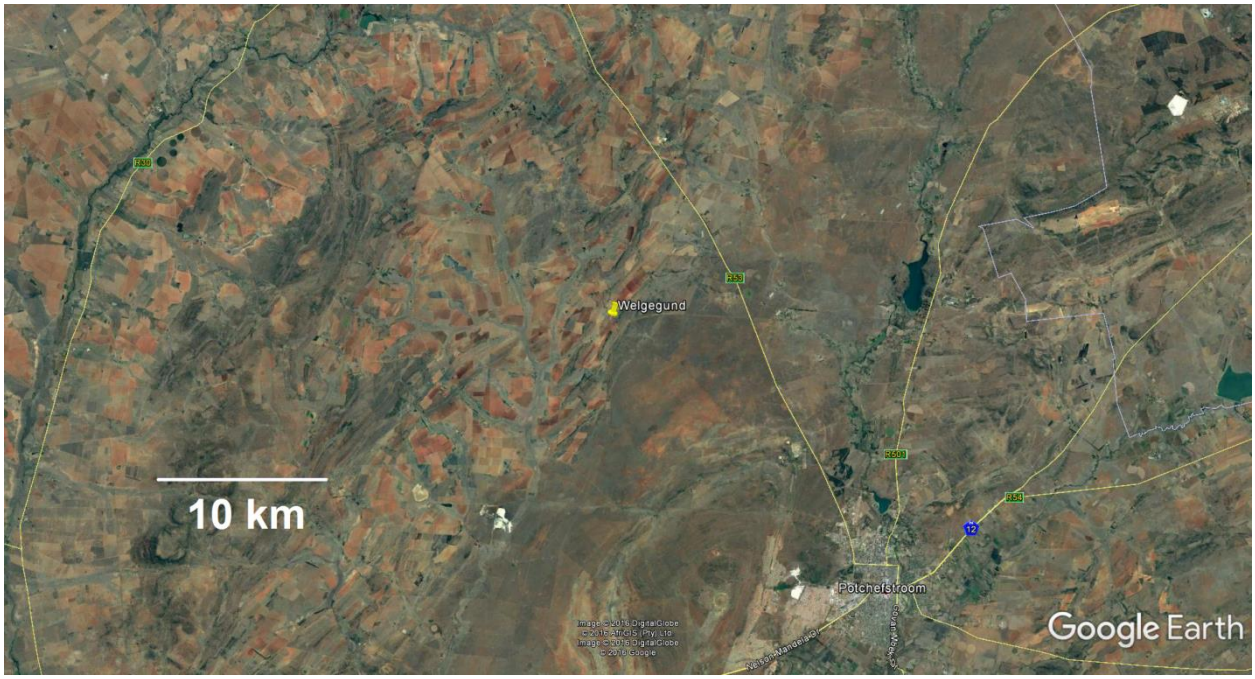

(a) Welgegund

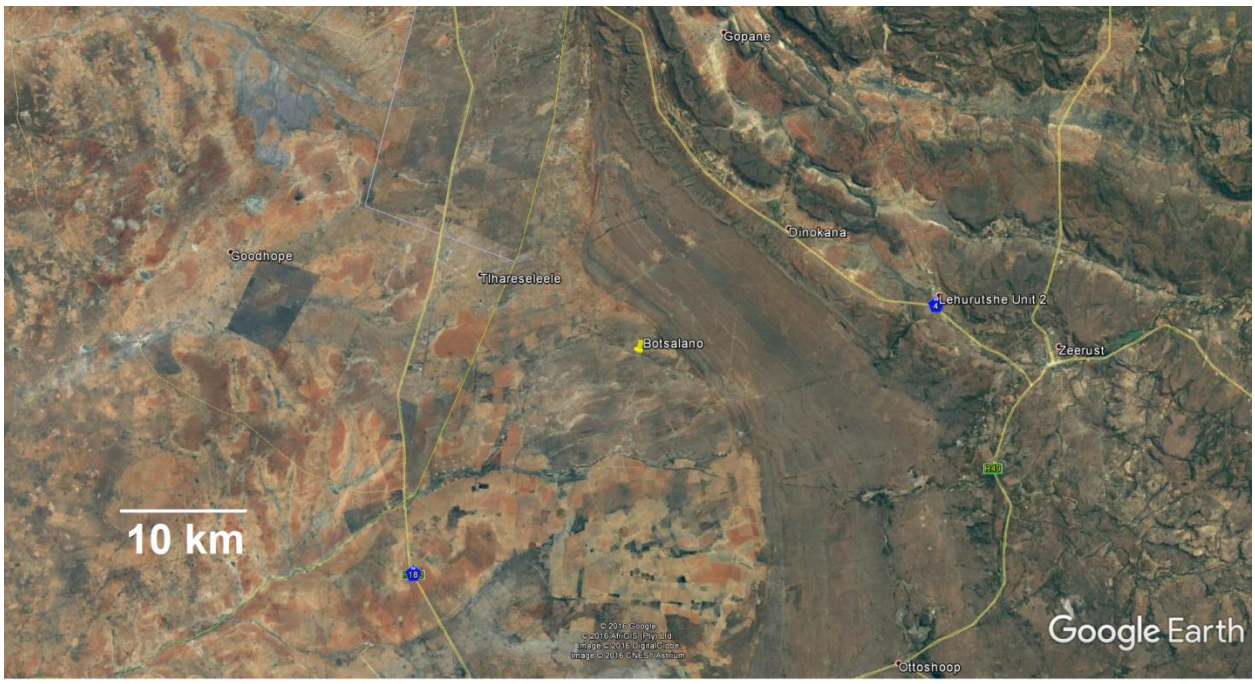

(b) Botsalano

Figure 4.4: Google map showing the locations and surrounding areas around (a) Welgegund, (b) Botsalano, (c) Louis Trichardt and (d) Skukuza monitoring stations (showed by yellow place marks) (*Google Maps, 2017*)

(c) Louis Trichardt

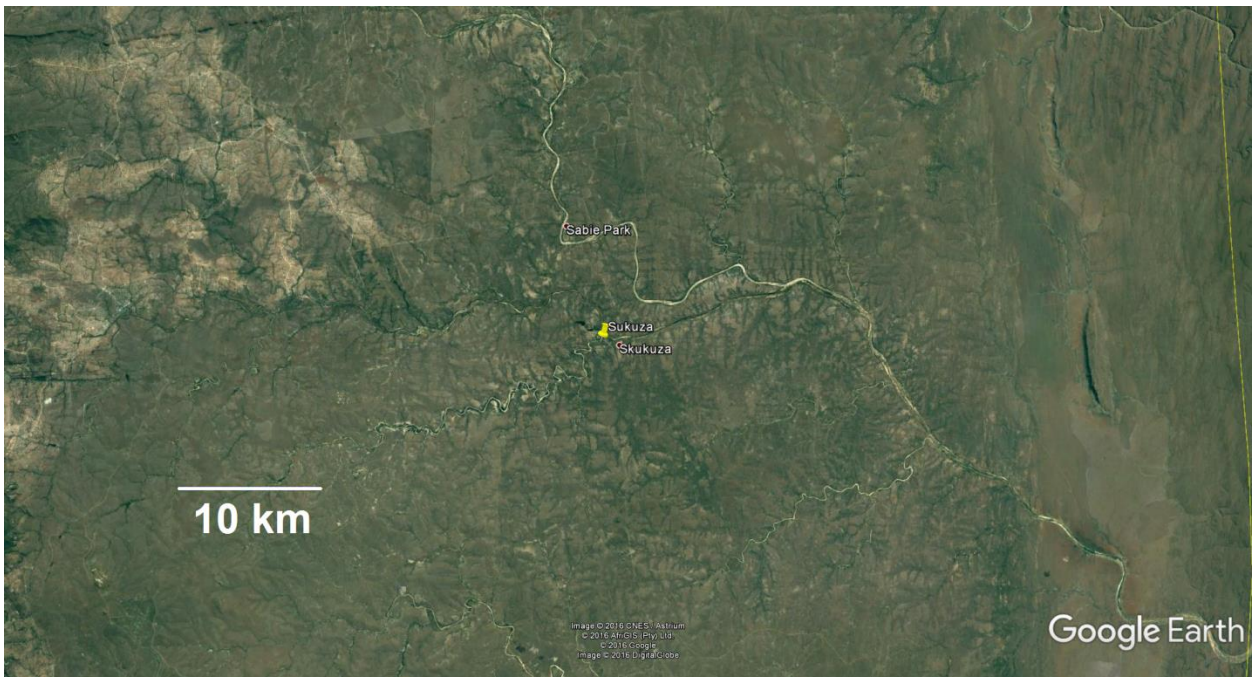

(d) Skukuza

Figure 4.4 (*continued)*: Google map showing the locations and surrounding areas around (a) Welgegund, (b) Botsalano, (c) Louis Trichardt and (d) Skukuza monitoring stations (shown by yellow place mark) (*Google Maps, 2017*)

The eBC and EC concentrations presented for all the sites considered (Figure 4.1) should also be contextualised. The background site with the lowest PM_{10} eBC concentrations reported here, i.e. Welgegund, had similar or higher eBC mass concentration values than typical western European background sites. eBC mass concentrations of 0.2 to 0.3 μgm^{-3} have been reported for western parts of northern Europe (e.g. Yttri et al., 2007). At natural and rural European background sites, values of 0.3 to 0.5 and 0.6 to 1.6 μgm^{-3} have been reported, respectively (e.g. Putaud et al., 2004; Hyvärinen et al., 2013). The other South African background sites reported here, i.e. Botsalano, Louis Trichardt and Skukuza, had higher mean and median values than the afore-mentioned European background/natural sites. The industrial/urban/household affected sites reported here, i.e. Elandsfontein, Marikana, Vaal Triangle and Amersfoort had higher average eBC or EC mass concentration levels than, for instance, an urban site in a large European city, where BC mass concentrations had an average of approximately 1.0 μgm^{-3} (Järvi et al., 2008; Viidanoja et al., 2002). In general, it can therefore be stated that eBC or EC mass concentrations across the measurement sites considered are relatively high, although lower than polluted areas in for instance China where concentrations of ~ 6-11 μgm^{-3} have been reported (USEPA, 2012).

Apart from the spatial information and possible indication of contributing sources obtained from Figure 4.1, it is also evident from the comparison of the PM_1 and PM_{10} eBC data of Welgegund that most of the eBC resides in the PM_1 size fraction, which was expected.

4.2 Temporal variations

4.2.1 Seasonal variations

In order to determine seasonal patterns, only the site where continuous measurements were conducted was considered. Monthly statistical distributions of eBC mass concentrations for Elandsfontein, Welgegund and Marikana measurement sites are presented in Figure 4.5. As is evident from these figures, there is a distinct and similar seasonal pattern observed at all three sites, with the highest eBC mass concentrations measured during June to October months. These months coincide with the colder winter months of June to August as well as the dry season occurring between May and middle October on the South African Highveld. Venter et al. (2012) previously indicated that household combustion for cooking and space heating in informal and semi-formal settlements during winter could be a significant eBC mass concentration source on a local scale. However, it has not yet been determined whether such household combustion could also make a significant regional contribution in South Africa. During the dry season, increased savannah and grassland fires occur, which contributed to increased atmospheric eBC concentrations (Bond et al., 2004, Saha and Despiau, 2009). The influence of both of these potential eBC sources, i.e. household combustion, and savannah and grassland fires, will be discussed later in Section 5.1. Obviously, increased atmospheric stability during the colder months (Garstang et al., 1996) will also lead to trapping of low level emissions, resulting in possible higher eBC concentrations. This is discussed in greater detail in the next section.

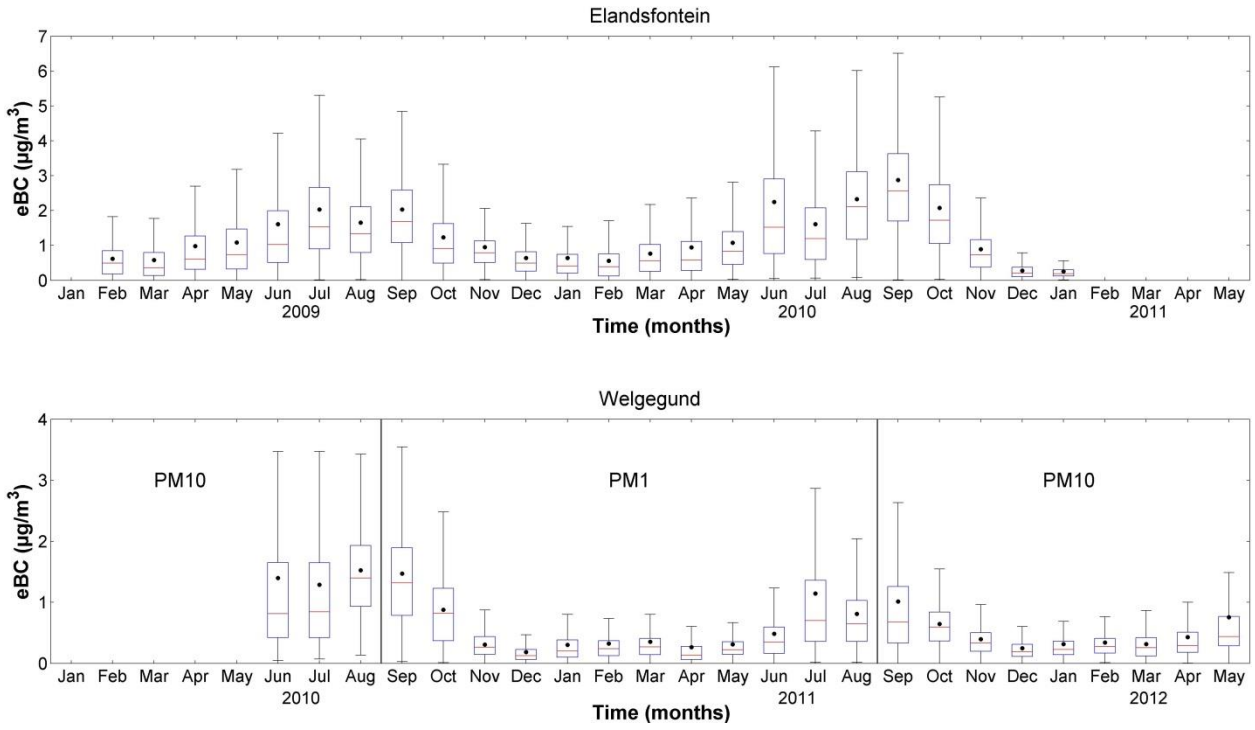

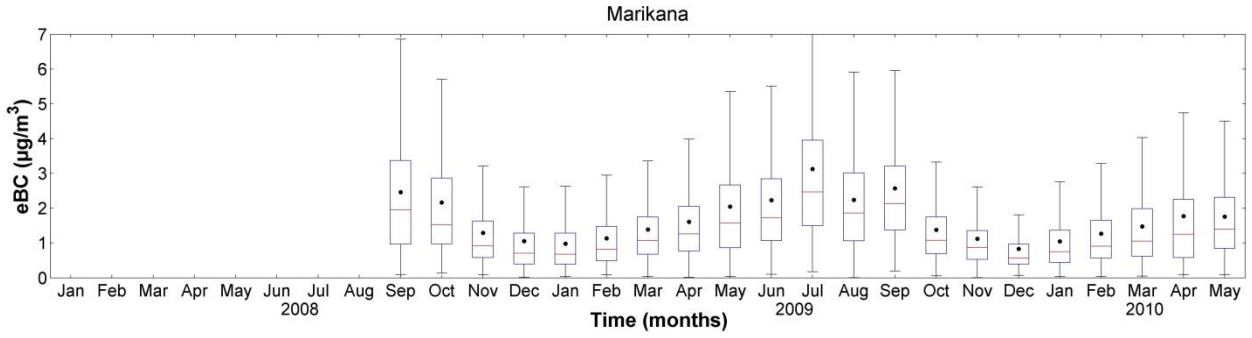

Figure 4.5: Monthly statistical distribution of PM_{10} (unless stated otherwise on figure) eBC concentrations at the three sites where continuous measurement data were gathered, i.e. Elandsfontein, Welgegund and Marikana. The red line of each box is the median, the black dots indicate the mean, the top and bottom edges of the box are the 25th and 75th percentiles and the whiskers ±2.7σ (99.3% coverage if the data has a normal distribution)

4.2.2 Diurnal variations

Average diurnal and seasonal diurnal plots (separate for summer, autumn, winter and spring) for the stations where continuous eBC mass concentration data were gathered, i.e. Elandsfontein, Marikana and Welgegund (both PM_1 and PM_{10}), are presented in Figure 4.6.

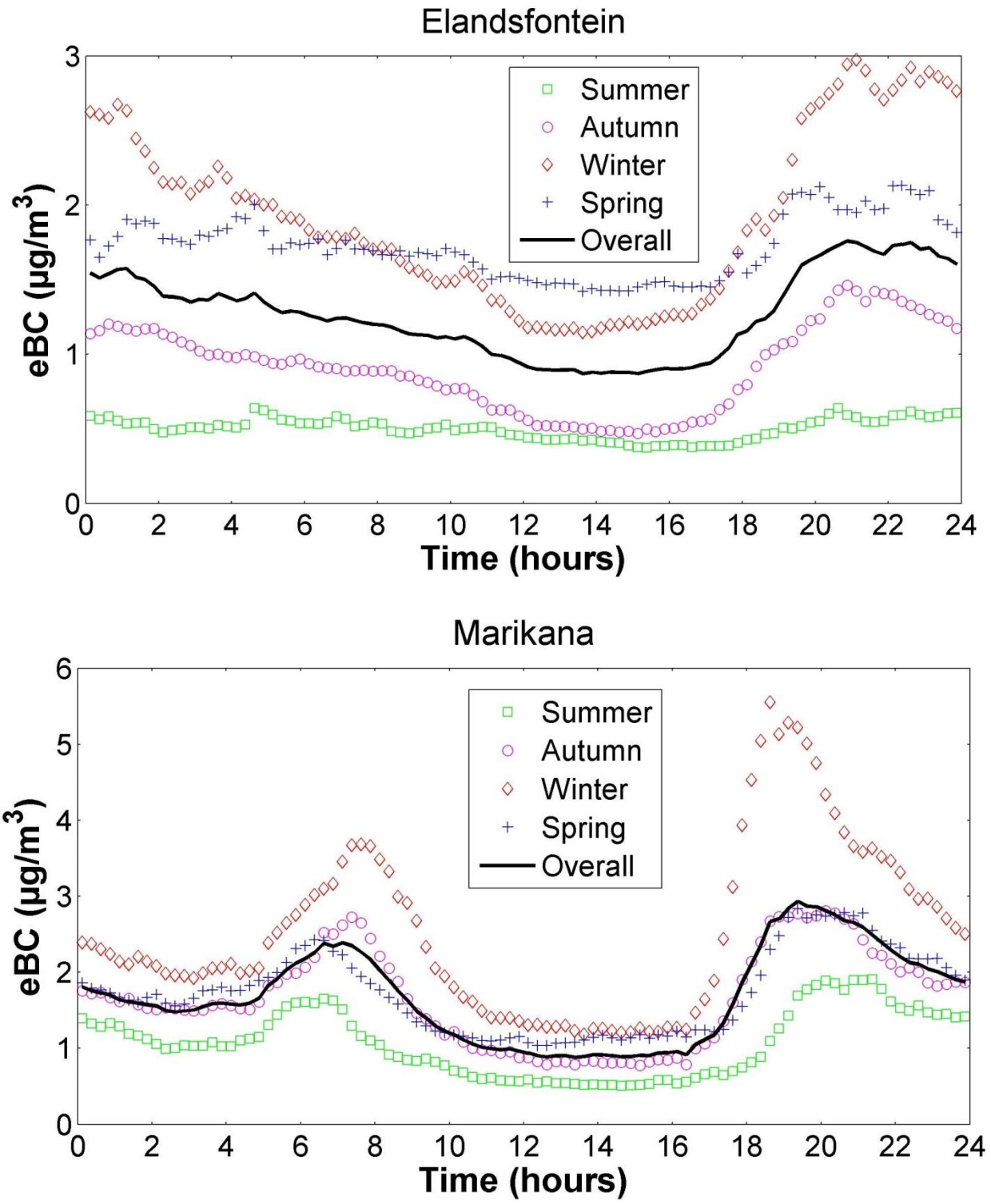

Figure 4.6: Overall and seasonal average eBC diurnal patterns observed for Elandsfontein, Welgegund and Marikana. Summer: DJF, Autumn: MAM, Winter: JJA and Spring: SON

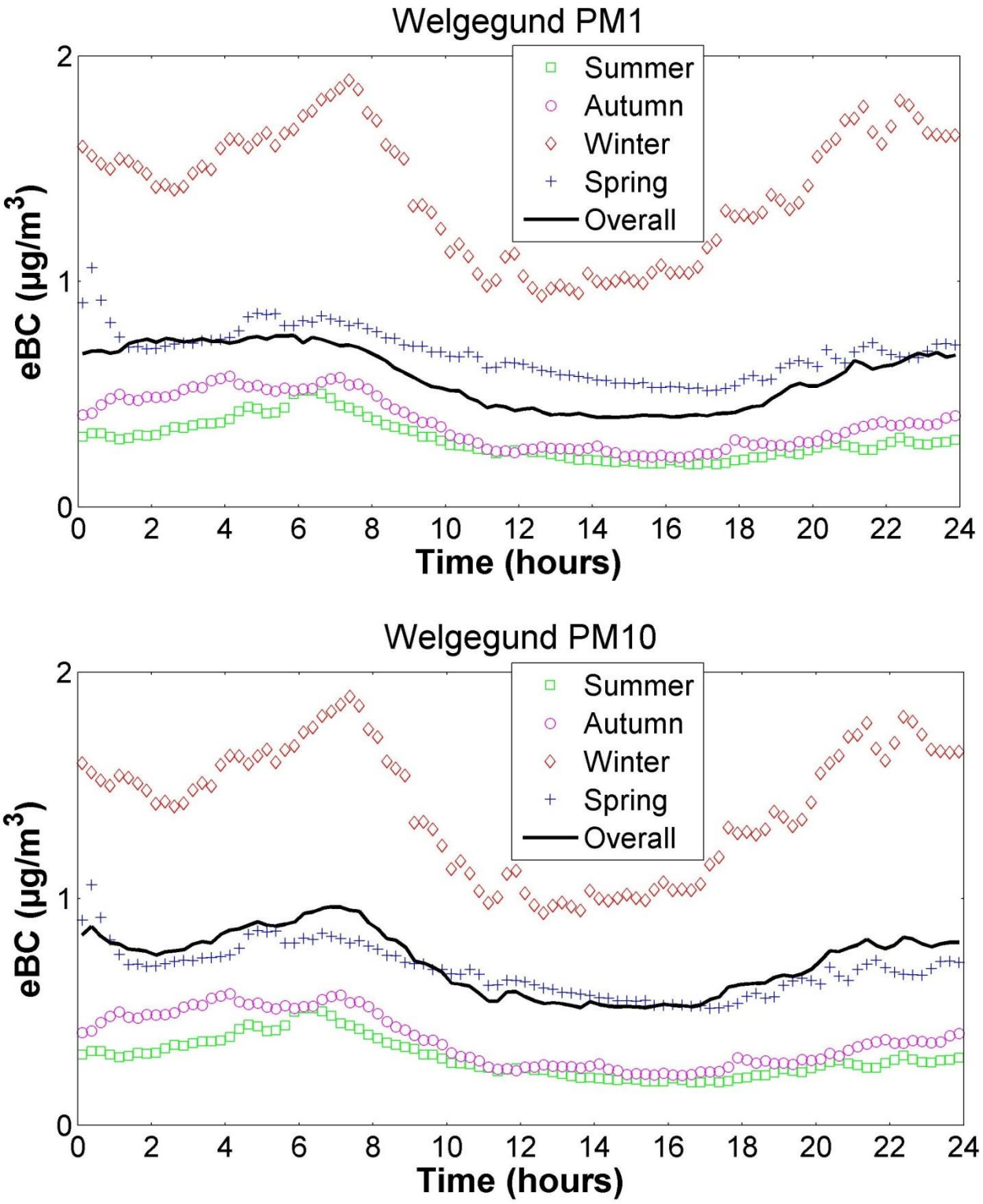

Figure 4.6 (*continued*): Overall and seasonal average eBC diurnal patterns observed for Elandsfontein, Welgegund and Marikana. Summer: DJF, Autumn: MAM, Winter: JJA and Spring: SON

The Elandsfontein diurnal plots indicate that the main source of eBC is not high stack emissions. The area in which Elandsfontein is situated is a well-known international NO_2 hotspot, with tropospheric column densities similar to what is observed over south-east Asia (Lourens et al., 2012; Lourens et al., 2016). It is widely accepted that NO_2 in this hotspot mainly originates from NOx emission from coal-fired power stations. The troposphere over the Highveld is strongly layered, with several inversion layers occurring. These layers prevent vertical mixing to a large degree (Garstang et al., 1996). The afore-mentioned NOx emissions are released into the atmosphere via high stacks, which are typically taller than 300m. The effective stack heights (actual stack heights plus rise due to emissions being hot) were designed to ensure that the NOx emissions are released above the lowest inversion layers, to prevent excessive local pollution and ensure distribution over a wider area. Collet et al. (2010) proved that NO_2 concentrations at Elandsfontein peak after 11:00 am, due to the breakdown of the lowest inversion layers, which allows downward mixing of the NOx tall stack emissions. Therefore, if eBC mainly originated from these large point sources with tall stacks, eBC concentrations would also have peaked, after the breakdown of the night-time inversion layers that would allow downward mixing of tall stack emitted eBC. However, this is clearly not the case. Additionally, the winter diurnal plot for Elandsfontein indicates substantially higher values during night-time when the planetary boundary layer (PBL) is less well mixed (i.e. strong low level inversion layers that trap surface emissions), which re-enforces the notion that the major origin of eBC is from low-level sources, rather than industrial high stacks.

At Elandsfontein the daily evolution of the PBL starts approximately three to four hours after sunrise (which varies between 05:07 and 06:56 local time), which results in increasing atmospheric mixing down from the upper troposphere, including high stack emissions (Korhonen et al., 2014). Considering all the afore mentioned, the most likely eBC sources during winter (June to August) and the dry season (May to middle October) are surface emissions from household combustion, and savannah and grassland fires of which the plumes do not punch through the PBL. This is an important finding, since industries on the Mpumalanga Highveld are often blamed for all forms of pollution, due to the NO_2 hotspot over this area.

In contrast to Elandsfontein, eBC concentrations at Marikana peaked in the early mornings (05:00-09:00) and again in the early to late evenings (17:30-22:00). These times correlate with the peak times for household combustion for space heating and cooking in the nearby informal and semi-formal settlements (Venter et al., 2012). Seasonal timing of the peak eBC concentration in the diurnal plots confirms that household combustion is the main source at this site. In winter, during which time daylight hours are shorter, the peak morning eBC concentration is at ~07:00 and the evening peak at ~18:00; whereas, during summer, with longer daylight hours, the peak morning eBC concentration is at ~06:00 and the evening peak at ~20:00. During the cold winter months, space heating is a priority, apart from cooking, while in summer, household combustion would mainly be used for cooking. These seasonal household combustion use patterns are reflected by the diurnal eBC patterns for Marikana.

The eBC diurnal plots of Welgegund do not indicate well-defined peaks as observed for Marikana. This is

expected, since there are no informal or semiformal settlements located close to the Welgegund station. Additionally, there are also no large point sources close to Welgegund, as there are at Elandsfontein. Therefore, only sources that have a regional influence are likely to contribute to eBC levels at Welgegund. It is therefore likely that savannah and grassland fires, especially during winter and early spring, are mainly responsible for eBC levels measured at Welgegund and mainly long-range transportation during the wet season. The lower PBL during the evenings and early mornings (Gierens et al., 2018) will concentrate the eBC and contribute to eBC levels rising in the evening and only decreasing three to four hours after sunrise, as suggested by Korhonen et al. (2014). This effect is strongest in the winter months.

4.2.3 Inter-annual differences

According to the seasonal eBC patterns for the sites where active monitoring took place, as presented in Figure 4.5, inter-annual variations can be expected. Detailed assessment of these variations was not considered in this study, since measurements covering several years would be required – the datasets considered were ≤ 2 years. However, some reasons for these variations can be postulated. Obviously, changes in availability patterns of large industrial point sources (i.e. whether they operate or not, or operate at reduced levels) and traffic volume could results in inter-annual variations. However, it is very difficult to assess such variations. Beukes et al. (2018) recently proposed a method that can be used to assess the availability patterns of industrial sources, but this method must still be developed and validated further. Additionally, meteorological patterns may vary from year to year, which will influence aspects such as circulation patterns, wet deposition (rain), biomass growth that will influence savannah and grassland activities and winter temperatures that will impact the frequency and intensity of household combustion for space heating. All the factors will influence ambient eBC concentrations. To practically illustrate this, one of the aspects, i.e. annual savannah and grassland fire frequencies, is considered further. Figure 4.7 illustrates the occurrences and locations of savannah and grassland fires throughout southern Africa relative to the location of all monitoring sites for years covering the monitoring periods of all sites (2008 to 2012). As evident from this figure, there are significant inter-annual differences in fire frequencies and spatial areas affected, which can mainly be related to changes in *El Niño*-Southern Oscillation (ENSO) patterns (Masifure et al., 2016 for ENSO).

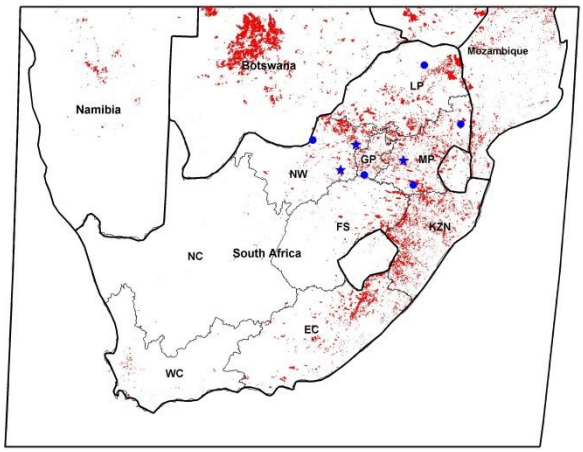

2008

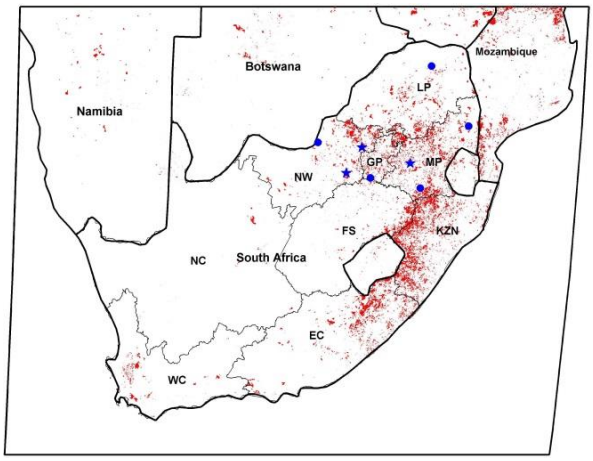

2009

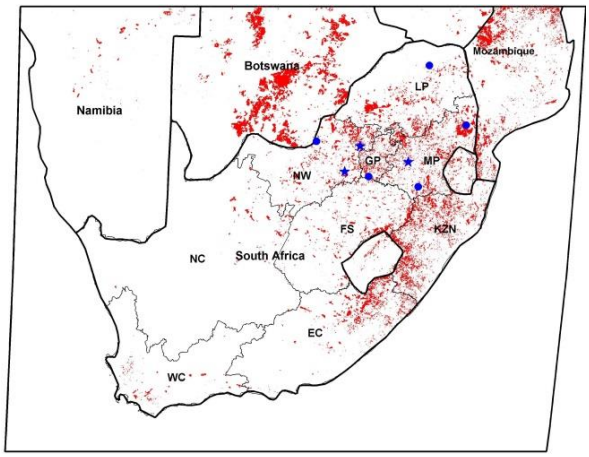

2010

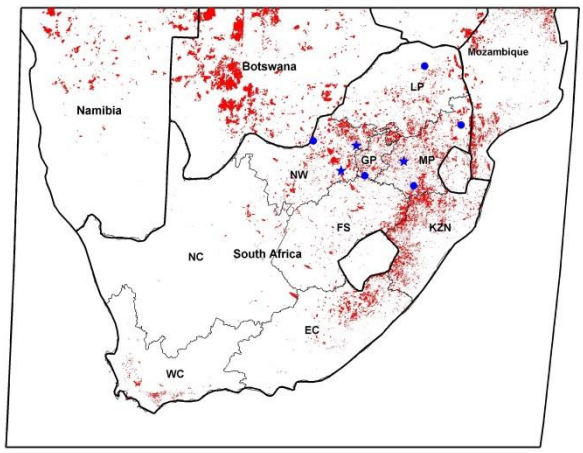

2011

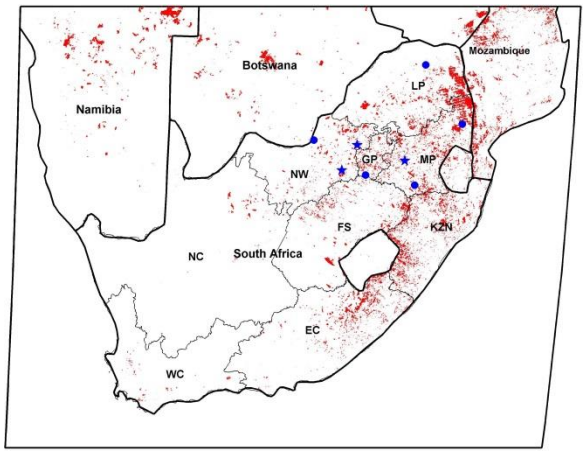

2012

Figure 4.7: Modis fire detected savannah and grassland fires (red) relative to the location of all the online monitoring sites (blue dots indicate sites where filters were collected and analysed offline blue stars for sites where continuous online measurements were conducted) for years covering the monitoring periods of all sites (2008 to 2012)

4.3 Conclusion

BC levels (expressed as eBC or EC) at all the South African measurements sites considered were in general higher than levels reported for comparative sites (comparing like with like, i.e. background, urban or industrially influenced) in first world countries, but lower than levels reported for highly polluted areas (e.g. certain sites in China) (Section 4.1). Large variations in EC and eBC concentrations were observed for the monitoring sites (Figure 4.1), which indicated that different sites are likely influenced by different sources. Specific deduction could not be made regarding sources influencing the DEBITS sites (LT, SK, VT, AF and BT), due to the lower temporal resolution of the data. Only general source deduction could be made for these sites, which included that sites located further east in South Africa are likely to be influenced more by savannah and grassland fires (See Figure 4.7), due to differences in biome productivity. Well defined seasonal and diurnal patterns were observed for sites where active measurements were conducted (EL, MA and WE). The seasonal patterns (Figure 4.5) indicated that savannah and grassland fires, as well as household combustion could be significant sources for all sites, since maximum eBC concentrations were observed in the cold winter months, or early spring when fire frequencies peaked. Diurnal patterns (Figure 4.6) indicated that WE and MA are likely influenced most by regional and long-range transport of eBC, and domestic combustion, respectively. The diurnal patterns for EL (Figure 4.6) proved that industrial high stack emissions are not the most significant source at this site. Lastly, although not investigated in detail, inter-annual variations in eBC levels were evident (Figure 4.5), which can be explained in differences in temporal activity patterns of anthropogenic sources and meteorological patterns.

CHAPTER 5 EQUIVALENT BC SOURCE IDENTIFICATION FOCUSING ON ELANDSFONTEIN SITE

As indicated in Chapter 4, there are various possible sources for eBC, e.g. industrial, household combustion, traffic, and savannah and grassland fires. This chapter considers possible significant contributing sources of eBC in greater detail for Elandsfontein (EL), Marikana (MA) and Welgegund (WE), with specific focus on Elandsfontein (EL).

5.1 eBC source identification

Figure 5.1 indicates fire pixel counts calculated from MODIS collection 5 burned area product (Roy et al., 2008) within the entire southern Africa (10-35˚S and 10-41˚E) region indicated on the primary y-axis, as well as fire pixel counts within a radius of 125 km around measurement sites where high resolution EBD data was gathered (EL, MA and WE) on the secondary y-axis.

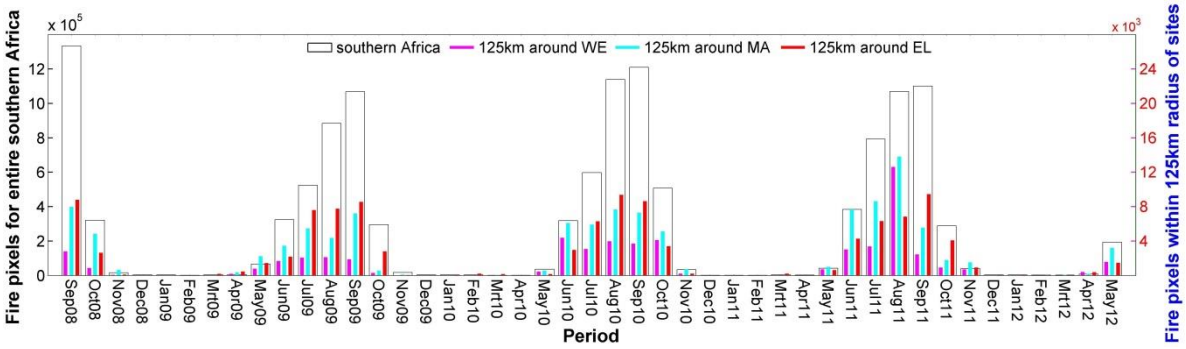

Figure 5.1: Fire pixels within the entire southern Africa (10-35˚S and 10-41˚E) indicated on the primary y-axis, as well as fires pixels within 125 km radii around Elandsfontein, Marikana and Welgegund measurement sites for their entire monitoring periods, indicated on the secondary y-axis as determined from MODIS collection 5 burned area product (Roy et al., 2008)

It is important to note that it is difficult to separate the influence of various sources at a specific site, since the measured eBC originates from a mixture of contributing sources. Therefore Figure 5.1 was considered first, since it provided guidance about which periods would be best to consider for the different eBC sources. This figure shows that peak fire frequencies were detected during July, August and September for southern Africa, as well as within 125 km radii around EL, MA and WE. For instance, there are very few savannah and grassland fires during December to February (DJF) every year in the northern interior of South Africa. The savannah and grassland fires during the summer period only occur in the southern Western Cape and will not influence eBC levels in the northern interior significantly. This is illustrated in Figures 5.2 and (b), which indicate significant fires during DJF in the southern Western Cape (Figure 5.2a), if compared to

detected fires during July to September (JAS) (Figure 5.2b).

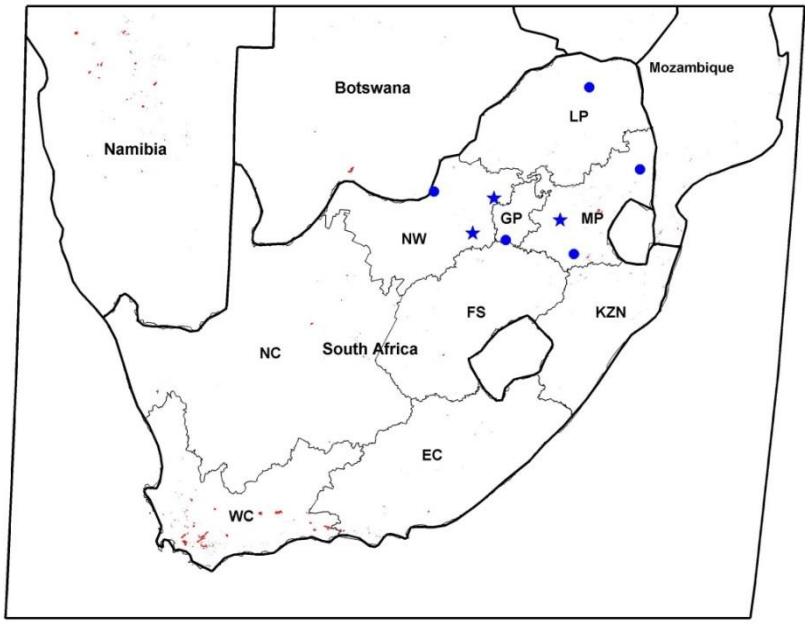

(a)

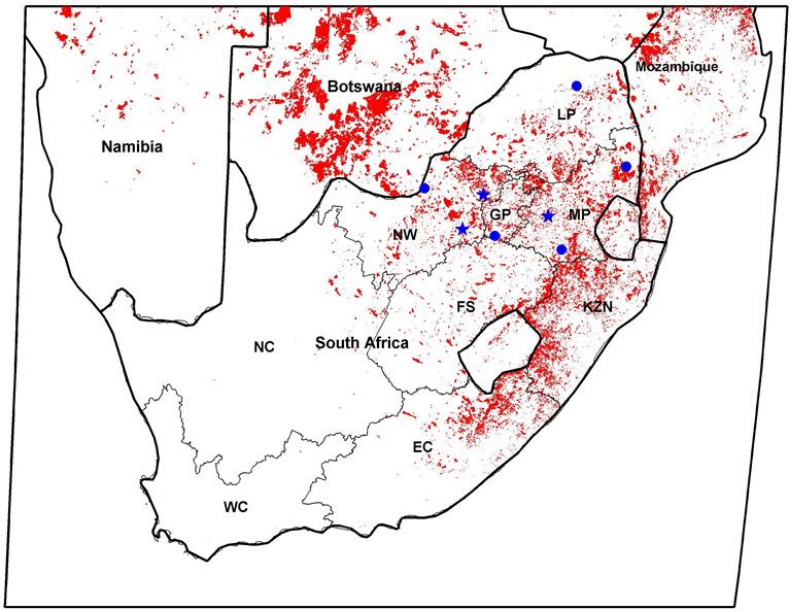

Figure 5.2: Modis burned area (See Figure 5.1) detected fires (red) during (a) summer (DJF) and (b) peak fire frequency (JAS) months for the years 2009 and 2011 combined. Blue dots indicate sites where filters were collected and analysed offline, while blue stars indicate sites where continuous online measurements were conducted (Roy et al., 2008)

In addition to the above-discussed temporal-spatial variation of savannah and grassland fires, minimal household combustion takes place during summer months (December to February), since it is the warmest months in the South African interior. This is illustrated in Figure 5.3 that presents the statistical spread of

temperatures measured during the sampling campaigns at EL, MA and WE. Since it is coldest in June and July (Figure 5.3), the effect of household combustion for space heating can be best isolated then.

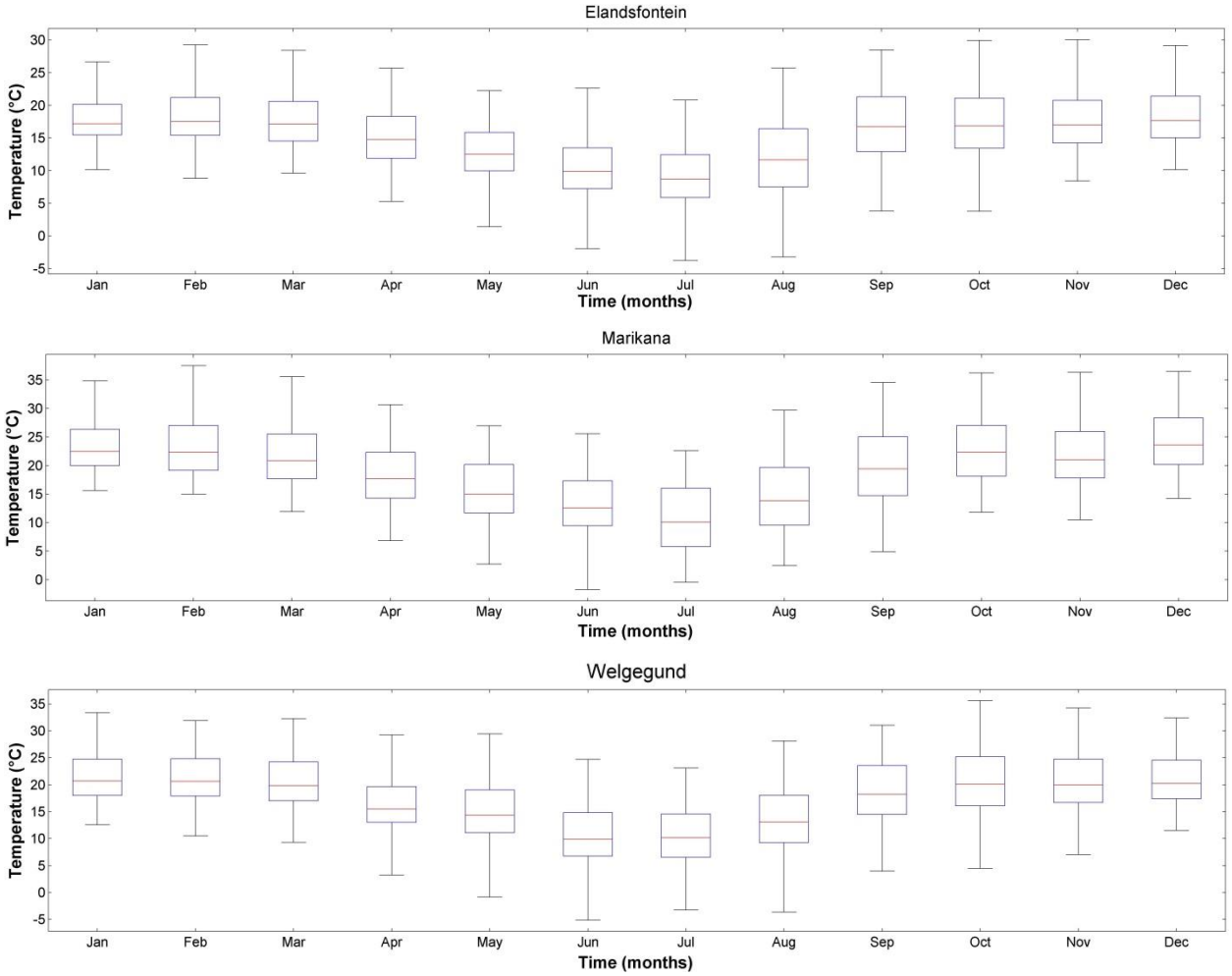

Figure 5.3: Statistical spread of temperatures measured at EL, MA and WE during the measurement campaigns. The red line of each box is the median, the top and bottom edges of the box are the 25th and 75th percentiles and the whiskers ±2.7σ (99.3% coverage if the data has a normal distribution)

It is clear for the overall southern African fire frequencies, as well as those around each site (Figure 5.1) that August and September have the highest savannah and grassland fire intensities. This is the driest period, just before the onset of the first rains, usually in middle October, which is illustrated by the actual rain event frequencies presented in Figure 5.4. However, the influence of household combustion is also not that strong during September to middle October; since it is already becoming warmer (see Figure 5.3) and less space heating is required. By considering aerosol particle concentrations at Marikana, Vakkari et al. (2014) proved that the evening peak associated with household combustion was significantly lower in September than in June to July.

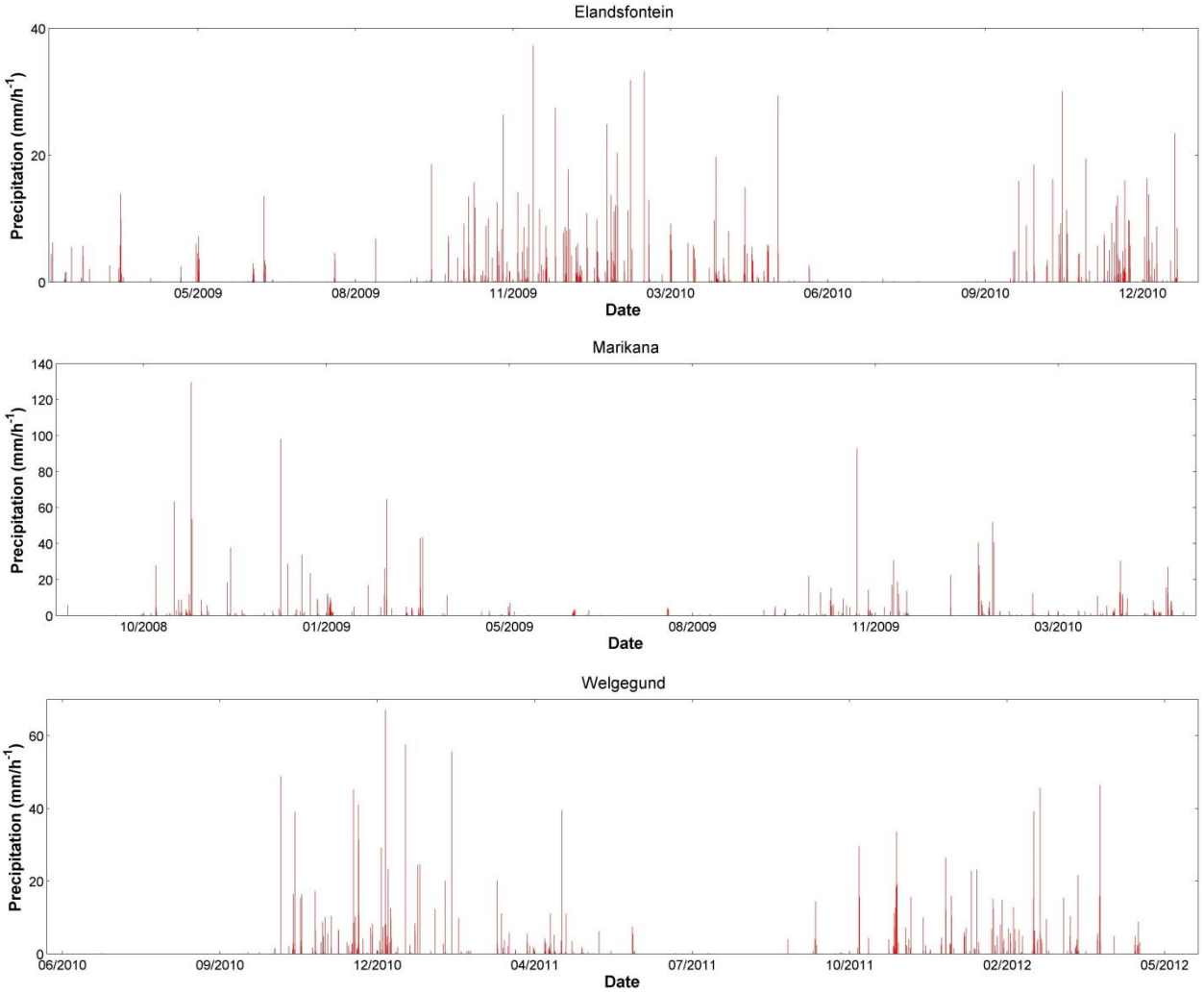

Figure 5.4: Seasonal distribution of rainfall measured at Elandsfontein, Marikana and Welgegund monitoring stations for the measurement periods considered in this study

Considering all the afore-mentioned (i.e. timing of savannah and grassland fires, and household combustion), it is best to isolate industrial and traffic related eBC sources during December to February, when household combustion for space heating, and savannah and grassland fire emissions are low in the South African interior. In the following sections, eBC contributions from the above-mentioned sources, i.e. industrial, traffic, savannah and grassland fires, and household combustion, will be explored in greater detail for Elandsfontein site only. This site was chosen since it can be affected by all the afore-mentioned

sources, while the other sites where continuous high resolution data were gathered will mainly be influenced by savannah and grassland fires (Welgegund) and household combustion (Marikana).

5.1.1 Industrial contribution

Numerous large industrial point sources linked to coal utilisation occur in the South African interior, e.g. coal-fired power stations that produce most of South Africa's electricity, large petrochemical operations utilising coal gasification, as well as numerous pyro-metallurgical smelters utilising coal and coal-related products as carbonaceous reductants for the production of various steels and alloys, exist around Elandsfontein (Collet et al., 2010; Lourens et al., 2011; Beukes et al., 2012). Previously, it has been indicated that some of these large point sources contribute significantly to certain pollutant concentrations, e.g. the NO_2 hotspot observed with satellite observations over the Highveld, mainly due to coal-fired power stations that do not de-SO_x or de-NO_x and traffic emissions (Lourens et al., 2012). However, the possible contributions of these large point sources to atmospheric BC concentrations have not yet been investigated for South Africa.

As previously indicated, Elandsfontein is situated within the well-known NO_2 hotspot, with various large points sources located in close proximity (Collet et al., 2010; Lourens et al., 2011). The diurnal eBC concentration plots of Elandsfontein (Figure 4.3) indicated that it is unlikely that industrial high stack emissions were the main source of eBC at this site. However, this postulate has to be proven. In Figure 5.5, eBC concentrations measured at Elandsfontein were plotted against the shortest distances that back trajectories passed any large point source, during the summer months (December to February), when minimal household combustion (Figure 5.3), as well as savannah and grassland fires occur (Figures 5.2). Although there was no clear correlation (Figure 5.5), the results indicated that at least some trajectories passing closer to these large industrial point sources had significant eBC concentrations. This suggests that eBC contributions from large industrial point sources cannot be ignored, notwithstanding the diurnal patterns indicating that high stack industrial emissions were not the main eBC source (Figure 4.3).

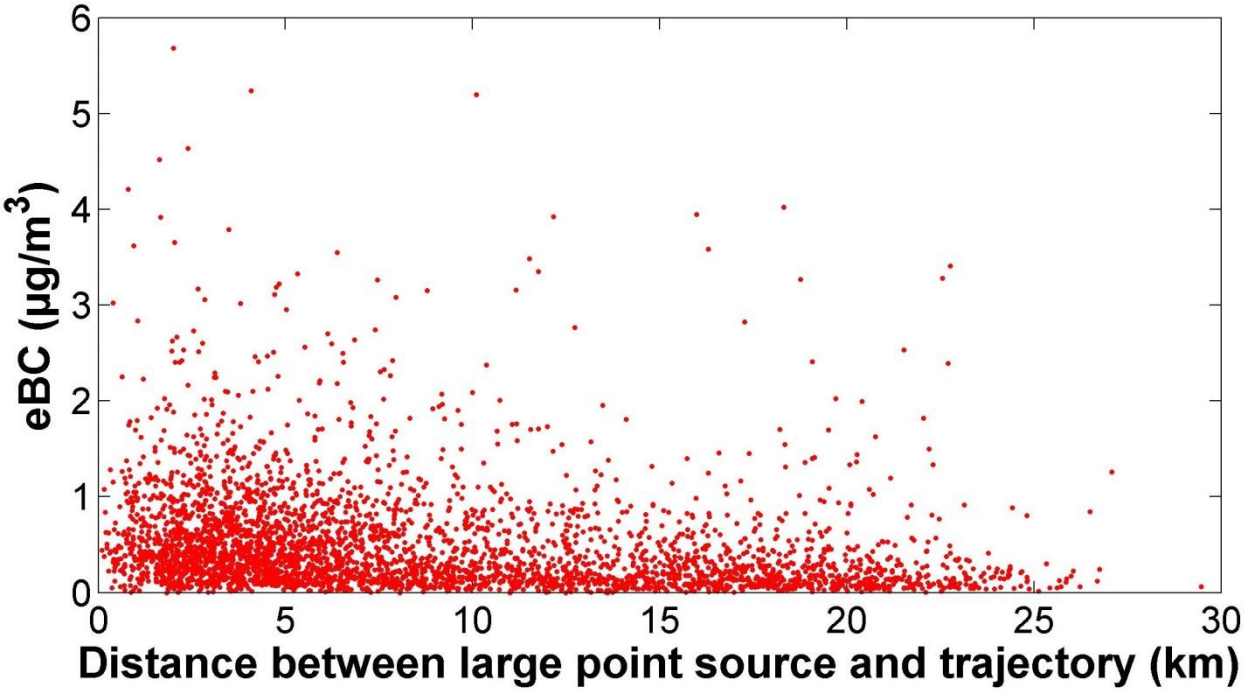

Figure 5.5: Hourly average eBC concentrations plotted against the shortest distances that hourly arriving back trajectories passed large point sources during the summer months (i.e. December to February) at Elandsfontein

In order to quantify the possible fractional contributions of industries to eBC levels, eBC peaks that coincided with peaks of other pollutants (Figure 3.9 and associated discussions), which are characteristic of large point sources in that area were considered for the December to February periods. Two distinct types of contributing sources were identified, i.e. eBC peaks that coincided with SO_2, NO_2 and NO, as well as those that only coincided with H_2S. Examples of both these types of identified coinciding peaks are indicated in Figures 5.6 and 5.7 below.

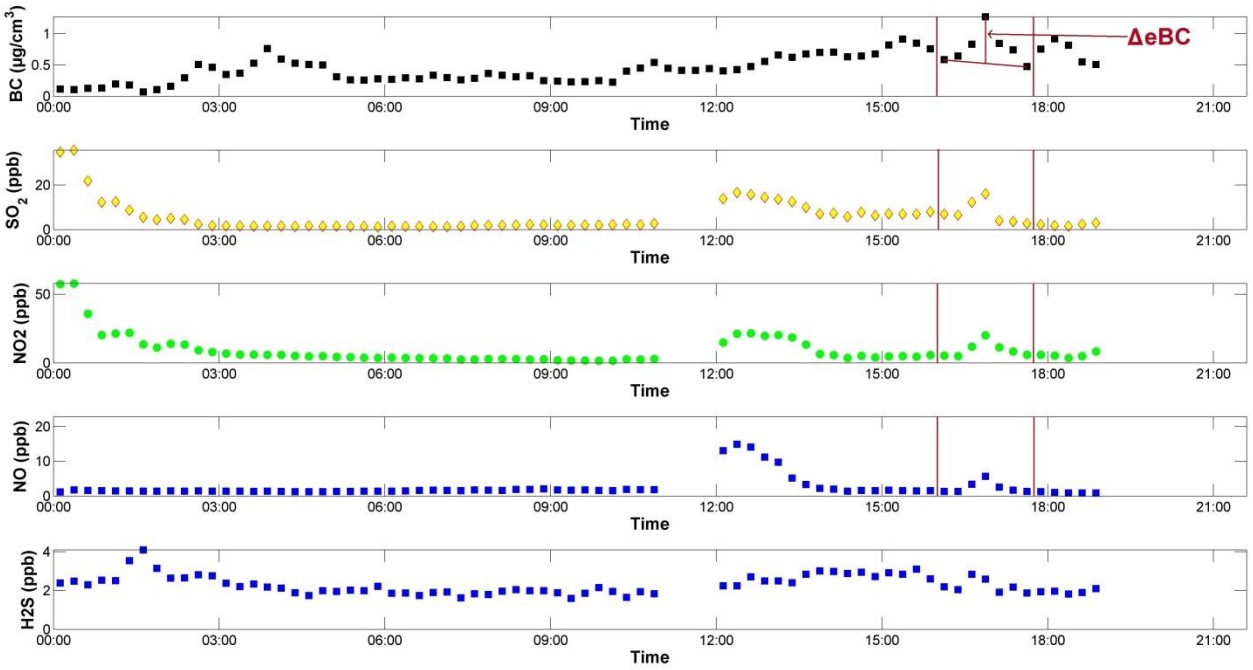

Figure 5.6: Example to illustrate coincidental peaks of SO_2, NO_2 and NO with eBC. Excess eBC (Δ eBC) defined as the eBC concentration above the baseline for this example is also indicated in the top panel

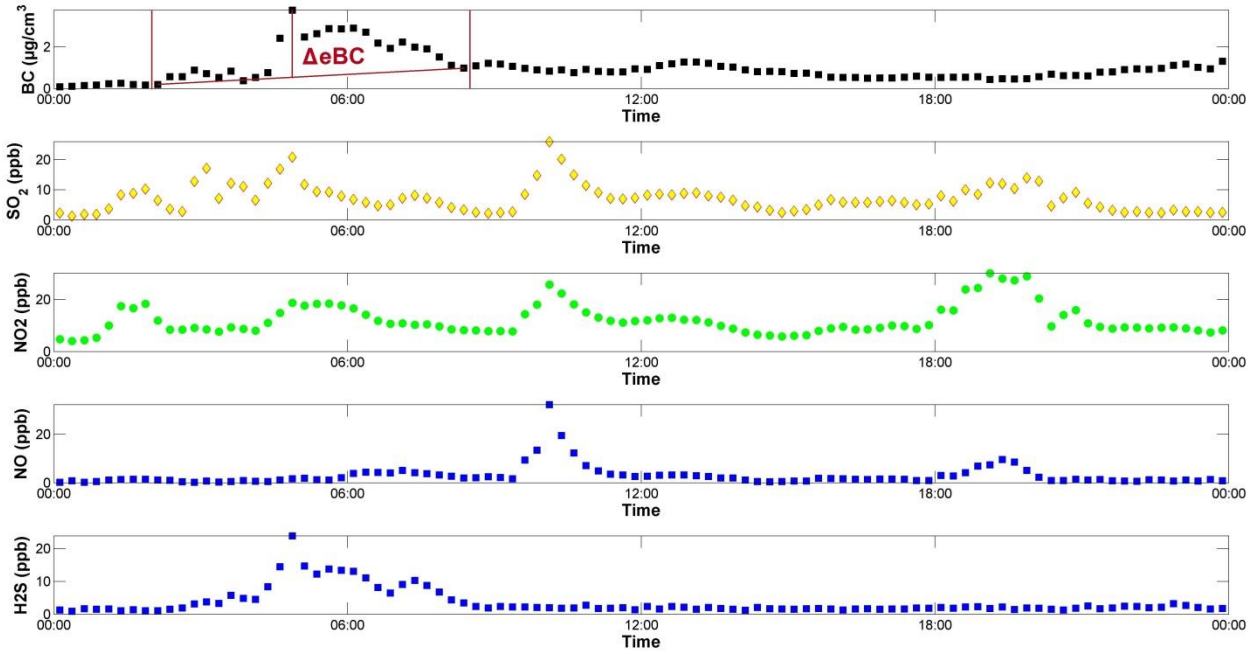

Figure 5.7: Example to illustrate coincidental peaks of H_2S with eBC. Excess eBC (Δ eBC) defined as the eBC concentration above the baseline for this example is also indicated in the top panel

From literature, it is known that plumes from coal-fired power plants on the South African Highveld are characterised by coincidental SO_2, NO_2 and NO increases (Collet et al., 2010; Lourens et al., 2011). Although it is not shown here, eBC plumes that were associated with these species were confirmed to have

originated from coal-fired power stations with back trajectory analyses. However, H_2S peaks that coincided with the eBC peaks could have been from various sources, e.g. the large petrochemical plant near Secunda, pyro-metallurgical smelters in the area or smouldering coal dumps that burn as a result of spontaneous combustion. In order to identify the origin of the eBC peaks that were associated with H_2S only, a map on which all back trajectories that arrived at Elandsfontein during these eBC peaks were plotted is presented in Figure 5.8, together with a wind rose for such events.

From these Figures, it is evident that the back trajectories that were associated with simultaneous eBC and H_2S concentration peaks only passed over the sector between the northwest and northeast from Elandsfontein. This is the area where all the pyro-metallurgical smelters are located. Smouldering coal dumps occur in all directions from Elandsfontein. Additionally, no trajectories associated with coincidental eBC and H_2S increases had passed over the petrochemical operation. It therefore seems likely that the eBC contribution associated with H_2S originates from the pyro-metallurgical smelters in the sector located between northwest and northeast from Elandsfontein.

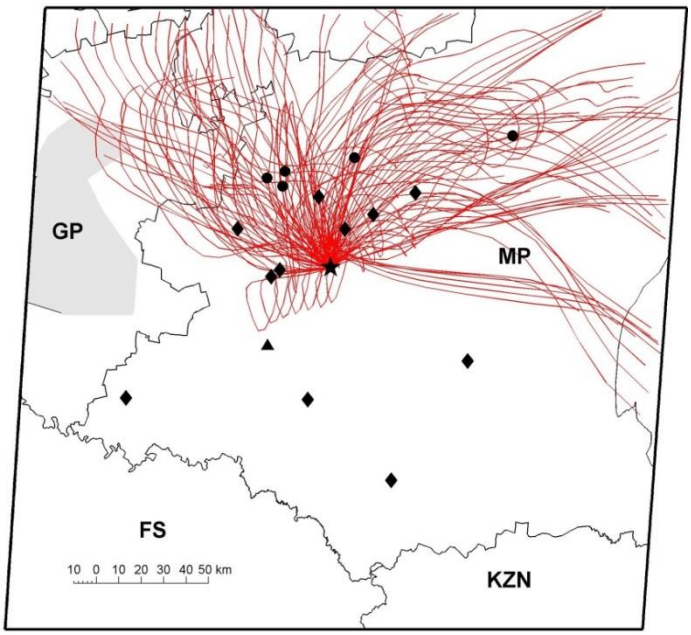

(a)

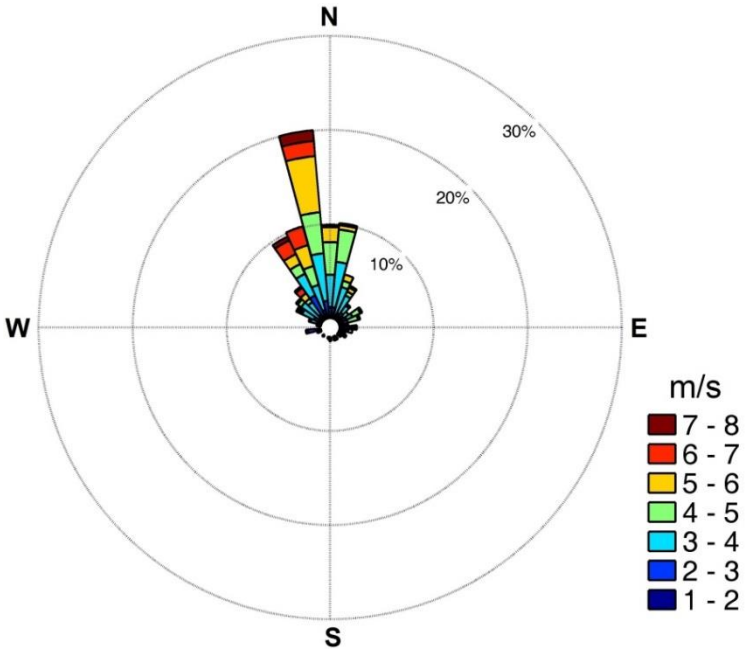

(b)

Figure 5.8: (a) All 24-hour back trajectories associated with peaks characterised by coincidental increases in eBC and H_2S during December to February. Elandsfontein site is indicated by the black star. Dots, diamonds and triangles indicate pyro-metallurgical smelters and char plants, coal-fired power plants and a large petrochemical operation, respectively. (b) The wind rose shows the prevailing wind direction during periods when eBC plumes that coincided with H_2S plumes were observed

5.1.2 Traffic contribution

From literature, it seems feasible to associate increased BC concentrations with traffic emissions, particularly diesel-powered vehicles (Cachier, 1995; Cooke and Wilson, 1996; Bond and Sun, 2005). Such plumes were identified with the method described earlier (Figure 3.9 and associated discussions) which identified coincidental increases of eBC with other pollutants. To isolate traffic contribution, only eBC plumes that coincided with NO_2, as indicated in Figure 5.9 were considered.

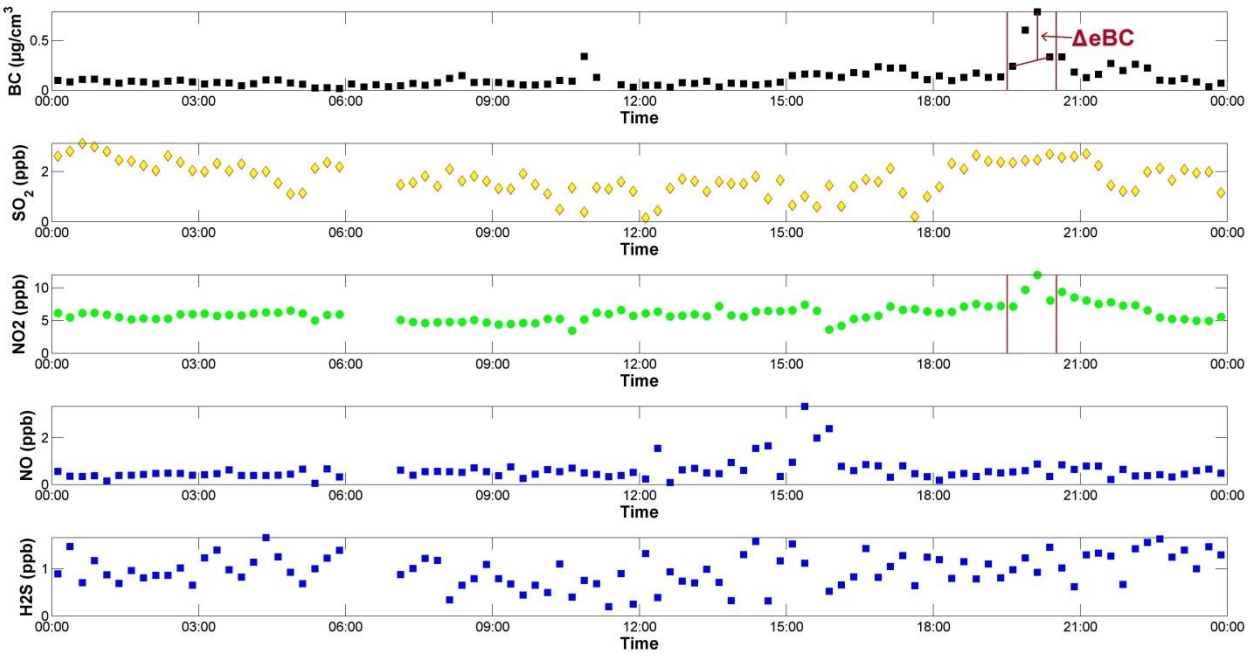

Figure 5.9: Example to illustrate coincidental peaks of NO_2 with eBC. Excess eBC (Δ eBC) defined as the eBC concentration above the baseline for this example is also indicated in the top panel

The Mpumalanga Highveld around Elandsfontein is the area where most thermal coal is mined in South Africa, which is mostly transported by diesel trucks via various roads criss-crossing the area as indicated in Figure 5.10a. However, the closest tarred road, i.e. the R35, passes Elandsfontein approximately 4.7 km to the east. This road is also one of the most utilised for coal road transportation. Additionally, to the north of Elandsfontein, numerous such tarred roads are located, e.g. the national N12 and N4 highways pass Elandsfontein approximately 38 km to the north and north-west respectively. It therefore seems reasonable that the traffic-related eBC back trajectory map (Figure 5.10a) is somewhat biased toward the east and north, although limited contributions from other sectors are also evident. The wind rose showing the prevailing wind direction during periods when eBC plumes that coincided with NO_2 plumes (Figure 5.10b) also indicates the sources to be mainly from the east, i.e. where the R35 passes Elandsfontein.

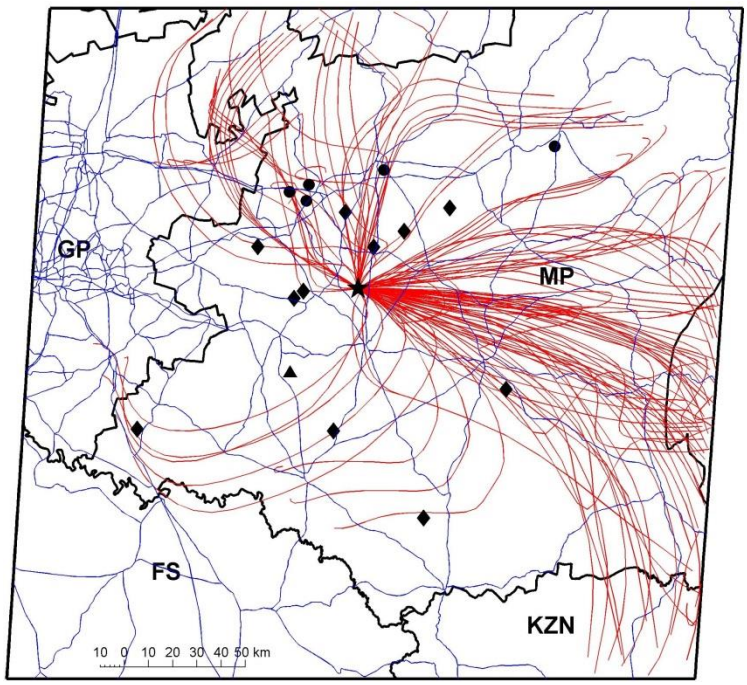

(a)

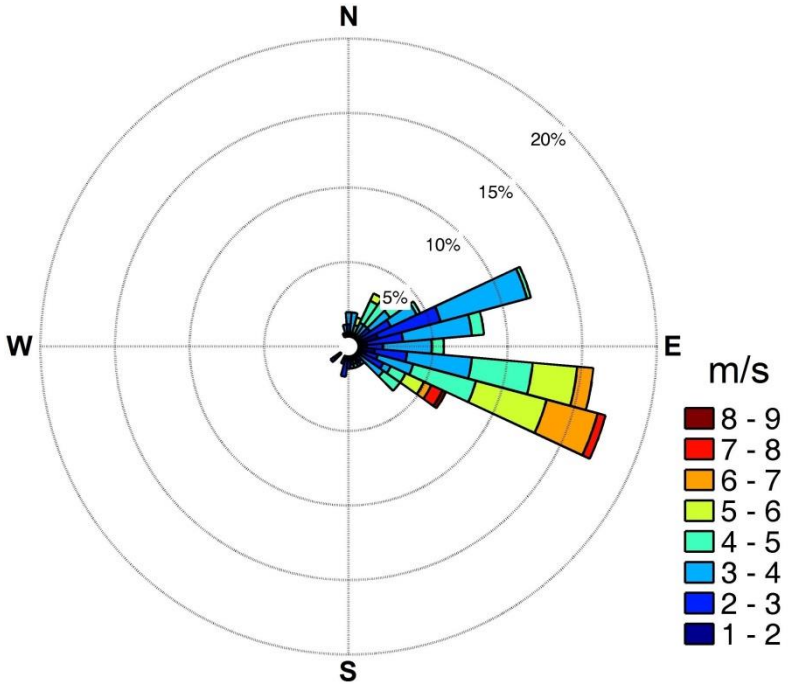

(b)

Figure 5.10: (a) All 24-hour back trajectories associated with peaks characterised by coincidental increases in eBC and NO_2 during December to February. The Elandsfontein site is indicated by the black star. The dots, diamonds and triangle indicate pyro-metallurgical smelters and char plants, coal-fired power plants and a large petrochemical operation, respectively. Roads are indicated with blue lines. (b) The wind rose shows the prevailing wind direction during periods when eBC plumes that coincided with NO_2 plumes were observed

5.1.3 Household combustion contribution

Various authors (e.g. Venter et al., 2012 and Nkosi et al., 2018) have indicated that household combustion for space heating and cooking in in- and semi-formal settlements contributes significantly to poor air quality in such settlements. In Figure 5.11, the relationships between monthly average and median eBC, against monthly mean and median temperatures for Elandsfontein, are presented. As is evident from the results presented in Figure 5.11, there is a significant correlation between eBC concentration and temperature, if August and September are ignored (indicated with hollow markers in Figure 5.11). During these months, significant eBC contributions can be expected from savannah and grassland fires (see Figure 5.1). The correlation between eBC concentration and temperature indicates that household combustion for space heating contributes significantly to eBC levels measured at Elandsfontein, especially during the colder months when household combustion is used more frequently for space heating.

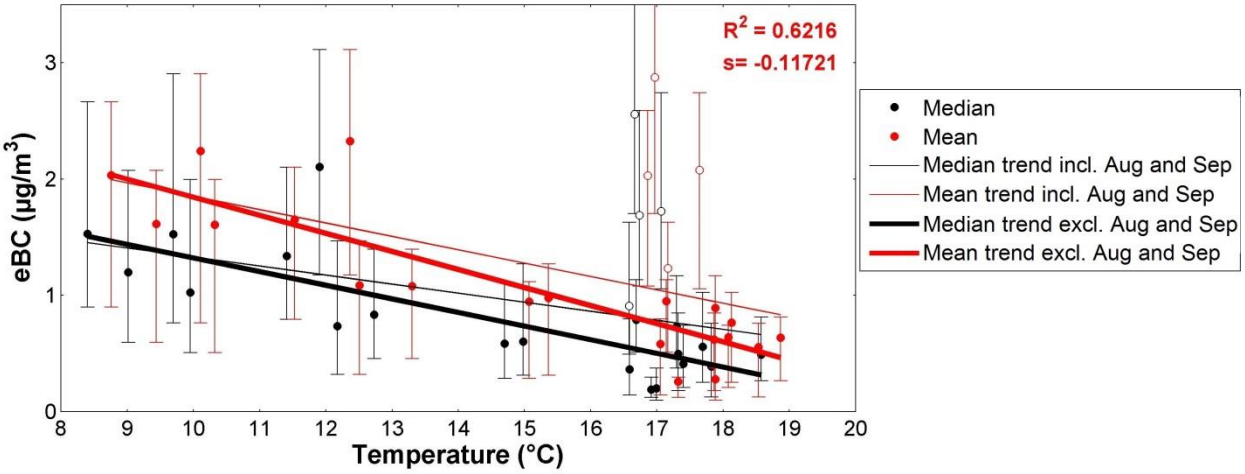

Figure 5.11: Monthly median and mean eBC (with bars indicating 25th and 75th percentiles) plotted against monthly median and mean temperatures for Elandsfontein

Similar to what was done for large industrial point sources (Figure 5.5), eBC concentrations were drawn as a function of the closest distance that back trajectories had passed in- and semi-formal settlement for Elandsfontein. However, this was done only for the winter months of June and July for both years, since household combustion contributions could be better isolated from savannah and grassland fire contributions during these periods. These results are presented in Figure 5.12. Although not conclusive, the results presented indicate that, in general, higher eBC concentrations were observed when trajectories passed closer to in- and semi-formal settlements in June and July.

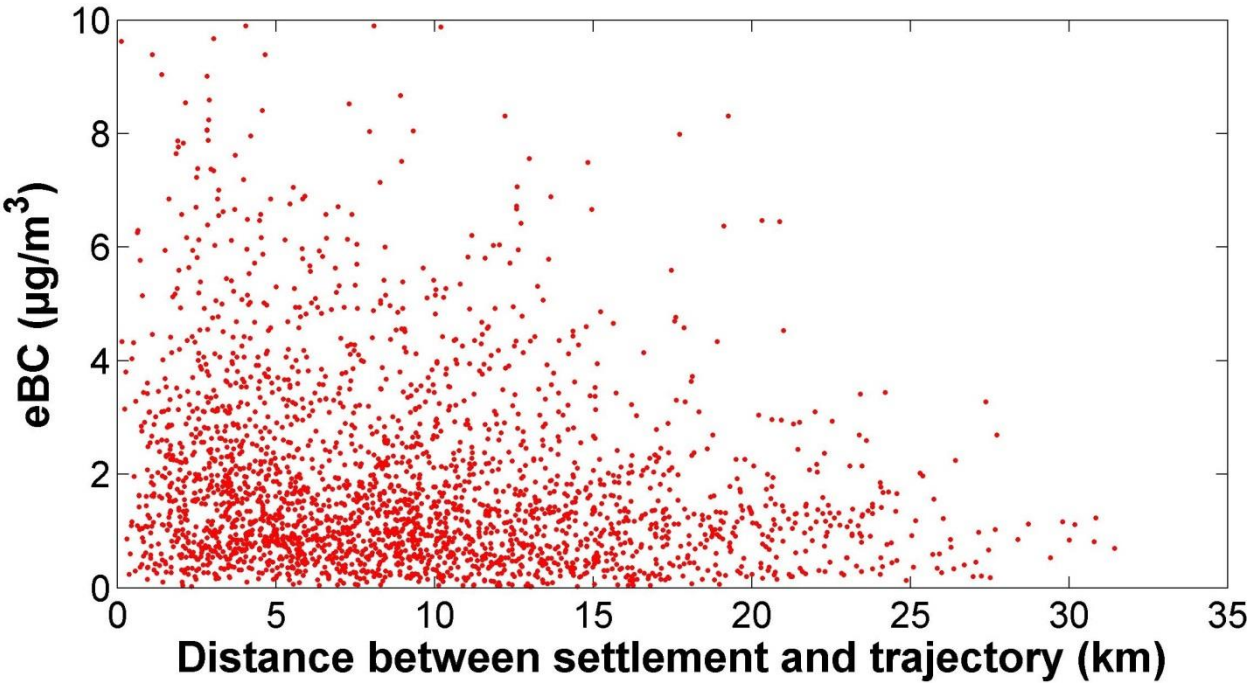

Figure 5.12: eBC concentration plotted against the shortest distances that hourly arriving back trajectories passed in- or semi-formal settlements during the winter months of June and July at Elandsfontein

Household combustion could result in the emission of various atmospheric species (Venter et al., 2012). In this study, tracers for household combustion were determined from species that simultaneously increased with eBC, including NO_2, SO_2 and H_2S, but not NO characterised household plumes measured at Elandsfontein. An example of such simultaneous increases in NO_2, SO_2 and H_2S is presented in Figure 5.13. Low-grade coal that is burned in ineffective stoves is commonly used for household combustion in the Mpumalanga Highveld, due to such coal being relatively inexpensive, and the use of which results in NO_x, SO_2 and H_2S emissions. During the cold winter months of June and July, strong inversion layers trap pollutants emitted closer to ground level and prevent the mixing and subsequent transportation of these pollutants. The low-level emissions from in- and semi-formal settlements are therefore not dispersed before the inversion layers break up during mid-morning. A previous study has indicated that the PBL starts growing around 10:00 local time at Elandsfontein during the winter months (Korhonen et al., 2014). It can therefore be accepted that the low-level inversion layers also start dissipating at that time. The long residence time of air masses around in- and semi-formal settlements in winter before being dispersed, coupled with additional transport time results in NO being oxidised to NO_2 prior to these plumes being measured at Elandsfontein.

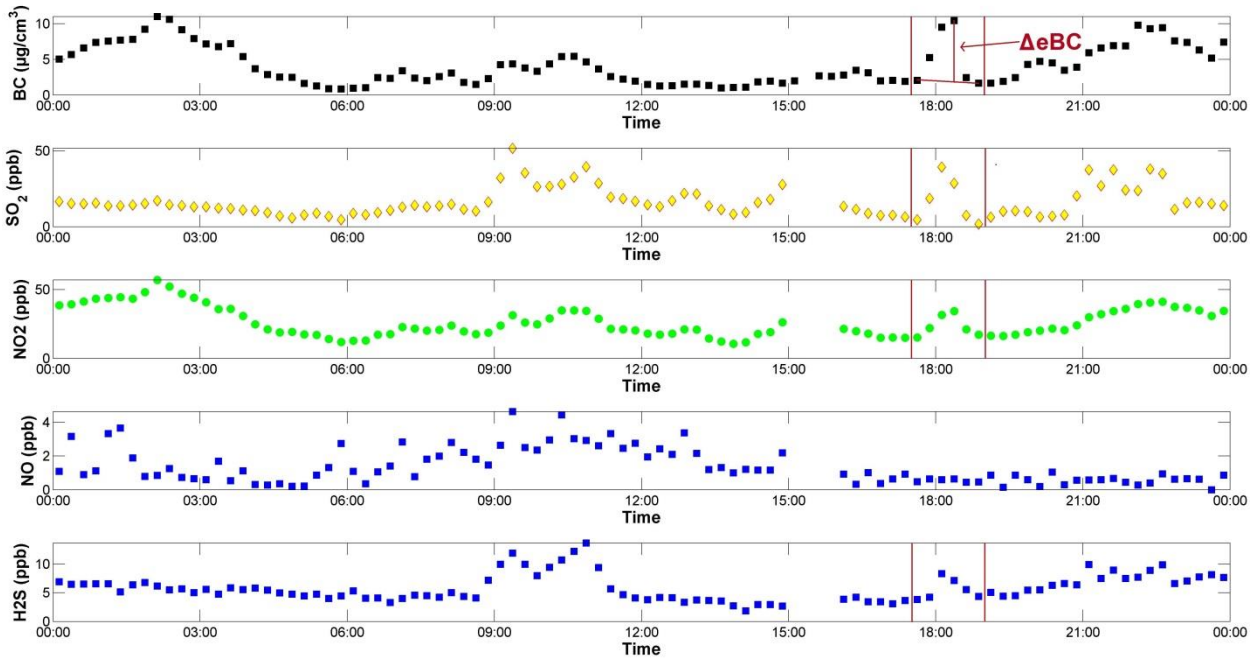

Figure 5.13: Example to coincidental peaks of SO_2, NO_2 and H_2S, but not NO. Excess eBC (Δ eBC) defined as the eBC concentration above the baseline for this example is also indicated in the top panel

Figure 5.14a indicates back trajectories associated with household combustion contribution to eBC levels (for time periods with coincidental increases in eBC with NO_2, SO_2 and H_2S, but not NO). Most of these back trajectories passed over Thubelihle and Kriel residential settlements, which are located 12.4 and 13.8 kilometres from Elandsfontein, respectively. Apart from this relatively local eBC influence from household combustion, most trajectories associated with household combustion eBC plumes passed over the sector between east and north-north-east, where the cities of Witbank and Middelburg, as well as the Johannesburg-Pretoria mega-city are located. These large cities have many more large in- and semi-formal settlements than the smaller towns in the area. Figure 5.14b presents the wind rose showing the prevailing wind direction during periods when eBC plumes that coincided with NO_2, SO_2 and H_2S plumes were observed, indicating sources to be mainly from more or less the same direction as most of the back trajectories.

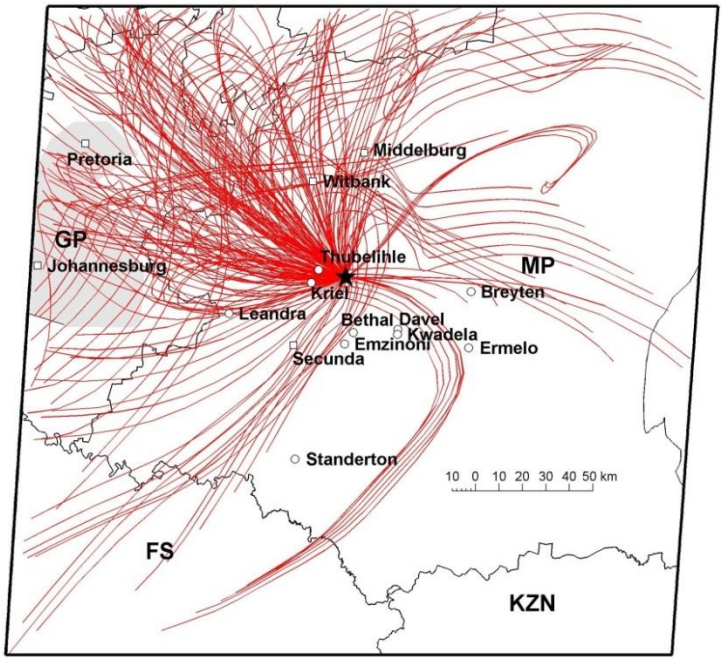

(a)

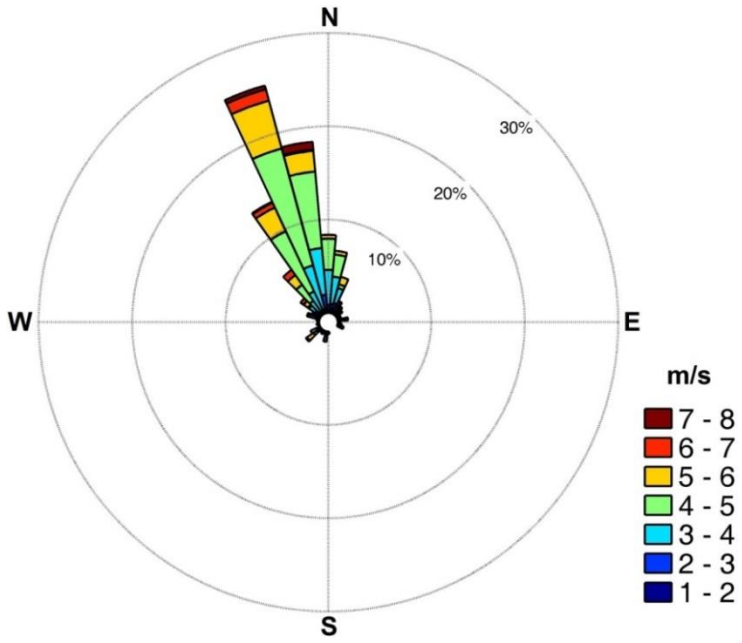

(b)

Figure 5.14: (a) Map indicating 24-hour back trajectories associated with peaks characterised by coincidental increases in eBC with NO_2, SO_2 and H_2S, but not NO in June and July. Elandsfontein site is indicated by the black star. b) The wind rose shows the prevailing wind direction during periods associated with arrival times of plumes associated with household combustion

5.1.4 Savannah and grassland fire contribution

Vakkari et al. (2014) recently indicated how savannah and grassland fire emission aerosols are changed via atmospheric oxidation in South Africa. To positively identify savannah and grassland fire plumes, the afore-mentioned authors used CO and eBC as coincidental increasing species. However, CO was not measured at Elandsfontein and therefore the positive identification of savannah and grassland plume could not be undertaken using this method. Additionally, the plumes of savannah and grassland fires occurring in neighbouring countries arriving at Elandsfontein will be diluted and aged. Such regional fires lift the entire eBC baseline, rather than exhibiting well-defined plumes that can be separated from the baseline (Mafusire et al., 2016), as was done for the industrial, traffic and household combustion sources. Thus far in this thesis, August and September have been considered as the months in which savannah and grassland fires frequencies peak. However, some household combustion might still occur in August due to space heating, since it is still a relatively cold month. Therefore, to determine the overall baseline increase as a result of savannah and grassland fires, only September was considered as being representative of savannah and grassland fires, while the summer months (December to February) can be considered as the baseline. By subtracting the September eBC mean from the summer mean, the eBC baseline increased by 2.01μgm^{-3}. This increase will be contextualised with the previously investigated sources in the next section.

5.1.5 Contextualisation of eBC source strengths

Up to now, individual eBC sources for Elandsfontein were discussed. However, their strengths were not compared with one another. In Figure 5.8, the comparison of the Δ eBC from coal-fired power stations, pyro-metallurgical smelters, traffic, household combustion, as well as savannah and grassland fires for Elandsfontein is presented. The relative savannah and grassland fire source strength is not statistically presented with a box and whisker like other sources, but only with a black star that indicates the mean eBC baseline increase during September when compared to the summer months of December to February. The data presented in Figure 5.15 were normalised to account for variations in the planetary boundary layer (PBL) height at Elandsfontein. This was done by using the monthly average PBL daily maximum heights reported by Korhonen et al. (2014) for 2010 at Elandsfontein. Unfortunately, no such data existed for 2009, therefore the 2009 monthly PBL heights were assumed to be similar to 2010. Thereafter, the ratios of the average PBL daily maximum heights for each of the periods during which certain sources could be better isolated (i.e. December to February for large point sources and traffic emission; and June to July to household combustion) were calculated and compared to the average PBL daily maximum heights for August and September (period with peak savannah and grassland fire occurrence). The Δ eBC for each of the sources identified during the December to February and June to July periods where then adjusted with these ratios to account for variations in the PBL, which could have a significant dilution or concentration effect on the measured eBC values, from which the Δ eBCs were derived. The results indicate the

significant source strength of household combustion, as well as savannah and grassland fires, as measured at Elandsfontein. However, coal-fired power stations, pyro-metallurgical and/or char plants and traffic contribute throughout the year, while household combustion, as well as savannah and grassland fires only contribute significantly in May to August, and June to September, respectively. Bond et al. (2013) indicated relatively high BC emissions from biofuel cooking (calculated for Africa in total), but did not indicate space heating to contribute significantly. However, our data seem to prove that space heating does contribute considerably to eBC levels in South Africa, particularly during cold winter months (June-July).

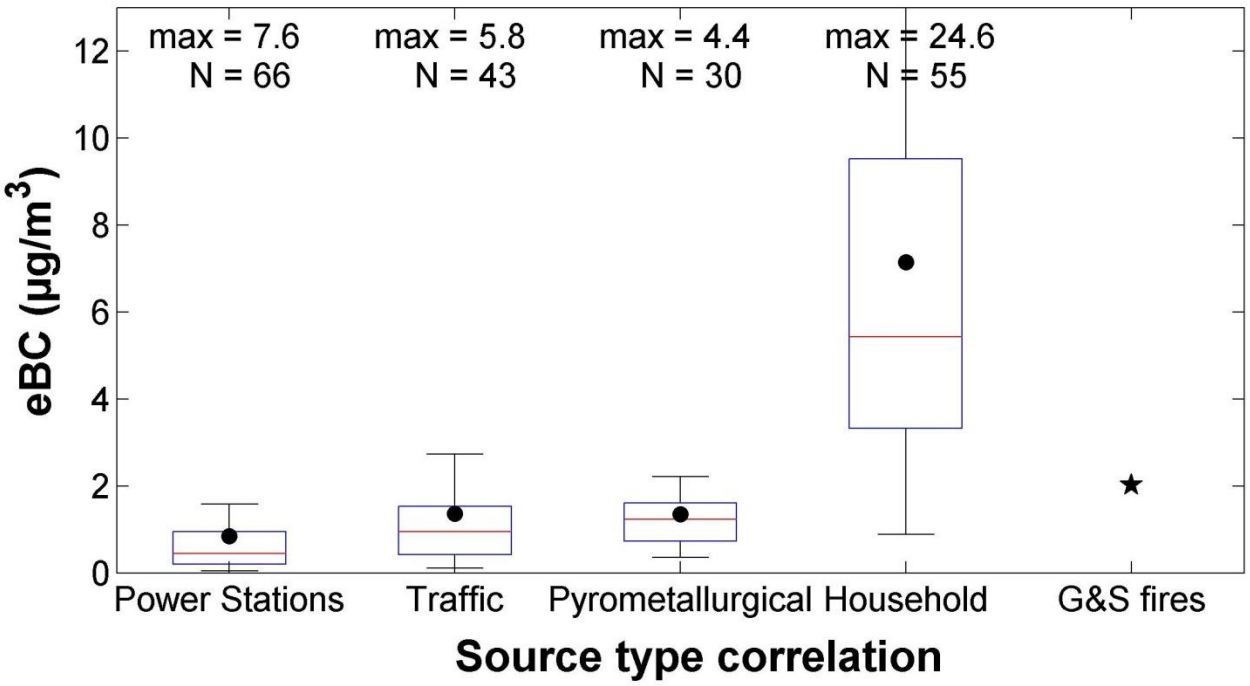

Figure 5.15: Δ eBC measured during plumes when eBC increases originated from coal-fired power station, traffic, pyro-metallurgical smelters and household combustion as measured at Elandsfontein. The overall mean baseline increase due to savannah and grassland (G&S) fires in September are indicated with a black star. This data was normalised to variations in boundary layer at Elandsfontein (Korhonen et al., 2014)

Vakkari et al. (2014) used Δ eBC in relation to other species to characterise differences in plumes of savannah and grassland fires. In a similar manner, these ratios for Δ eBC divided by species that were characteristic of the different plume types identified (i.e. representing industrial, traffic or house hold combustion) were determined and are presented in Figure 5.16. Since so little BC data is available for South Africa, the median and/or mean values indicated in this figure could be used in subsequent modelling studies as emission factors to estimate eBC if only the concentration(s) of the species that were used in calculating these ratios are known.

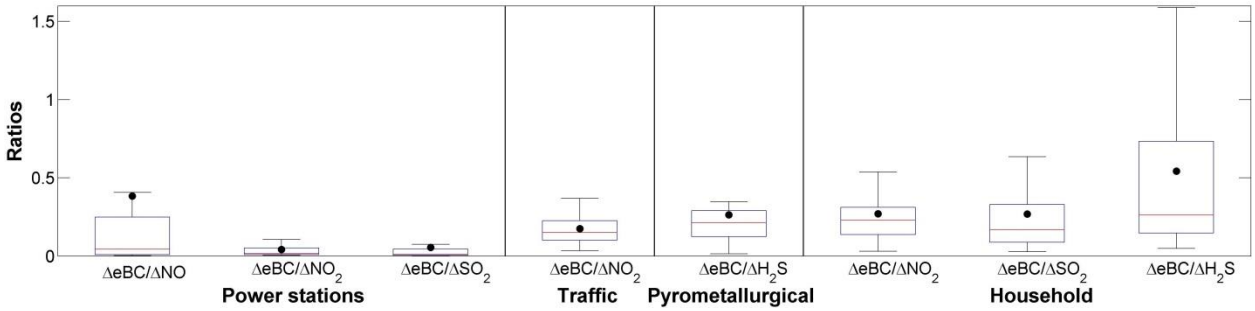

Figure 5.16: Ratio of Δ eBC divided by Δ of other species relevant to the identification of each source type, except for grassland and savannah fires measured at Elandsfontein.

5.2 Conclusion

Possible contributing eBC sources were explored in greater detail for Elandsfontein only. Industrial sources could be isolated best during the summer months of December to February, since very few savannah and grassland fires, as well as household combustion for space heating occur then. Coincidental plumes of SO_2, NO_2, NO and eBC were used to identify plumes from coal-fired power stations, while coincidental increases of H_2S and eBC characterised eBC contributions from pyrometallurgical smelters. During summer, coincidental increases of NO_2 and eBC were used to identify traffic emissions. The contribution of household combustion was isolated during the coldest winter months of June and July. Coincidental increases of NO_2, SO_2 and H_2S, with eBC, which did not correlate to NO increases, were found to characterise household combustion plumes. Back trajectory analyses and wind roses supported the validity of all the aforementioned source associations. Savannah and grassland fire plumes could not be isolated since CO was not measured at Elandsfontein. However, the general baseline increase in eBC levels between September (the peak fire frequency period) and the summer months (with virtually no savannah and grassland fires) could be calculated and attributed to savannah and grassland fire eBC emissions. At Elandsfontein, the eBC concentration in September was comparable to the eBC concentration in June to July, which indicates that at this location domestic heating and regional scale savannah and grassland fires are equally significant sources of eBC.

Although the source strengths of coal-fired power stations, pyro-metallurgical smelters and traffic emissions were lower than that of household combustion, as well as savannah and grassland fires, the first mentioned sources contribute throughout the year, while the latter only contributed significantly in May to August, and June to September, respectively. Of the fresh industrial plumes, the highest eBC concentrations were associated with pyro-metallurgical smelters. This is a significant finding, since coal-fired power stations and petrochemical operations have in the past been attributed for most of the pollution problems on the Mpumalanga Highveld (mainly due to the fact that this area has been identified as NO_2 hotspot). Therefore, contributions resulting from pyrometallurgical sources in this area need to be considered in greater detail in future studies to obtain a comprehensive picture. Lastly, the calculated emission ratios of

eBC and gaseous species that were presented could be used in future modelling studies as emission factors for sources in South Africa.

CHAPTER 6 MATHEMATICAL CONFIRMATION OF eBC SOURCES AT ELANDSFONTEIN

Various multivariate analysis methods can be used to conduct or confirm source apportionment. These methods provide both descriptive and inferential procedures that allow the search for patterns in the data, or test hypotheses about patterns of a priori interest. With multivariate descriptive techniques one can peer beneath the tangled web of variables on the surface and extract the essence of the system. Some examples of these methods include multivariate linear regression (MLR) andprincipal component analysis (PCA), amongst others (Rencher, 2002). MLR was used in this study.

6.1 MLR analysis

MLR explores the linear relationship between one or more y's (the dependent or response variables) and one or more x's (the independent or predictor variables). It uses a linear model to relate the y's to the x's and is concerned with the estimation and testing of the parameters in the model. In this thesis, MLR was used to mathematically verify in an independent manner (i.e. mathematically, without the possible source-related prejudices of the candidate) if the source deductions made in Chapter 5 were valid. This method has been used by various authors to conduct data analysis and gain insight (e.g. Venter et al., 2015, Du Preez et al., 2015; Jaars et al., 2014).

6.2 Mathematical confirmation of eBC sources at Elandsfontein

Four scenarios were investigated with MLR analyses. Firstly, MLR analysis was conducted for the entire monitoring period at Elandsfontein. As evident from Figure 6.1(a), the RMSE difference between the experimental (actual measured) and the calculated eBC concentration if only one independent parameter was included in the optimum MLR solution was approximately 1.54. The RMSE difference could be reduced by including more independent parameters in the optimum MLR solution. However, it was found that the inclusion of more than nine independent parameters did not further reduce the RMSE difference significantly. From the MLR analysis conducted for the entire measurement period at Elandsfontein, the actual MLR equation obtained is presented as Equation 3. With this equation, eBC concentration at Elandsfontein could be calculated. The comparisons between actual and calculated (with Equation 3) eBC concentrations are presented in Figure 6.1 (b). From this comparison, it is evident that Equation 3 could be used to predict eBC at Elandsfontein relatively accurately.

$$y = -33.7038 + (0.0050 \times O_3) + (0.0387 \times SO_2) + (0.0006 \times NO_2) + (0.0722 \times H_2S) + (-0.0174 \times RH) + (0.0997 \times WS) + (0.0005 \times WD) + (0.0421 \times P) + (2.27433 \times T\text{-grad}) \quad \text{Eq. 3}$$

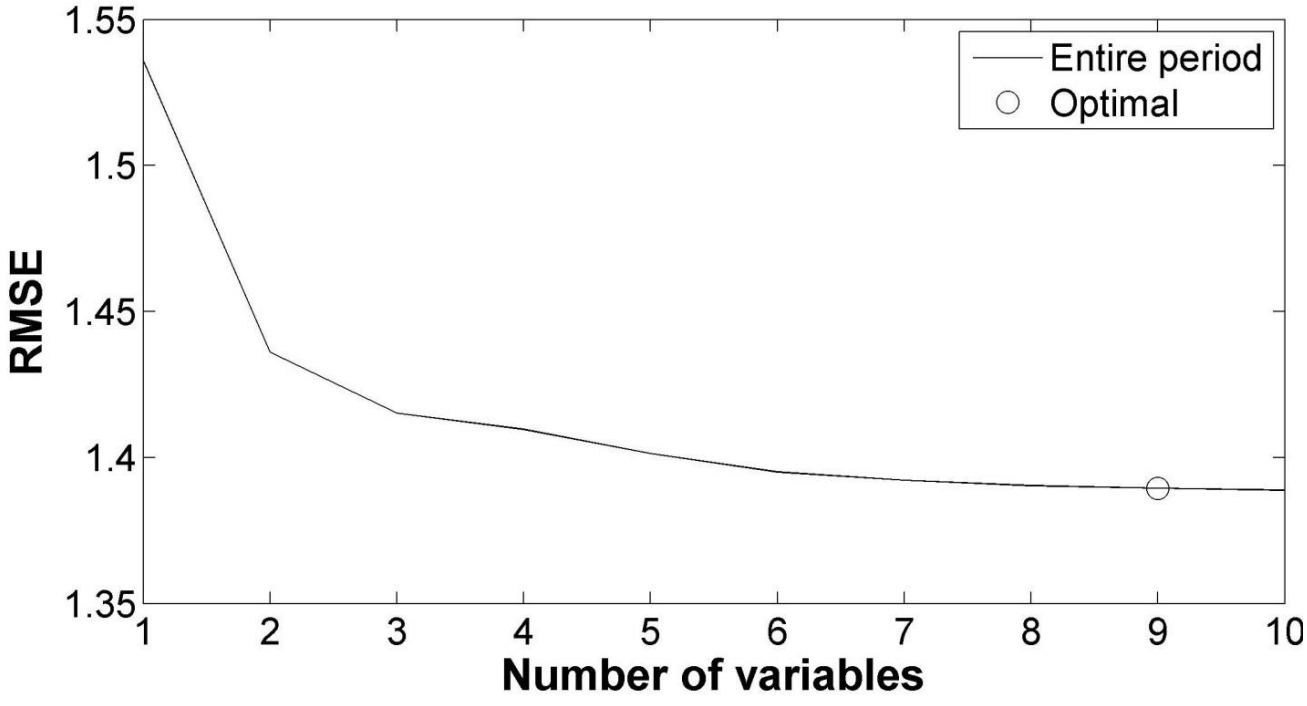

(a)

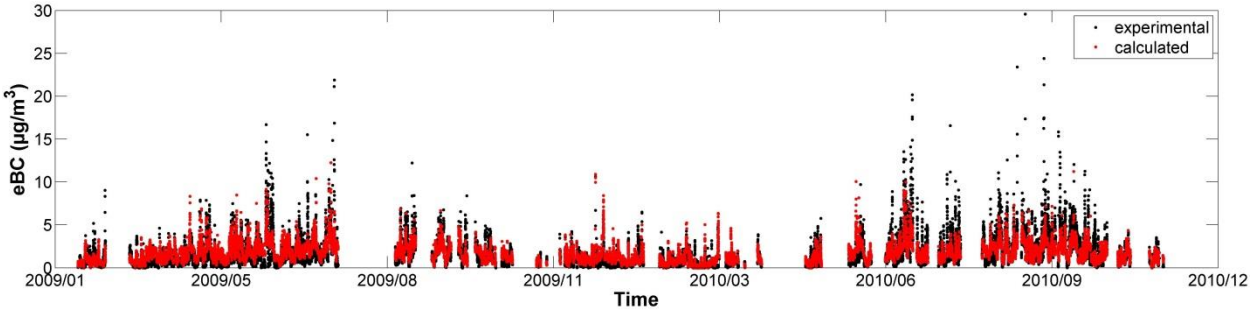

(b)

Figure 6.1: (a) RMSE difference between the MLR calculated eBC and the actual measured eBC at Elandsfontein for the entire measurement period. (b) Actual eBC compared with calculated (using Eq. 3) for the entire monitoring period at Elandsfontein

To further verify whether the eBC contribution sources were identified correctly in Chapter 5, MRL analyses were also conducted for the different time periods defined for isolation of the various sources, i.e. December to February for industrial and traffic sources, June and July for household combustion, and August and September for savannah and grassland fires. As is indicated in Equation 4 and Figure 6.2 (a), the optimum MLR solution obtained for the December to February period included seven independent variables in the equation. Firstly, the fact that fewer independent variables were required to reduce the RMSE optimally, if compared with the overall period in Figure 6.2 (a) indicates that the December to February period is less complicated (which could imply, but does not necessarily mean less sources) in

terms of contributing sources than the overall period. Secondly, the identity of the independent variables and the sign (positive or negative) associated with them in Equation 4 are noteworthy. For instance, increased O_3 concentrations led to lower eBC, which indicates that aged air masses had lower eBC than fresh plumes do. This supports the notion that relatively nearby industry and traffic sources dominated eBC levels at this site, during the specified time period. The increased eBC associated with increased NO_2 and H_2S concentrations in Equation 4 supports the identity of the specific source types previously identified, i.e. coal-fired power stations, pyrometallurgical smelters, as well as traffic emissions. The remaining independent variables in Equation 4 are associated with meteorological parameters, which could indicate that meteorological patterns (e.g. atmospheric stability as indicated by T-gradient) could have a significant influence on plumes containing eBC measured at Elandsfontein.

$$y = -30.3494 + (-0.0170 \times O_3) + (0.0002 \times NO_2) + (0.1005 \times H_2S) + (0.1350 \times T) + (0.0102 \times RH) + (0.0338 \times P) + (1.8185 \times \text{T-gradient}) \quad \text{Eq. 4}$$

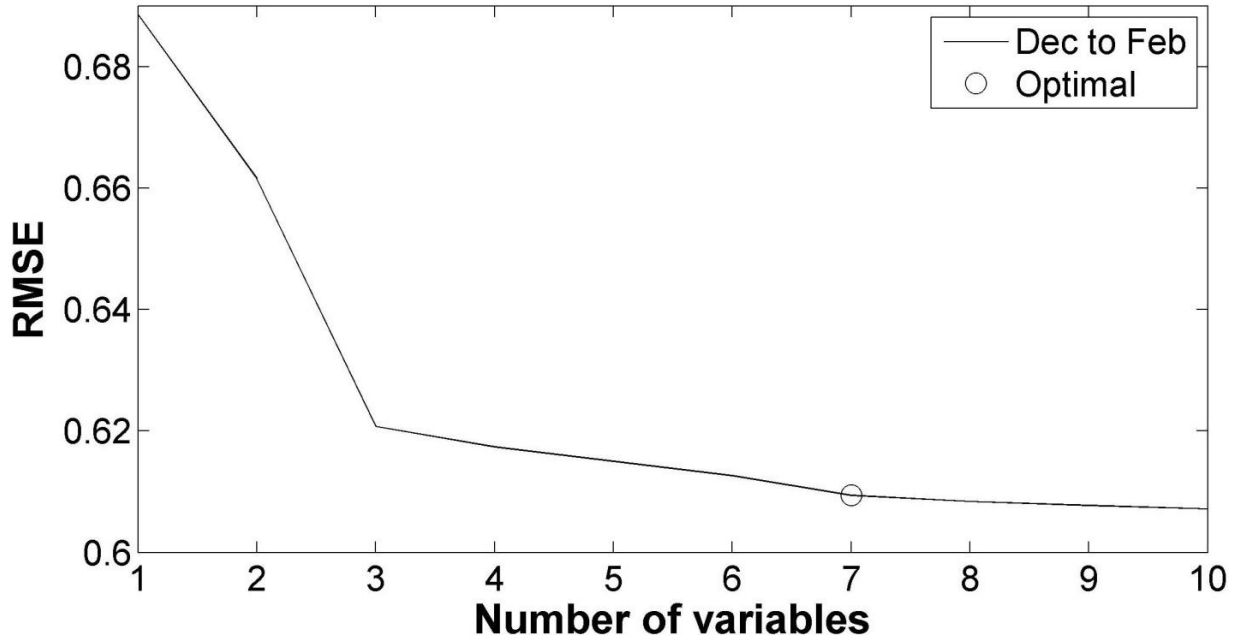

(a)

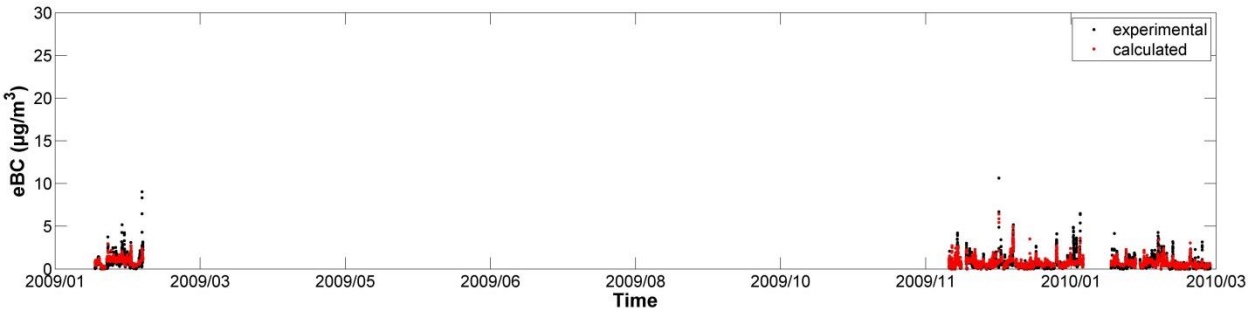

(b)

Figure 6.2: (a) RMSE difference between the MLR calculated eBC and the actual measured eBC at Elandsfontein for the summer (DJF) period. (b) Actual eBC compared with calculated (using

Eq. 4) for the summer (DJF) period at Elandsfontein

For the June and July periods, Equation 4 and the lower left panel of Figure 6.3 (a) indicate that the optimum MLR solution included only four independent variables in the equation. The fact that fewer independent variables were required to reduce the RMSE optimally, if compared with the overall period in Figure 6.3 (a) indicates that the December to February period was influenced by fewer eBC sources. This low number of independent variables confirm that this time period was dominated by a much less complicated source mixture than the overall time period. During June to July, it was previously indicated that household combustion dominated eBC contributions, which is confirmed by the SO_2- and NO_2-associated eBC increases indicated by Equation 5. As stated earlier, the household combustion plumes measured at Elandsfontein are likely to be NO depleted, due to the stagnant nature of air masses during the evening and early morning that result in the oxidation of NO to NO_2. This phenomenon is also indicated by Equation 4. Lastly, increased relative humidity (RH) will be associated with increased moisture-induced particle growth that could result in quicker aerosol deposition and therefore reduced eBC levels.

$$y = 1.7061 + (0.0453 \times SO_2) + (-0.1059 \times NO) + (0.0855 \times NO_2) + (-0.0191 \times RH) \quad \text{Eq. 5}$$

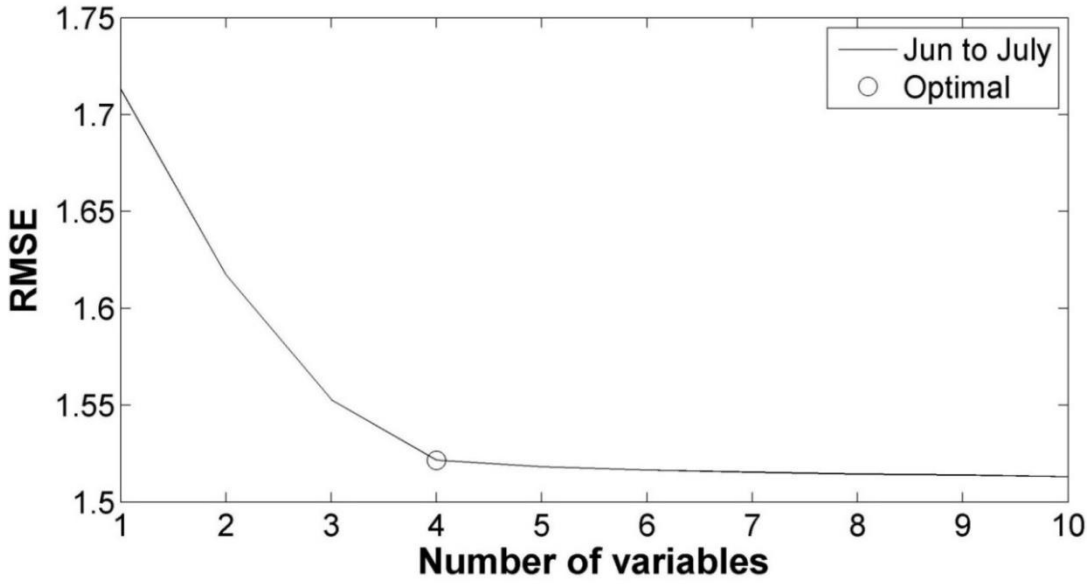

(a)

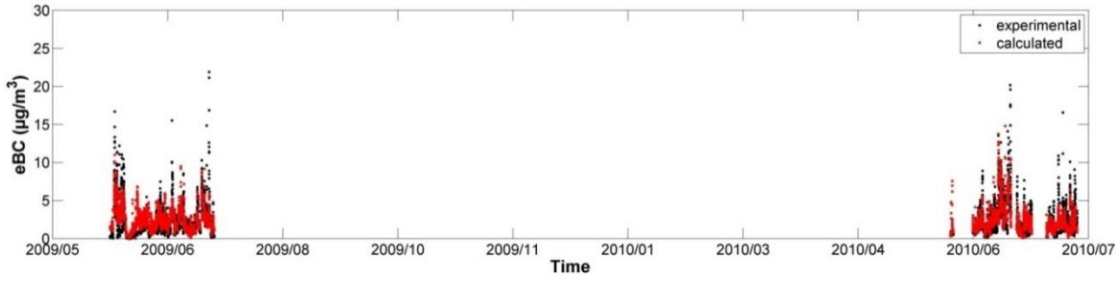

(b)

Figure 6.3: (a) RMSE difference between the MLR calculated eBC and the actual measured eBC for the

winter (JJ) period at Elandsfontein. (b) Actual eBC compared with calculated (using Eq. 5) for the winter (JJA) period at Elandsfontein

For the August and September periods, Equation 6 and Figure 6.4 (a) indicate that the optimum MLR solution included eight independent variables in the equation. Although not as low as for the June and July period, this low number of independent variables confirms that the August and September period eBC sources were less complicated than for the overall time period. According to Equation 6, increased O_3 for August to September had a positive constant associated with it, which indicates that aged savannah and grassland fire plumes increase the eBC concentrations, while the NO_2 and SO_2 positive constant associations and the negative NO constant association indicate that household combustion also contributes to eBC concentrations during this time. This makes sense, since August is regarded as a winter month with significant household combustion for space heating taking place. However, since the August and September periods already include warmer spring months (September for both years) with lower household combustion, the H_2S, T, RH and T-grad relationships observed in summer also already make a meaningful contribution.

$$y = -2.549 + (0.0511 \times O_3) + (0.0316 \times SO_2) + (-0.5737 \times NO) + (0.1840 \times NO_2) + (0.0433 \times H_2S) + (0.0469 \times T) + (0.0145 \times RH) + (2.4877 \times \text{T-grad}) \quad \text{Eq. 6}$$

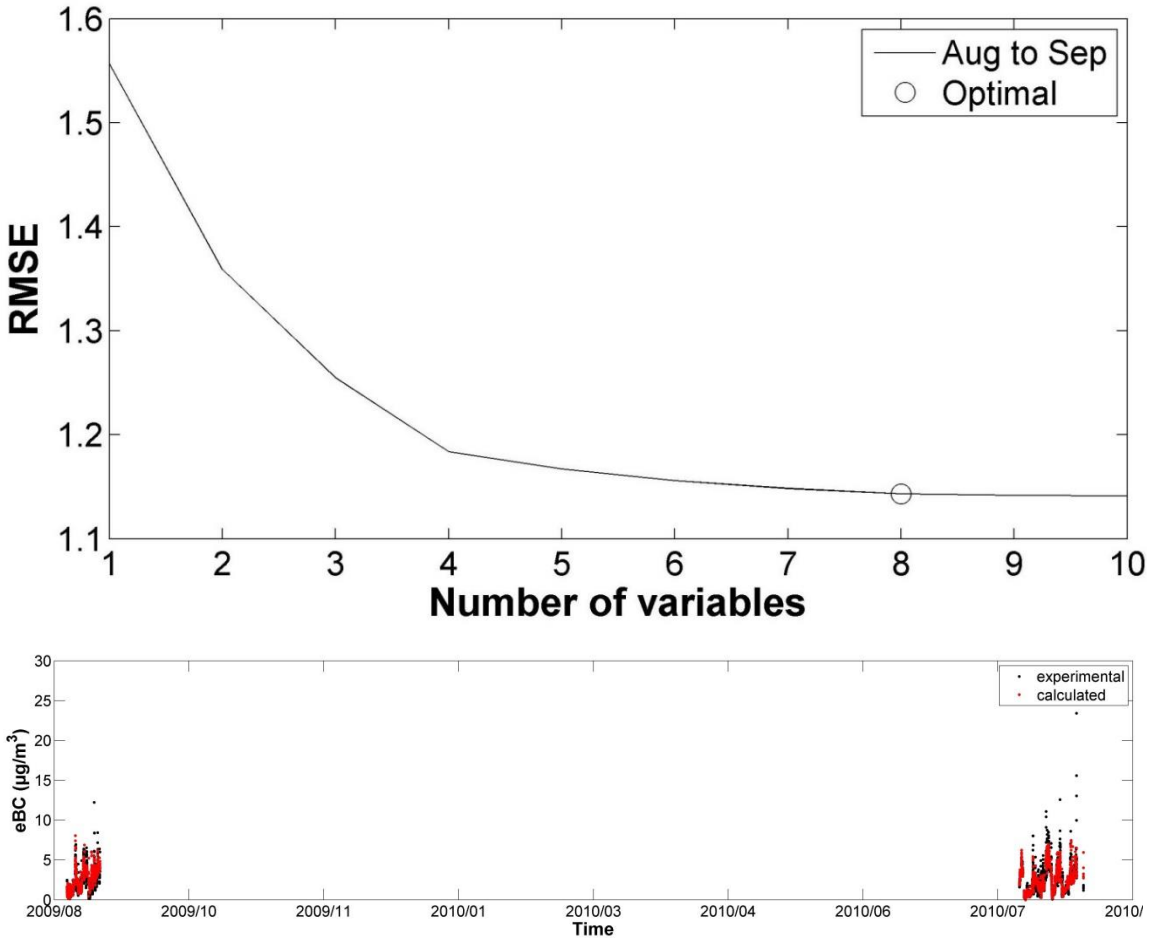

Figure 6.4: (a) RMSE difference between the MLR calculated eBC and the actual measured eBC at Elandsfontein for August and September. (b) Actual eBC compared with calculated (using Eq. 6) for the entire monitoring period at Elandsfontein

6.3 Conclusion

The statistical/mathematical results obtained in this chapter confirmed that the sources identified in Chapter 5 were correct. The lower number of independent variables for selected periods (which correlated with specific source types), comparison to the MLR solution for the entire sampling period, confirmed the seasonal dominance of certain sources.

CHAPTER 7: MAIN CONCLUSIONS, PROJECT EVALUATION AND FUTURE PERSPECTIVES

In this chapter, the main conclusions are presented. This is followed by a project evaluation, within the context of the objectives set in Chapter 1. Thereafter, future perspectives (e.g. research gaps and opportunities) identified during the course of this study are presented.

7.1 Main conclusions

Analyses of eBC and EC spatial concentration patterns at eight sites indicate that concentrations in the South African interior are in general higher than what has been reported for the developed world, e.g. Western Europe. The highest levels were observed at the Vaal Triangle, which were attributed to EC emissions from household combustion emanating from in- and semi-formal settlements, as well as traffic and large point sources. eBC or EC levels at Elandsfontein, Amersfoort and Marikana were similar, but likely originated from different sources. Elandsfontein and Amersfoort lie within the well-known NO_2 hotspot over the Mpumalanga Highveld and are therefore likely to be influenced by industrial activities in this area, while Marikana is in close proximity to in- and semi-formal settlements. The background sites, i.e. Welgegund, Botsalano, Louis Trichardt and Skukuza, had lower eBC or EC levels. All these background sites are likely to be affected most by regional savannah and grassland fires, which are common in southern Africa.

Similar seasonal patterns were observed at all three sites where high resolution eBC data were collected, i.e. Elandsfontein, Marikana and Welgegund, with the highest eBC concentrations measured in June to October. These months coincide with the cold winter months of June to August that indicate possible contributions from household combustion, as well as the dry season on the South African Highveld occurring between May and mid-October, which indicates contributions from savannah and grassland fires. Diurnal patterns indicated that, at Elandsfontein, industrial high stack emissions were not the most significant source, since no peaks were observed after the breakup of lower-level inversion layers. The diurnal patterns at Marikana revealed household combustion for space heating and cooking to be the most significant sources. At Welgegund, the most significant source contribution was most likely regional savannah and grassland fires.

Possible contributing eBC sources were explored in greater detail for Elandsfontein only. Industrial sources could be isolated best during the summer months of December to February, since very few savannah and

grassland fires, as well as household combustion for space heating occur then. Coincidental plumes of SO_2, NO_2, NO and eBC were used to identify plumes from coal-fired power stations, while coincidental increases of H_2S and eBC characterised eBC contributions from pyrometallurgical smelters. During summer, coincidental increases of NO_2 and eBC were used to identify traffic emissions. The contribution of household combustion was isolated during the coldest winter months of June and July. Coincidental increases of NO_2, SO_2 and H_2S, with eBC, which did not correlate with NO increases, were found to characterise household combustion plumes. Back trajectory analyses and wind roses supported the validity of all the aforementioned source associations. Savannah and grassland fire plumes could not be isolated, since CO was not measured at Elandsfontein. However, the general baseline increase in eBC levels between September (the peak fire frequency month) and the summer months (December to February, with virtually no savannah and grassland fires) could be calculated and attributed to savannah and grassland fire eBC emissions. At Elandsfontein, the eBC concentration in September was comparable to the eBC concentration in June to July, which indicates that, at this location, domestic heating and regional scale savannah and grassland fires are equally significant sources of eBC. Furthermore, multilinear regression (MLR) analyses supported the seasonality of eBC sources at Elandsfontein.

Although the source strengths of coal-fired power stations, pyro-metallurgical smelters and traffic emissions were lower than that of household combustion, as well as savannah and grassland fires, the first-mentioned sources contribute year round, while the latter only contributed significantly in May to August, and June to September, respectively. Of the fresh industrial plumes, the highest eBC concentrations were associated with pyro-metallurgical smelters. This is a very significant finding, since coal-fired power stations and petrochemical operations have in the past been blamed for most of the pollution problems on the Mpumalanga Highveld (mainly due to the NO_2 hotspot over this area). Therefore, pyrometallurgical sources in this area need to be considered in greater detail in future studies. The calculated emission ratios of eBC and gaseous species that were presented could be used in future studies to assess the eBC emission inventories for industrial and domestic sources in South Africa.

Although this was a technical study (focusing on the science), some policy-related decisions/deductions could be made from it, i.e. targeted sector-specific reduction measure to address BC emissions. Since BC is a short-lived climate forcing species (and air quality pollutant, as part of fine particulate matter), reductions in ambient levels could have a significant regional benefit. However, such decisions/deductions should be cost-effective and considered only after a tailored assessment that accounts for the countries' resources and needs has been completed to ensure lasting human health, environmental and climate benefits. The results presented in this PhD provide a strong foundation for the afore-mentioned and indicates the need to expand related research in South Africa.

7.2 Project evaluation

In order to evaluate the success and shortcomings of this study, specific objectives set at the beginning of the study have to be considered. These study objectives with specific outcomes are presented below:

- ***Objective 1****: Assess spatial and temporal (seasonal and diurnal) trends of BC over the northern interior of South Africa. Data from several measurement sites will be considered and general deduction with regard to possible sources will be derived from the spatial and temporal trends.*

Outcome/evaluation: This study provided an assessment of spatial and temporal (seasonal and diurnal) trends of BC over the South African interior using data collected from several BC measurement sites (EL, MA, WE, LT, SK, VT, AF and BT). During this assessment, preliminary possible BC source deductions from the trends were also made. Detailed findings from this assessment are presented in Chapter 4.

- ***Objective 2:*** *Determine potential contributing source strengths for at least one of the measurement sites for which high resolution continuous data were available.*

Outcome/evaluation: Potential contributing sources strengths of BC were assessed using data collected from Elandsfontein monitoring site only, since it is the site that was deemed to be influenced by the most complex (diverse) source mixture. The other two sites, where continuous high resolution data were collected (i.e. Welgegund and Marikana), were influenced mainly by single dominant sources (i.e. savannah and grassland fires at Welgegund; household combustion at Marikana). These findings are presented in Chapter 5.

- ***Objective 3:*** *Use a multivariant statistical method to confirm that the above-mentioned deductions made regarding source contributions were valid. Such a statistical evaluation will prevent biases that could have arisen due to preconceptions of the candidate.*

Outcome/evaluation: Potential contributing source deductions made from the source assessment (Chapter 5) were validated and confirmed using a multilinear regression method. These findings are presented in Chapter 6.

Given the above-mentioned outcome evaluations within the context of the specific objectives, the candidate considers the project as successful. However, this does not imply that the project was perfect or that all research graphs have been addressed. Remaining research and knowledge gaps that can be considered are discussed in the next section.

7.3 Future perspectives

To further enhance the BC knowledge base in South Africa and to address research gaps that were identified during the study, the following future work should be considered:

- Although this thesis presents the most comprehensive eBC spatial, temporal and source contribution assessments for the South African interior that has been published in the peer-reviewed public domain to date, the spatial coverage of eBC measurements is still limited in the country. Limited studies by, for example Fieg et al. (2015), only show basic BC analysis of data collected from some of the national DEA BC monitoring stations with findings published in the local peer reviewed domain, i.e. the Clean Air Journal (Feig et al., 2015). A comprehensive analysis of the data from these stations should be considered and resourced to improve SA's understanding of BC and its associated impacts (on human health, the environment and global warming).
- In this study, a comprehensive source apportionment of BC was undertaken for the Elandsfontein monitoring site only. A similar approach, as presented in this study, could be followed to conduct BC source apportionment for other sites where comprehensive datasets are acquired.
- BC contributions resulting from pyrometallurgical sources in the Mpumalanga Highveld need to be considered in greater detail in future studies. To date, emissions for these sources have not received as much attention as the coal-fired power stations and petrochemical operations.
- Expansion on the spatial coverage of BC measurements sites to include areas that are currently not covered by the national DEA BC monitoring programme (as outlined in Chapter 2) is recommended; therefore, expanding BC monitoring to cover additional areas outside of the national priority areas, prioritising residential areas with the aim of characterising the impacts of BC on human health.
- The calculated emission ratios of eBC and gaseous species that were presented in Chapter 5 could be used in future modelling studies as emission factors for BC emission sources in South Africa.
- In this study, ambient BC levels were not converted/translated to local and/or regional climatic impacts, which is critical in order to assess current and future impacts and contributions of BC to global warming. Compared to CO_2 (long lifetime in the atmosphere), BC (a short-lived climate pollutant) is a regional and local contributor to global warming (that causes climate change) due to its short lifetime in the atmosphere (days to weeks). Using the information presented in this PhD coupled with related national and international studies (e.g. DEA BC monitoring network, Ramanathan (2008)), a nationwide BC reduction policy/strategy/plan can be formulated for South Africa. According to Ramanathan (2008) and Mokdad (2004),

reductions in BC emissions may be the fastest means of slowing global warming and climate change in the short term; and can form part of a viable climate change mitigation strategy, whereas reductions in GHG emissions will take longer to influence atmospheric concentrations and will have less impact on climate on a short timescale. However, extensive reductions in GHG emissions remain essential to limit climate change over the long term. Emission sources and ambient BC concentrations vary spatially and temporally, resulting in climate effects that are more regionally and seasonally dependent compared to the effects of other long-lived and well-mixed GHGs such as CO_2. It should therefore be acknowledged that mitigation efforts for BC will produce different climate results depending on the region, season, and emissions sources (Lippmann et al., 2003; USEPA, 2012; Bond, 2013; IPCC, 2013).

- The recently released scientific IPCC Special Report on assessing the impacts of 1.5 degrees global warming (IPCC, 2018) confirms that the climate is warming at a much faster rate/pace than it was anticipated and that the globe is expected to reach the 1.5 degrees global warming by the year 2030 (12 years from now!). A global warming of 3.4 degrees will be experienced by 2100, with the African continent warming at a rate much higher than this global 3.4 degrees. This warming will have devastating impacts on water, food security, ecosystems, human health, human settlements, infrastructure etc., with huge adaptation costs associated with these impacts Therefore, there is a need to consider reducing short-lived climate pollutants such as BC to limit the pace of global warming that has been projected by this recent IPCC special report.
- Therefore, focusing on reducing BC nationally will contribute to SA's climate change mitigation strategies, plans and efforts and will ensure that SA meets its international climate change commitments as outlined in the country's nationally determined commitments (NDCs) that were submitted to the United Nations Framework Convention on Climate Change (UNFCCC) as part of the Paris Agreement (PA) signed in 2015. The IPCC 2018 report also warns that the NDCs submitted by all global countries as part of the PA that is currently being implemented fall short and will not be sufficient to slow down the projected global warming; and encourages countries to review their mitigation commitments to explore potential mitigation efforts and areas that can be strengthened to keep global warming to below 1.5 degrees Celsius.
- Investing in BC reduction as part of SA's mitigation system will help reduce regional and localised global warming and strengthen the country's NDC. This will ensure that SA does not only depend on other major GHG emitting countries (such as the United States of America and China) to reduce its GHG emissions to address its regional and local impacts of climate change.

BIBLIOGRAPHY

Andreae, M.O., and Gelencser, A. Black carbon or brown carbon? The nature of light absorbing carbonaceous aerosols. Atmospheric Chemistry and Physics, 6, 3131-3148, doi: 10.5194/acp-6-3131, 2006.

Aurela, M., Beukes, J.P., Vakkari, V., Van Zyl, P.G., Teinilä, K., Saarikoski S., and Laakso L. The composition of ambient and fresh biomass burning aerosols at a savannah site. South African Journal of Science, 112(5/6), Article no: 2015-0223, doi: 10.17159/ sajs.2016/20150223, 2016.

Awang, N.R., Ramli, N.Y., Ahmad, S., and Elbayoumi, M. Multivariate methods to predict ground level ozone during daytime, night-time, and critical conversion time in urban areas. Atmospheric Environment 43, 3918-3924, doi: 10.5094/APR.2015.081, 2015.

Backman, J., Virkkula, A., Vakkari, V., Beukes, J. P., Van Zyl, P. G., Josipovic, M., Piketh, S., Tiitta, P., Chiloane, K., Petäjä, T., Kulmala, M., and Laakso, L. Differences in aerosol absorption Ångström exponents between correction algorithms for a particle soot absorption photometer measured on the South African Highveld. Atmospheric Measurement Techniques Discussion, 7, 4285-4298, doi: 10.5194/amt-7-4285, 2014.

Baldauf, R. W., Lane, D. D., Marotz, G. A., and Wiener, R. W. Performance evaluation of the portable MiniVOL particulate matter sampler. Atmospheric Environment, 35, 6087- 6091, 2001.

Beukes, J. P., Van Zyl, P. G., and Ras, M. Treatment of Cr (VI) - containing wastes in the South African ferrochrome industry – review of currently applied methods, The Southern African Institute of Mining and Metallurgy, , 112, 413-418, 2012.

Beukes, J.P., Vakkari, V., Van Zyl, P.G., Venter, A.D., Josipovic, M., Jaars, K., Tiita, P., Siebert, S., Pienaar, J.J., Kulmala, M., and Laakso, L. Welgegund: long-term land atmosphere measurement platform in South Africa. iLeaps Newsletter, 12, 24-25, 2013.

Beukes, J.P., Vakkari, V., Van Zyl, P.G., Venter, A.D., Josipovic, M., Jaars, K., Tiitta, P., Kulmala, M., Worsnop, D., Pienaar, J.J., Virkkula, A., and Laakso, L. Source region plume characterisation of the interior of South Africa as observed at Welgegund, Clean Air Journal, 23(1), 7-10, 2013.

Beukes, J.P., Vakkari, V., van Zyl, P.G., Venter, A.D., Josipovic, M., Jaars, K., Tiitta, P., Laakso, H., Kulmala, M., Worsnop, D., Pienaar, J.J., Järvinen, E., Chellapermal, R., Ignatius, K., Maalick, Z., Cesnulyte, V., Ripamonti, G., Laban, T.L., Skrabalova, L., du Toit, M., Virkkula, A., Siebert S.J., and Laakso, L. Source region plume characterisation of the interior of South Africa, as measured at Welgegund, as measured at Welgegund, in preparation, 2014.

Beukes, J.P., Venter, A.D., Josipovic, M., Van Zyl, P.G., Vakkari, V., Jaars, K., Dunn, M., and Laakso, L. Automated Continuous Air Monitoring. Comprehensive Analytical Chemistry, 70, 183-208, 2015. http://dx.doi.org/10.1016/bs.coac.2015.09.006, 2015.

Beukes J.P., Van Zyl, P.G., Sofiev, M., Soares, J., Liebenberg-Enslin, H., Shackleton, N., and Sundström, A.-M. The Journal of the Southern African Institute of Mining and Metallurgy, 118 619-624. The use

of satellite observations of fire radiative power to estimate the availabilities (activity patterns) of pyrometallurgical smelters. http://dx.doi.org/10.17159/2411-9717/2018/v118n6a9, 2018.

Bohren, C.F., and Huffman D.R. Absorption and Scattering of Light by Small Particles, Wiley, Canada. 1983.

Bond, T., Streets, D.G., Yarber, K.F., Nelson, S.M., Woo, J.H., and Klimont, Z. A technology-based global inventory of black and organic carbon emissions from combustion. Journal of Geophysical Research, 109, doi: 10.1029/2003JD003697, 2004.

Bond, T., and Sun, H. Can Reducing Black Carbon Emissions Counteract Global Warming?? Environmental Science and Technology, 39, 16, 5921–5926, DOI: 10.1021/es048042, 2005.

Bond, T.C., Doherty, S.J., Fahey, D.W., Forster, P.M., Berntsen, T., DeAngelo, B.J., Flanner, M.G., Ghan, S., Kärcher, B., Koch, D., Kinne, S., Kondo, Y., Quinn, P., Sarofim, M.C., Schultz, M.G., Schulz, M., Venkataraman, C., Zhang, H., Zhang, S., Bellouin, N., Guttikunda, S.K., Hopke, P.K., Jacobson, M.Z., Kaiser, J.W., Klimont, Z., Lohmann, U., Schwarz, J.P., Shindell, D., Storelvmo, T., Warren, S.G., and Zender, C.S. Bounding the role of black carbon in the climate system: A scientific assessment. Journal of Geophysical Research: Atmospheres, 118, 5380-5552, doi:10.1002/jgrd.50171, 2013.

Cachier, H. Combustion carbonaceous aerosols in the atmosphere: implications for ice core studies. In: Robert, J.D. (Ed.), Ice Core Studies of Global Biogeochemical Cycles. NATO ASI Series Springer, Berlin, 313- 346, 1995.

Cao, G.L., Zhang, X.Y., and Zheng, F.C. Inventory of black carbon and organic carbon emissions from China. Atmospheric Environment, 40 (34), 6516–6527, 2006.

Carruthers, V. Wildlife of Southern Africa. Struik Publishers, Cape Town, 1997.

Chang S.G., and T. Novakov. Formation of pollution particulate nitrogen compounds by NO-soot and NH_3-soot gas particle surface reactions. Atmospheric Environment 9, 495-504, 1975.

Chow, J.C., Watson, J.G., Pritchett, L.C., Pierson, W.R., Frazier, C.A., and Purcell, R.G. The DRI thermal/optical reflectance carbon analysis system: description, evaluation and applications in U.S. Air quality studies. Atmospheric Environment, 27, 1185-1201, doi: 10.1016/0960-1686(93)90245-T, 1993.

Chow, J.C., Watson, J.G., Crow, D., Lowenthal, D.H., and Merrifield, T. Comparison of IMPROVE and NIOSH carbon measurements. Aerosol Science and Technology, 34, 23-24, 2001.

Coakley, J. A., Cess, R. D., Yurevich, F. B. The effect of tropospheric aerosols on the Earth‘s radiation budget: a parameterisation for climate models. Journal of Atmospheric Science, 40, 116–138, 1983.

Collett, K, Piketh, S., and Ross, K. An assessment of the atmospheric nitrogen budget on the South African Highveld. South African Journal of Science, 106, doi:10.4102/sajs.v106i5/6.220, 2010.

Conradie, E.H., Van Zyl, P.G., Pienaar, J.J., Beukes, J.P., Galy-Lacaux, C., Venter, A.D., and Mkhatshwa, G.V. The chemical composition and fluxes of atmospheric wet deposition at four sites in South Africa. Atmospheric Environment, doi: 10.1016/j.atmosenv.2016.07.033, 2016.

Cooke, W.F., and Wilson, J.N. A global black carbon aerosol model. Journal of Geophysical Research 101D, 19395-19408, doi: 10.1029/96JD00671, 1996.

Cooke, W.F., Jennings, S.G., and Spain, T.G. Black carbon measurements at Mace Head. Journal of Geophysical Research, 102D, 25339-25346, 1997.

Draxler, R. R., and Hess, G. D. Description of the HYSPLIT 4 Modelling System, NOAA Technical Memorandum ERL ARL-224, 2004.

Department of Environmental Affairs (DEA). Climate Change Adaptation Plans for South African Biomes, prepared by Council for Scientific and Industrial Research (CSIR), Pretoria, 2015.

Du Preez, S.P., Beukes, J.P., and Van Zyl., P.G. Cr (VI) Generation During Flaring of CO-Rich Off-Gas from Closed Ferrochromium Submerged Arc Furnaces. Doi: 10.1007/s11663-014-0244-3, 2015.

Environmental Analysis Facility (EAF). DRI Standard operating procedure, 86p. Laboratoired'Aérologie – UMR 5560. http://www.aero.obs-mip.fr/spip.php?article489, (accessed 16 June 2017), 2008.

EPA (Environmental Protection Agency), Recommendations for Reducing Emissions for the Legacy Diesel Fleet. U.S. Environmental Protection Agency, Washington, DC. Available at http://www.epa.gov/cleandiesel/documents/caaac-apr06.pdf (accessed 19 January 2018), 2006.

EPA. Reducing black carbon emissions in South Asia, Washington, DC.

Available at http://nepis.epa.gov/Exe/ ZyPDF.cgi/P100EF3D.PDF?Dockey=P100EF3D.PDF (accessed 1.May.15), 2012a.

EPA. Report to Congress on Black Carbon. U.S. Environmental Protection Agency, Washington, DC. Available at http://www.epa.gov/blackcarbon/ (accessed 19 January .2018), 2012b.

Feig, Gregor T., Vertue Beverley, Naidoo, Seneca Ncgukana Nokulunga, and Mabaso Desmond. Measurement of atmospheric black carbon in the Vaal Triangle and Highveld Priority Areas. Received: 17 April 2015; Reviewed: 15 May 2015, Accepted 4 June 2015. http://dx.doi.org/10.17159/2410-972X/2015/v25n1a4, 2015.

Fenger, J. Urban air quality. Journal of Atmospheric Environment, 33, 4877-4900, 1999.

Fleming, G., and van der Merwe, M. Spatial disaggregation of greenhouse gas emission inventory data for Africa South of the Equator,

http://gis.esri.com/library/userconf/proc00/professional/papers/PAP896/p896.htm (date accessed: 12 March 2017), 2004.

Formenti, P., Elbert, W., Maenhaut, W., Haywood, J., Osborne, S., and Andreae, M.O. Inorganic and carbonaceous aerosols during the Southern African Regional Science Initiative (SAFARI 2000) experiment: Chemical characteristics, physical properties and emission data for smoke from African biomass burning. Journal of Geophysical Research, 108(D13), 8488, doi: 10.1029/2002JD002408, 2003.

Forster, P., Ramaswamy, V., Artaxo, P., Berntsen, T., Betts, R., Fahey, D.W., Haywood,J., Lean, J., Lowe, D.C., Myhre, G., Nganga, J., Prinn, R., Raga, G., Schulz, M., and Van Dorland, R. Changes in Atmospheric Constituents and in Radiative Forcing. In: Climate Change 2007: The Physical Science Basis. Contribution of Working Group I to the Fourth Assessment Report of the Intergovernmental Panel on Climate Change [Solomon, S., D., Qin, M., Manning, Z., Chen, M., Marquis, K.B., Averyt, M. Tignor

and H.L. Miller (Eds.)]. Cambridge University Press, Cambridge, United Kingdom and New York, NY, USA, 2007.

Freiman, M.T., and Piketh, S.J. Air transport into and out of the industrial Highveld region of South Africa. Journal of Applied Meteorology, 42, 994–1002, 2003.

Galy-Lacaux, C., Al Ourabi, H., Lacaux, J.P., Pont, V., Galloway, J., Mphepya, J., Pienaar, K., Sigha, L., and Yoboué, V. Dry and wet atmospheric nitrogen deposition in Africa. IGAC Newsletter, 27, 6-11, 2003.

Garstang, M., Tyson, M., Swap, R., Edwards, M., Kållberg, P., and Lindesay, J.A.: Horizontal and vertical transport of air over southern Africa. Journal of Geophysical Research, 101, 23721-23736. 1996.

Gautam, R., Hsu, C.N., Lau, K.-M., Kafatos, M. Aerosol and rainfall variability over the Indian monsoon region: distributions, trends and coupling. Annals of Geophysics, 27, 3691-3703, 2009.

Gierens, R.T., Henriksson, S., Josipovic, M., Vakkari, V., Van Zyl, P.G., Beukes, J.P., Wood, C.R., and O'Connor, E.J. Observing continental boundary-layer structure and evolution over the South African savannah using a ceilometer. Theoretical and Applied Climatology, published online, doi: 10.1007/s00704-018-2484-7, 2018.

Google Maps, date accessed: April 2017 and August 2018.

Guillame, B., Liousse, C., Galy-Lacaux, C., Rosset, R., Gardrat, E., Cachier, H., Bessagnet, B., and Poisson, N. Modeling exceptional high concentrations of carbonaceous aerosols observed at Pic du Midi in spring-summer 2003: Comparison with Sonnblick and Puy de Dôme. Atmospheric Environment, 42, 5140-5149, doi: 10.1016/j.atmosenv.2008.02.024, 2008.

Gurja, B.R., Butler, T.M., Lawrence, M.G., Lelieceld, J. Evaluation of emissions and air quality in megacities. Atmospheric Environment 42, 1593-1606, 2008.

Hamilton, R.S., and Mans-field, T.A. Airborne particulate elemental carbon: its sources, transport and contribution to dark smoke and soiling. Atmospheric Environment, 25A, 715-723, 1991.

Hansen, A.D.A., Rosen, H., and Novakov, T. The Aethalometer: an instrument for the real-time measurement of optical absorption by aerosol particles. Science of the Total Environment, 36, 191-196, 1984.

Hansen, A.D.A., Bodhaine, B.A., Dutton, E.G., and Schnell, R.C. Aerosol black carbon measurements at the South Pole: initial results 1986-1987. Geophysical Research Letters, 15, 1193 - 1196, 1988.

Hansen, J., M. Sato, R. Ruedy, A. Lacis, and V. Oinas.: Global warming in the twenty-first century: An alternative scenario. Proceedings of the National Academy of Sciences of the United States of America, 9875-9880, 2000.

Hansen, J and Makiki, Sato. Figure 1 in Trends of Measures Climate Forcing Agents, Proceedings of the National Academy of Sciences of the USA, 98, 14778, 14779, 2001.

Hansen, J., M. Sato, R. Ruedy, L. Nazarenko, A. Lacis, G.A. Schmidt, G. Russell, I. Aleinov, M. Bauer, S. Bauer, N. Bell, B. Cairns, V. Canuto, M. Chandler, Y. Cheng, A. Del Genio, G. Faluvegi, E. Fleming, A. Friend, T. Hall, C. Jackman, M. Kelley, N.Y. Kiang, D. Koch, J. Lean, J. Lerner, K. Lo, S.

Menon, R.L. Miller, P. Minnis, T. Novakov, V. Oinas, J.P. Perlwitz, J. Perlwitz, D. Rind, A. Romanou, D. Shindell, P. Stone, S. Sun, N. Tausnev, D. Thresher, B. Wielicki, T. Wong, M. Yao, and S. Zhang, 2005: Efficacy of climate forcings. Journal of Geophysical Research., 110, D18104, doi: 10.1029/2005JD005776, 2005.

Hansen, J and Nazarenko, L. The effective forcing for the assigned snow albedo change in the most realistic cases 1 and 2 is Fe ~0.6 Wm^{-2} in the Northern Hemisphere or Fe ~0/3 Wm^{-2} globally. 2007(a).

Hansen, J., M. Sato, R. Ruedy, P. Kharecha, A. Lacis, R.L. Miller, L. Nazarenko, K. Lo, G.A. Schmidt, G. Russell, I. Aleinov, S. Bauer, E. Baum, B. Cairns, V. Canuto, M. Chandler, Y. Cheng, A. Cohen, A. Del Genio, G. Faluvegi, E. Fleming, A. Friend, T. Hall, C. Jackman, J. Jonas, M. Kelley, N.Y. Kiang, D. Koch, G. Labow, J. Lerner, S. Menon, T. Novakov, V. Oinas, J.P. Perlwitz, J. Perlwitz, D. Rind, A. Romanou, R. Schmunk, D. Shindell, P. Stone, S. Sun, D. Streets, N. Tausnev, D. Thresher, N. Unger, M. Yao, and S. Zhang. Climate simulations for 1880-2003 with GISS modelE. Climate Dynamics, 29, 661-696, doi: 10.1007/s00382-007-0255-8, 2007 (b).

Highwood, E., and Kinnersley, R. When smoke gets in our eyes: The multiple impacts of atmospheric black carbon on climate, air quality. Environment International, 32, 4, 560-566, 2006.

Hirsikko, A., Vakkari, V., Tiitta, P., Manninen, H.E., Gagné, S., Laakso, H., Kulmala, M., Mirme, A., Mirme, S., Mabaso, D., Beukes, J.P., and Laakso, L. Characterisation of sub-micron particle number concentrations and formation events in the western Bushveld Igneous Complex, South Africa. Atmospheric Chemistry and Physics, 12, 3951-3967, doi: 10.5194/acp-12-3951-2012, 2012.

Hyvärinen, A.P., Vakkari, V., Laakso, L., Hooda, R.K., Sharma, V.P., Panwar, T.S., Beukes, J.P., Van Zyl, P.G., Josipovic, M., Garland, R.M., Andreae, M.O., Pöschl, U., and Petzold, A. Correction for a measurement artifact of the Multi-Angle Absorption Photometer (MAAP) at high black carbon mass concentration levels. Atmospheric Measurement Techniques, 6, 81-90, doi: 10.5194/amt-6-81-2013, 2013.

HYSPLIT User's Guide-Version 4. Last revised: April 2013.

http://www.arl.noaa.gov/documents/reports/hysplit_user_guide.pdf. (Accessed: April 2016).

IEA (International Energy Agency) Report. CO_2 emissions from fuel combustion. Accessed 13 February 2014 and 2016.

IPCC. Second Assessment Report, Climate Change – Working Group I: The Science of Climate Change, 1995.

IPCC. Third Assessment Report, Climate Change – Working Group I: The Scientific Basis, 2001. Changes in Atmospheric Constituents and in Radiative Forcing, in climate change 2007: the physical science basis. Contribution of working group I to the fourth assessment report of the intergovernmental panel on climate change 129, 132. Available at http://www.ipcc.ch/ipccreports/ar4-wg1.htm, 2007.

IPCC. Summary for Policymakers. In Climate Change: The Physical Science Basis. Contribution of Working Group I to the Fifth Assessment Report of the Intergovernmental Panel on Climate Change [Stocker, T.F., D. Qin, G.K. Plattner, M. Tignor, S.K. Allen, J. Boschung, A. Nauels, Y. Xia, V. Bex

and P.M. Midgley (Eds.)]. Cambridge University Press, Cambridge, United Kingdom and New York, NY, USA. 2013.

IPCC. Summary for Policymakers. Global warming of 1.5 °C. An IPCC special report on the impacts of global warming of 1.5 °C above pre-industrial levels and related global greenhouse gas emission pathways, in the context of strengthening the global response to the threat of climate change, sustainable development, and efforts to eradicate poverty. Formally approved at the First Joint Session of Working Groups I, II and III of the IPCC and accepted by the 48th Session of the IPCC, Incheon Republic of Korea, 6 October 2018.

Jaars, K., Beukes, J.P., Van Zyl, P.G., Venter, A.D., Josipovic, M., Pienaar, J.J., Vakkari, V., Aaltonen, H., Laakso, H., Kulmala, M., Tiitta, P., Guenther, A., Hellén, H., Laakso, L., and Hakola, H. Ambient aromatic hydrocarbon measurements at Welgegund, South Africa. Atmospheric Chemistry and Physics, 14, 4189-4227, doi: 10.5194/acpd-14-4189-2014, 2014.

Jacobson, M. Strong Radiative Heating Due to the Mixing State of Black Carbon in Atmospheric Aerosols. Nature, 409, 695-697, 2001.

Jacobson, M. Control of fossil fuel particulate black carbon and organic matter, possibly the most effective method of slowing global warming. Journal of Geophysical Research, 107, D19 19, 2002.

Jacobson, M. Climate response of fossil fuel and biofuel soot, accounting for soot's feedback to snow and sea ice albedo and emissivity, 109. Journal of Geophysical Research: Atmospheres, 109, D21201, doi: 10.1029/2004JD004945, 2004.

Janssen, N., Hoek, G., Simic-Lawson, M., Fischer, P., van Bree, L., ten Brink, H., Keuken, M., Atkinson, R., Anderson, H., Brunekreef, B., and Flemming R. Cassee.: Black carbon as an additional indicator of the adverse health effects of airborne particles compared with PM_{10} and $PM_{2.5}$. Environmental Health Perspectives, 119, 12, 2011.

Janssen, N., Gerlofs-Nijland, M., Lanki, T., Salonen, R., Cassee, F., Hoek, G., Fischer, P., Brunekreef, B. and Krzyzanowski, M. Health effects of black carbon. The WHO European Centre for Environment and Health Report. ISBN: 978 92 890 0265 3. Publications WHO Regional Office for Europe, 2012.

Järvi, L., Junninen, H., Karppinen, A., Hillamo, R., Virkkula, A., Mäkelä, T., Pakkanen, T., Kulmala, M. Temporal variations in black carbon concentrations with different time scales in Helsinki during 1006-2005. Atmospheric Chemistry and Physics, 8, 1017-1027, 2008.

Kanakidou, M., Seinfeld, J.H., Pandis, S.N., Barnes, I., Dentener, F.J., Facchini, M.C., Van Dingenen, R., Ervens, B., Nenes, A., Nielson, C.J., Swietlicki, E., Putaud, J.P., Balkanski, Y., Fuzzi, S., Horth, J., Moortgat, G.K., Winterhalter, R., Myhre, C.E.L., Tsigaridis, K., Vignati, E., Stephanou, E.G., and Wilson, J. Organic aerosol and global climate modelling: a review. Atmospheric chemistry and Physics, 5, 1053-1123, doi: 1680-7324/acp/2005-5-1053, 2005.

Karnosky, D.F., Percy, K.E., Chappelka, A.H., Simpson, C., and Pikkarainen, J. Air Pollution, Global Change and Forests in the New Millennium. Academic Press, Netherlands, 2003.

Kerminen, V.M., MaK kelaK , T.E., Ojanen, C.H., Hillamo, R.E., Vilhunen, J.K., Rantanen, L., Havers,

N., von Bohlen, A., and Klockow, D. Characterisation of particulate phase in the exhaust from a diesel car. Environmental Science and Technology, 31, 1883-1889, 1997.

Kim, D., and Ramanathan, V. Solar radiation budget and radiative forcing due to aerosols and clouds. Journal of Geophysical Research, 113 (D02203), doi: 10.1029/2007JD008434, 2008.

Korhonen, K., Giannakaki, E., Mielonen, T., Pfüller, A., Laakso, L. Vakkari, V., Baars, H., Engelmann, R., Beukes, J.P., Van Zyl, P.G, Ramandh, A., Ntsangwane, L., Josipovic, M., Tiitta, P., Fourie, G., Ngwana, I., Chiloane, K., and Komppula. M. Atmospheric boundary layer top height in South Africa: measurements with lidar and radiosonde compared to three atmospheric models. Atmospheric Chemistry and Physics, 13, 17407-17450, 2014.

Kuik, F., Lauer, A., Beukes, J.P., Van Zyl, P.G., Josipovic, M., Vakkari, V., Laakso, L., and Feig, G.T. The anthropogenic contribution to atmospheric black carbon concentrations in southern Africa: a WRF-Chem modelling study. Atmospheric Chemistry and Physics, 15, 8809–8830, doi: 10.5194/acp-15-8809-2015, 2015.

Kulmala, M., Asmi, A., Lappalainen, H., Carslaw, K. S., Pöschl, U., Baltensperger, U., Hov, Ø., Brenguier, J.-L., Pandis, S. N., Facchini, M. C., Hansson, H.-C., Wiedensohler, A., and O'Dowd, C.D. Introduction: European Integrated Project on Aerosol Cloud Climate and Air Quality interactions (EUCAARI). Integrating aerosol research from nano to global scales. Atmospheric Chemistry and Physics 9, 2825-2841, 2009.

Laban, T.L., van Zyl, P.G., Beukes, J.P., Vakkari, V., Jaars, K., Borduas-Dedekind, N., Josipovic, M., Thompson, A.M., Kulmala, M., and Laakso, L. Seasonal influences on surface ozone variability in continental South Africa and implications for air quality. Atmospheric Chemistry and Physics. Discussion, https://doi.org/10.5194/acp-2017-1115, in review, 2018.

Laakso, L., Vakkari, V., Virkkula, A., Laakso, H., Backman, J., Kulmala, M., Beukes, J.P., van Zyl, P.G., Tiitta, P., Josipovic, M., Pienaar, J.J., Chiloane, K., Gilardoni, S., Vignati, E., Wiedensohler, A., Tuch, T., Birmili, W., Piketh, S., Collett, K., Fourie, G.D., Komppula, M., Lihavainen, H., de Leeuw, G., and Kerminen, V.-M.: South African EUCAARI measurements: seasonal variation of trace gases and aerosol optical properties. Atmospheric Chemistry and Physics, 12, 1847-1864, doi: 10.5194/acp-12-1847-2012, 2012.

Liousse, C., Penner, J.E., Chuang, C., Walton, J.J., Eddleman, H., and Cachier, H. A global three-dimensional model study of carbonaceous aerosols. Journal of Geophysical Research, 105, 26871-26890, 1996.

Lippmann, M., Cohen, B.S., and Schlesinger, R.S. Environmental Health Science. New York: Oxford University Press, 2003.

Liu, J.G., and Diamond, J. China's environment in a globalizing world. Nature 435, 1179-1186, 2005.

Lourens, A.S., Beukes, J.P., and Van Zyl, P.G. Spatial and temporal assessment of gaseous pollutants in the Highveld of South Africa. South African Journal of Science, 107(1/2), Article no: 269, 8 pages, doi: 10.4102/sajs.v107i1/2.269, 2011.

Lourens, A.S.M., Butler, T.M., Beukes, J.P., Van Zyl, P.G., Beirle, S., Wagner, T., Heue, K-P., Pienaar, J., Fourie, G.D., and Lawrence, M.G. Re-evaluating the NO_2 hotspot over the South African Highveld. South African Journal of Science, 108, 6 pp., doi: 10.4102/sajs.v108i11/12.1146.1146, 2012.

Lourens, A.S.M., Butler, T.M., Beukes, J.P., Van Zyl, P.G. Pienaar, J.J., and Lawrence, M.G. Investigating photochemical processes in the Johannesburg-Pretoria megacity using a box model. South African Journal of Science, 112(1/2), Article no: 2015-0169, 11 pages, doi: 10.17159/sajs.2016/2015-0169, 2016.

Mafusire, G., Annegarn, H.J., Vakkari, V., Beukes, J.P., Josipovic, M., Van Zyl, P.G., and Laakso, L. Submicrometer aerosols and excess CO as tracers for biomass burning air mass transport over southern Africa. Journal of Geophysical Research – Atmospheres, 121, 10262-10282, doi: 10.1002/2015JD023965, 2016.

Martins, J.J., Dhammapala, R.S., Lachmann, G., Galy-Lacaux, C., and Pienaar, J.J. Long-term measurements of sulphur dioxide, nitrogen dioxide, ammonia, nitric acid and ozone in southern Africa using passive samplers. South African Journal of Science, 103, 336-342, 2007.

Martins, J.J. Concentrations and deposition of atmospheric species at regional sites in southern Africa. MSc Thesis NWU Potchefstroom, 224p. 2009.

Maritz, P., Beukes, J.P., Van Zyl, P.G. Conradie, E.H., Liousse, C., Galy-Lacau, C., Castéra, P., Ramandh, A., Mkhatshwa, G., Venter, A.D., and Pienaar, J.J. Spatial and temporal assessment of organic and black carbon at four sites in the interior of South Africa. Clean Air Journal, 25(1), 20-33, doi: 10.17159/2410-972X/2015/v25n1a1, 2015.

Masiello, C.A. New directions in black carbon organic geochemistry. Marine Chemistry 92, 201-213, doi: 10.1016/j.marchem.2004.06.043, 2004.

Menon, S., J. Hansen, L. Nazarenko, and Y. Luo. Climate effects of black carbon aerosols in China and India. Science, 297, 2250-2253, 2002.

Michael Hogan. Abiotic factor. Encyclopedia of Earth. eds Emily Monosson and C. Cleveland. National Council for Science and the Environment, Washington DC, 2010.

Michael, Levitsky. Black Carbon and Climate Change: Considerations for International Development Agencies. Environment department papers; no. 112. Climate change series. World Bank, Washington, DC. World Bank. https://openknowledge.worldbank.org/handle/10986/18317, 2011.

MODIS: Obtaining and processing MODIS data. http://www.yale.ed u/ceo/Documentation/MODIS_data.pdf, 2016.

Mokdad, Ali H. Actual causes of death in the United States. Journal of American Medical Association, 291 (10), 1238-1245, 2004.

Moorthy, K.K., Nair, V.S., Babu, S.S., and Satheesh, S.K. Spatial and vertical heterogeneities in aerosol properties over oceanic regions around India: implications for radiative forcing. Quarterly Journal of the Royal Meteorological Society, doi: 10.1002/qj.525, 2009.

Mphepya, J.N., Pienaar, J.J., Galy-Lacaux, C., Held, G., and Turner, C.R. Precipitation Chemistry in Semi-

Arid Areas of Southern Africa: A Case Study of a Rural and an Industrial Site. Journal of Atmospheric Chemistry, 47, 1-24, 2004.

Mphepya, J.N., Galy-Lacaux, C., Lacaux, J.P., Held, G., and Pienaar, J.J. Precipitation Chemistry and Wet Deposition in Kruger National Park, South Africa. Journal of Atmospheric Chemistry, 53, 169-183. Doi: 10.1007/s10874-005-9005-7, 2006.

Myhre, G., Samset, B.H. Standard climate models radiation codes underestimate black carbon radiative forcing. Atmospheric Chemistry and Physics, 15, (5) 2883-2888, 2015.

NASA. http://gcmd.nasa.gov/records/ GCMD_gov.noaa.ncdc.C00075.html, accessed 22 May 2016.

Nieuwenhuijsen, M.J. Exposure assessment in occupational and environmental epidemiology. London: Oxford University Press. Tami Bond, Summary: Aerosols, Air Pollution as a Climate Forcing: A Workshop, Honolulu, Hawaii, April 29-May 3. Available at http://www.giss.nasa.gov/meetings/pollution2002/, 2003.

Nkosi, Ncobile C., Piketh, Stuart J., and Burger, Roelof P. Fine PM emission factors from residential burning of solid fuels using traditional cast-iron coal stoves. http://dx.doi.org/10.17159/2410-972X/2018/v28n1a10, 2018.

Novakov, T. 2nd International Conference on Carbonaceous Particles in the Atmosphere. The Science of Total Environment, 36, 1984.

Novakov, T., Chang, S.G., and Harker, A.B. Sulphates as pollution particulates: Catalytic formation on carbon (soot) particles, Science, 186, 259-261, 1974.

Ohara, T., Akimoto, H., Kurokawa, J., Horii, N., Yamaji, K., Yan, X., and Hayasaka, T. An Asian emission inventory of anthropogenic emission sources for the period 1980-2020. Atmospheric Chemistry and Physics, 7 (16), 4419-4444, 2007.

Penner, J.E., Ghan, S.J., and Walton, J.J. The role of biomass burning in the budget and cycle of carbonaceous soot aerosols and their climate impact. In: Levine, J.S. (Eds.), Global Biomass Burning: Atmospheric, Climatic, and Biospheric Implications. MIT Press, Cambridge, MA, 387- 393, 1991.

Penner, J.E., Eddleman, H., and Novakov, T. Towards the development of a global inventory for black carbon emissions. Atmospheric Environment, 27A, 1277-1295, 1993.

Petzold, A., Kramer, H., and Schönlinner, M. Continuous Measurement of atmospheric black carbon using a multi-angle Absorption photometer. Environmental Science and Pollution Research, Special Issue 4, 78-82, 2002.

Petzold, A., and Schönlinner, M. Multi-angle absorption photometry: a new method for the measurement of aerosol light absorption and atmospheric black carbon. Journal of Aerosol Science, 35, 421-441, doi: 10.1016/j.jaerosci.2003.09.005, 2004.

Pope, C.A., Burnett, R.T., Thun, M.J., Calle, E.E., Krewski, D., Ito, K., and Thurston, G.D. Lung cancer, cardiopulmonary mortality, and long-term exposure to fine particulate air pollution. Journal of the American Medical Association, 287 (9), 1132-1141, 2002.

Pöschl, U. Atmospheric Aerosols: composition, transformation, climate and health effects. Atmospheric

Chemistry: Reviews. Angewandte Chemie International Edition, 44, 7520-7540, Doi: 10.1002/anie.200501122, 2005.

Pretorius Ilze. Piketh Stuart, Burger Roelof, and Neomagus Hein. A perspective on South African coal fired power station Emissions. Journal of Energy in Southern Africa 26(3), 27-40, doi: http://dx.doi.org/10.17159/2413-3051/2015/v26i3a2127, 2015.

Putaud, J.-P., Raes, F., Van Dingenen, R., Brüggemann, E., Facchini, M.-C., Decesari, S., Fuzzi, S., Gehrig, R., Hüglin, C., Laj, P., Lorbeer, G., Maenhaut, W., Mihalopoulos, N., Müller, K., Querol, X., Rodriguez, S., Schneider, J., Spindler, G., ten Brink, H., Tørseth, K., and Wiedensohler, A. A European aerosol phenomenology: chemical characteristics of particulate matter at kerbside, urban, rural and background sites in Europe. Atmospheric Environment, 38, 2579-2595, doi:10.1016/j.atmosenv.2004.01.041, 2004.

Ramanathan, V., Crutzen, P.J., and Lelieveld, J. Indian Ocean experiment: an integrated analysis of the climate forcing and effects of the great Indo-Asian haze. Journal of Geophysical Research, 106, 28371-28398, 2001.

Ramanathan, V., and Carmichael, G. Global and regional climate changes due to black carbon. Nature Geoscience 1, 221-227. Doi: 10.1038/ngeo156, 2008.

Ramsuchit and Kornelius. Analysis of contributions to the PM10 concentration in a gold mine residential village. 16th International Union of Air Pollution Prevention Associations (IUAPPA) World Clean Air Conference. Conference Paper, 2013.

Rockstrom, J., Steffen, W., Noone, K., Persson, A., Chapin, F., Lambin, E., and Scheffer, M. A safe operating space for humanity. Nature 461 (7263), 472-475, doi: 10.1038/461472a. PMID 19779433, 2009.

Rencher, A.C. Methods of multivariate analysis, Second Edition, Brigham Young University, John Wiley & Sons, Inc. Publication, 605 Third Avenue, New York, NY 10158-001, 2002.

Rosen, H., and Hansen, A.D.A. Estimates of springtime soot and sulphur fluxes entering the Arctic troposphere: Implications to source regions. Atmospheric Environment, 19, 2203-2207, 1985.

Roy, D.P., Boschetti, L., Justice, C.O., and Ju, J. The collection 5 MODIS burned area product: Global evaluation by comparison with the MODIS active fire product. Remote Sensing of Environment, 112, 3690-3707p, doi: 10.1016/j.rse.2008.05.013, 2008.

Saha, A., and Despiau S. Seasonal and diurnal variations of black carbon aerosols over a Mediterranean coastal zone. Atmospheric Research, 92, 27-41, doi:10.1016/j.atmosres, 2009.

Saikawa Eri, Naik Vaishali, Horowitz Larry W., Liu Junfeng, Mauzerall Denise. Present and potential future contributions of sulphate, black and organic carbon aerosols from China to global air quality, premature mortality and radiative forcing. Atmospheric Environment, 43, 2814-2822, 2009.

Satheesh, S.K., Ramanathan, V., Li-Jones, X., Lobert, J.M., Podgorny, I.A., Prospero, J.M., Holben, B.N., and Loeb, G.N. A model for the natural and anthropogenic aerosols over the tropical Indian Ocean derived from Indian Ocean experiment data. Journal of Geophysical Research 104, 27421-27440, 1999.

Schmidt, M.W.I., and Noack, A.G. Black carbon in soils and sediments: Analysis, distribution, implications and current challenges. Global Biogeochemical Cycles 14, 777-793, 2000.

Sehloho, R.M. An assessment of atmospheric organic and black carbon at Welgegund. PhD thesis in preparation, North-West University, 2017.

Seinfeld, J.H., and Pandis, S.N. Atmospheric Chemistry and Physics: From Air Pollution to Climate Change. 3rd edition, John Wiley and Sons Inc. 2016.

Shen, G., Tao, S., Wei, S., Zhang, Y., Wang, R., Wang, B., Li, W., Shen, H., Huang, Y., Chen, Y., Chen, H., Yang, Y., Wang, W., Wei, W., Wang, X., Liu, W., Wang, X., and Masse Simonich, S. Reductions in emissions of carbonaceous particulate matter and polycyclic aromatic hydrocarbons from combustion of biomass pellets in comparison with raw fuel burning. Environmental Science and Technology, 46(11):6409-16, 2012.

Shindell, D.T., Levy II, H., Schwarzkopf, M.D., Horowitz, L.W., Lamarque, J.F., and Faluvegi, G. Multimodel projections of climate change from short-lived emissions due to human activities. Journal of Geophysical Research – Atmospheres, 113, D11109, doi: 10.1029/2007JD009152, 2008.

Slanina, S., and Zhang, Y. Aerosols connection between regional climatic change and air quality. IUPAC. Pure and Applied Chemistry, 76(6), 1241-1253, 2004.

Solomon, S., D. Qin, M. Manning, Z. Chen, M. Marquis, K.B. Averyt, M. Tignor and H.L. Miller (eds.) Climate Change 2007: The Physical Science Basis, Cambridge University Press, Cambridge, United Kingdom and New York, NY, USA, 2007.

South African National Environmental Management, Air Quality Act of 2004 (NEM AQA, 2004)

South African Air Quality Information System (SAAQUIS).

http://www.saaqis.org.za/Priority%20Areas.aspx, accessed: 15 May 2017.

South African Weather Service (SAWS), http://www.weathersa.co.za/, accessed: 15 May 2017).

Spengler John D., and Adgate, J. Climate change, indoor environments, and health. International Journal of indoor environment and health, 22, 89-95, 2012.

Stohl, A. Computation, accuracy and application of trajectories: a review and bibliography. Atmospheric Environment, 32(6), 947-966, doi: 10.1016/S1352-2310(97)00457-3, 1998.

Stohl, A. Characteristics of atmospheric transport into the Arctic troposphere. Journal of Geophysical Research, 111, D11306, doi: 10.1029/2005JD006888, 2006.

Streets, D.G., Bond, T.C., Carmichael, G.R., Fernandes, S.D., Fu, Q., He, D., Klimont, Z., Nelson, S.M., Tsai, N.Y., Wang, M.Q., Woo, J.H., and Yarber, K.F. An inventory of gaseous and primary aerosol emissions in Asia in the year 2000. Journal of Geophysical Research, 108 (D21), 8809, doi: 10.1029/2002jd003093, 2003.

Swap, R.J., Annegarn, H.J., Suttles, J.T., King, M.D., Platnick, S., Privette, J.L., and Scholes R.J. Africa burning: A thematic analysis of the Southern African Regional Science Initiative (SAFARI 2000), Journal of Geophysical Research, 108, 8465, doi: 10.1029/2003JD003747, 2003.

Swap, R.J., Aranibar, J.N., Dowty, P.R., Gilhooly (III), W.P., and Macko, S.A. Natural abundance of ^{13}C

and ^{15}N in C_3 and C_4 vegetation of southern Africa: patterns and implications. Global Change Biology, 10, 350-358, doi: 10.1046/j.1529-8817.2003.00702.x, 2004.

The World Bank and Institute for Health Metrics and Evaluation: The Cost of Air Pollution Strengthening the Economic Case for Action. Report, University of Washington, Seattle, 2016.

Tiitta, P., Vakkari, V., Croteau, P., Beukes, J.P., Van Zyl, P.G., Josipovic, M., Venter, A.D., Jaars, K., Pienaar, J.J., Ng, N.L., Canagaratna, M.R., Jayne, J.T., Kerminen, V.M., Kokkola, H., Kulmala, M., Laaksonen, A., Worsnop, D.R., and Laakso, L. Chemical composition, main sources and temporal variability of PM1 aerosols in southern African grassland. Atmospheric Chemistry and Physics, 14, 1909-1927, doi: 10.5194/acp-14-1909-2014, 2014.

Tummon, F., Solmon, F., Liousse, C., and Tadross, M. Simulation of the direct and semidirect aerosol effects on the southern Africa regional climate during the biomass burning season. Journal of Geophysical Research D: Atmospheres, 115(19). Article no: D19206, doi: 10.1029/2009JD013738, 2010.

Twomey, S. Pollution and Planetary Albedo. Atmospheric Environment, 8, 1251-1256, 1974.

Tyson P.D., Garstang M., Swap R., Kållberg P., and Edwards M. An air transport climatology for subtropical southern Africa. International Journal of Climatology, 16, 265-291, 1996.

Tyson, P.D., and Preston-Whyte, R.A. The weather and climate of Southern Africa. Oxford University Press, Cape Town, 2004.

United States Department of Energy Archives, 1985.

United States Environmental Protection Agency (USEPA). Report to Congress on Black Carbon Department of the Interior, Environment, and Related Agencies Appropriations Act, 2010, EPA-450/R-12-001, http://www.epa.gov/blackcarbon, 2012 (a).

U.S. EPA. Reducing Black Carbon Emissions in South Asia, Low Cost Opportunities. Office of International and Tribal Affairs, 2012 (b).

Vakkari, V., Laakso, H., Kulmala, M., Laaksonen, A., Mabaso, D., Molefe, M., Kgabi, N., and Laakso, L. New particle formation events in semi-clean South African savannah, Atmospheric Chemistry and Physics, 11, 3333–3346, doi: 10.5194/acp-11-3333-2011, 2011.

Vakkari, V., Kerminen, V.M., Beukes, J.P., Tiitta, P., van Zyl, P.G., Josipovic, M., Venter, A.D., Jaars, K., Worsnop, D.R., Kulmala, M., and Laakso, L. Rapid changes in biomass burning aerosols by atmospheric oxidation. Geophysical Research Letters, 03, 2014.

Van Tienhoven, A.M. Status of air pollution in South Africa. National Association for Clean Air (NACA) Conference. www.naca.org.za, 1999.

Venter, A.D., Vakkari, V., Beukes, J.P., Van Zyl, P.G., Laakso, H., Mabaso, D., Tiitta, P., Josipovic, M., Kulmala, M., Pienaar, J.J., and Laakso, L. An air quality assessment in the industrialised western Bushveld Igneous Complex, South Africa. South African Journal of Science, 108(9/10), Article no: 1059, 10 pages, doi: 10.4102/sajs.v108i9/10.1059, 2012.

Venter, A.D., Beukes, J.P., van Zyl, P.G., Brunke, E.G., Labuschagne, C., Slemr, F., Ebinghaus, R., and

Kock, H. Statistical exploration of gaseous elemental mercury (GEM) measured at Cape Point from 2007 to 2011. Atmospheric Chemistry and Physics, 15, 10271-10280, doi: 10.5194/acp-15-10271-2015, 2015.

Venter, A.D., Beukes, J.P., Van Zyl, P.G., Josipovic, M., Jaars, K., and Vakkari, V. Regional atmospheric Cr (VI) pollution from the Bushveld Complex, South Africa. Atmospheric Pollution Research, 7, 762-767, doi: 10.1016/j.apr.2016.03.009, 2016.

Viidanoja, J., Sillanpää, M., Laakia, J., Kerminen, V.-M., Hillamo, R., Aarnio, P., and Koskentalo, T. Organic and black carbon in $PM_{2.5}$ and PM_{10}: 1 year of data from an urban site in Helsinki, Finland. Atmospheric Environment, 36, 3183-3193, doi: 10.1016/S1352-2310(02)00205-4, 2002.

Virkkula A. Correction of the calibration of the 3-wavelength Particle Soot Absorption Photometer (3λ PSAP). Aerosol Science and Technology, 44, 706-712, 2010.

Yu, H., Kaufman, Y. J., Chin, M., Feingold, G., Remer, L.A., Anderson, T. L., Balkanski, Y., Bellouin, N., Boucher, O., Christopher, S., DeCola, P., Kahn, R., Koch, D., Loeb, N., Reddy, M. S., Schulz, M. Takemura, T. and Zhou, M. A review of measurement-based assessment of aerosol direct radiative effect and forcing. Atmospheric Chemistry and Physics, 6, 613-666, 2006.

Yttri, K.E., Aas, W., Bjerke, A., Cape, J.N., Cavalli, F., Ceburnis, D., Dye, C., Emblico, L., Facchini, M.C., Forster, C., Hanssen, J.E., Hansson, H.C., Jennings, S.G., Maenhaut, W., Putaud, J.P., and Torseth, K. Elemental and organic carbon in PM10: a one year measurement campaign within the European Monitoring and Evaluation Program EMEP. Atmospheric Chemistry and Physics, 7, 5711-5725, 2007.

Wang, R., Tao, S., Shen, H., Huang, Y., Chen, H., Balkanski, Y., Boucher, O., Ciais, P., Shen, G., Li, W., Zhang, Y., Chen, Y., Lin,N., Su, S., Li, B., Liu, J., and Liu, W. Trend in Global Black Carbon Emissions from 1960 to 2007. Environmental Science & Technology, 48 (12), 6780-6787, 2014.

Warren, S.G., and Wiscombe, W.J. A model for the spectral albedo of snow. II Snow containing atmospheric aerosols. Journal of Atmospheric Sciences, 37, 2734-2745, 1980.

Watson J.G., Chow, J.C., and Chen, L.W.A. Summary of organic and elemental carbon/black carbon analysis methods and intercomparisons. Aerosol and Air Quality Research, 5, 65-102, 2005.

Wolf, E.W., and Cachier, H. Concentrations and seasonal cycle of black carbon in aerosol at a coastal Antarctic station. Journal of Geophysical Research, 103D, 11033-11041, 1998.

World Health Organisation (WHO), 2017.

http://www.who.int/gho/urban_health/situation_trends/urban_population_growth_text/en/, accessed: 15 May 2017.

Zhou, X., Gao, J., Wang, T., Wu, W., and Wang, W. Measurement of black carbon aerosols near two Chinese megacities and the implications for improving emission inventories. Atmospheric Environment, 43, 3918-3924, 2009.